CONTRIBUTION OF THE CANONICAL WNT PATHWAY IN *TRIBOLIUM* ANTERIOR-POSTERIOR AXIS PATTERNING

by

JINPING FU

B.S., Zhejiang University, China, 2004

AN ABSTRACT OF A DISSERTATION

submitted in partial fulfillment of the
requirements for the degree

DOCTOR OF PHILOSOPHY

Division of Biology
College of Arts and Sciences

KANSAS STATE UNIVERSITY
Manhattan, Kansas

2014

Abstract

How animals polarize and establish the main axis during embryogenesis has been one of the most attractive questions in Biology. Increasing body of work in various model organisms implicates that most metazoans utilize the canonical Wnt signaling pathway to pattern the anterior-posterior (AP) axis, despite the limited evidence from arthropods. In *Drosophila*, a highly derived insect, canonical Wnt activity is not required for global AP patterning, but in typical insects including *Tribolium castaneum*, loss of canonical Wnt activity results in posterior truncation. To determine the effects of increased canonical Wnt levels, I analyzed the function of *axin*, encoding a highly conserved negative regulator of the pathway. *Tc-axin* transcripts are maternally localized to the anterior pole in freshly laid eggs. Parental RNAi for *Tc-axin* produced progeny phenotypes that ranged from mildly affected embryos with cuticles displaying a graded loss of anterior structures, to severely affected embryos lacking cuticles and condensing to the posterior pole of the egg without any definable structures. Altered expression patterns of several blastodermal markers indicated anterior expansion of posterior fates. Epistasis analysis of other canonical Wnt pathway components and the expansion of *Tc-caudal* expression, a Wnt target, suggest that the effects of *Tc-axin* depletion are mediated through this pathway and that canonical Wnt activity must be repressed for proper anterior development in *Tribolium*. These studies provide unique evidence that canonical Wnt activity must be carefully regulated along the AP axis in an arthropod, and support an ancestral role for Wnt signaling in defining AP polarity and patterning in metazoan development.

Additionally, as an anterior structure, the extraembryonic serosa is reduced in *Tc-axin* RNAi progeny. However, in *Tc-pangolin* (*Tc-pan*, a homolog of Wnt downstream component) RNAi progeny, an interesting phenotype was produced that serosa was not only

reduced but also separated into distinct anterior and dorsal domains. I carefully recorded this phenomenon with live imaging using a *Tribolium* transgenic line that expresses GFP in each nucleus. Through careful examination with embryonic fate-map markers, I found that the tissue between separated serosa domains is dorsally extended head lobe. And I also found that in severe phenotype, dorsal serosa was completely gone while anterior serosa not, suggesting independent regulation mechanisms for anterior and dorsal serosa formation. This descriptive data will complement future study in the genetic mechanism underlying serosa formation by providing more details in morphogenesis.

CONTRIBUTION OF THE CANONICAL WNT PATHWAY IN *TRIBOLIUM* ANTERIOR-POSTERIOR AXIS PATTERNING

by

JINPING FU

B.S., Zhejiang University, China, 2004

A DISSERTATION

submitted in partial fulfillment of the
requirements for the degree

DOCTOR OF PHILOSOPHY

Division of Biology
College of Arts and Sciences

KANSAS STATE UNIVERSITY
Manhattan, Kansas

2014

Approved by:

Major Professor
Dr. Susan J. Brown

Copyright

Abstract

How animals polarize and establish the main axis during embryogenesis has been one of the most attractive questions in Biology. Increasing body of work in various model organisms implicates that most metazoans utilize the canonical Wnt signaling pathway to pattern the anterior-posterior (AP) axis, despite the limited evidence from arthropods. In *Drosophila*, a highly derived insect, canonical Wnt activity is not required for global AP patterning, but in typical insects including *Tribolium castaneum*, loss of canonical Wnt activity results in posterior truncation. To determine the effects of increased canonical Wnt levels, I analyzed the function of *axin*, encoding a highly conserved negative regulator of the pathway. *Tc-axin* transcripts are maternally localized to the anterior pole in freshly laid eggs. Parental RNAi for *Tc-axin* produced progeny phenotypes that ranged from mildly affected embryos with cuticles displaying a graded loss of anterior structures, to severely affected embryos lacking cuticles and condensing to the posterior pole of the egg without any definable structures. Altered expression patterns of several blastodermal markers indicated anterior expansion of posterior fates. Epistasis analysis of other canonical Wnt pathway components and the expansion of *Tc-caudal* expression, a Wnt target, suggest that the effects of *Tc-axin* depletion are mediated through this pathway and that canonical Wnt activity must be repressed for proper anterior development in *Tribolium*. These studies provide unique evidence that canonical Wnt activity must be carefully regulated along the AP axis in an arthropod, and support an ancestral role for Wnt signaling in defining AP polarity and patterning in metazoan development.

Additionally, as an anterior structure, the extraembryonic serosa is reduced in *Tc-axin* RNAi progeny. However, in *Tc-pangolin* (*Tc-pan*, a homolog of Wnt downstream component) RNAi progeny, an interesting phenotype was produced that serosa was not only

reduced but also separated into distinct anterior and dorsal domains. I carefully recorded this phenomenon with live imaging using a *Tribolium* transgenic line that expresses GFP in each nucleus. Through careful examination with embryonic fate-map markers, I found that the tissue between separated serosa domains is dorsally extended head lobe. And I also found that in severe phenotype, dorsal serosa was completely gone while anterior serosa not, suggesting independent regulation mechanisms for anterior and dorsal serosa formation. This descriptive data will complement future study in the genetic mechanism underlying serosa formation by providing more details in morphogenesis.

Table of Contents

List of Figures

List of Tables

Acknowledgments

I owe my appreciations to all those individuals who have made this dissertation possible.

First of all, I want to express my gratitude to my advisor, Dr. Susan J. Brown, for her continuous support, great academic guidance and patience during my Ph.D. study. Her passion in both science and life will influence me in following many years.

I would like to thank Dr. Sunghun Park for serving on the committee as my outside chair and carefully reading my thesis. I thank all my committee members Dr. Kristin Michel, Dr. Michael A. Herman and Dr. Anna Zolkiewska for always being there to provide help and advice during those years.

Next I would like to give my appreciations to former and current members in Brown lab for their love and help. In particular, I want to thank Dr. Renata Bolognesi, Dr. Teresa Shippy, Dr. Yoshinori Tomoyasu, Dr. Sherry Miller, Dr. Ezzat El-Sherif, Xin Zhu and Nanyan Lu for their helpful academic discussions. I want to thank our many former and current technicians, especially Michelle Gordon Coleman and Barb Van Slyke, for enormous technical support.

Then I want to acknowledge my collaborations with Dr. Gregor Bucher, Dr. Nico Posnien, Georg Oberhofer and Peter Kitzmann from Bucher lab in Germany, Dr. Renata Bolognesi from Monsanto company, Tamara D. Fischera, Parker Rayla, Dr. Ezzat El-Sherif, and Xin Zhu from Brown lab. Without them, my research could not go this further.

I thank the Division of Biology for providing the financial support, the teaching experience and the friendly research environment. I thank all the former and current graduate students in the Division of Biology for sharing research and life experience during my Ph.D. years. I thank all my friends in Kansas State University for their friendship.

Finally I want to express my gratitude to the ones who have been so important in my life. I thank my parents Guoxiang Fu and Fengxian Lao, my little sister Jiaping Fu for

their endless love and support. I thank Dr. Cheng Jin for being a wonderful husband with continuous patience, love and encouragement. Without him, I could not go through all those difficulties. His love keeps my life in proper perspective and balance.

Chapter 1

Introduction

1.1 The canonical Wnt signaling pathway

The canonical Wnt signaling pathway is a fundamental regulator that can be found in all extant taxa of metazoans [1] and plays essential roles in various developmental processes. Recent comparative analyses suggest that canonical Wnt signal is an ancient anterior-posterior (AP) axis patterning mechanism in most metazoans [2–5].

As one of the three characterized Wnt signaling pathways, the canonical Wnt pathway is the only one that involves a transcription factor named β-catenin. As shown in Fig. 1.1, when Wnt signal is off, β-catenin is degraded in the cytosol by a destruction complex composed of Axin, GSK3β/Shaggy and APC. Without β-catenin, downstream target genes are not transcribed in the nucleus. When Wnt signal is on, the Wnt ligand binds to the receptor and initiates the degradation of the destruction complex. This allows rescued β-catenin to accumulate and translocate to the nucleus and subsequently activate downstream target genes alongside other transcription factors including TCF/LEF/Pan and BCL9/Lgs.

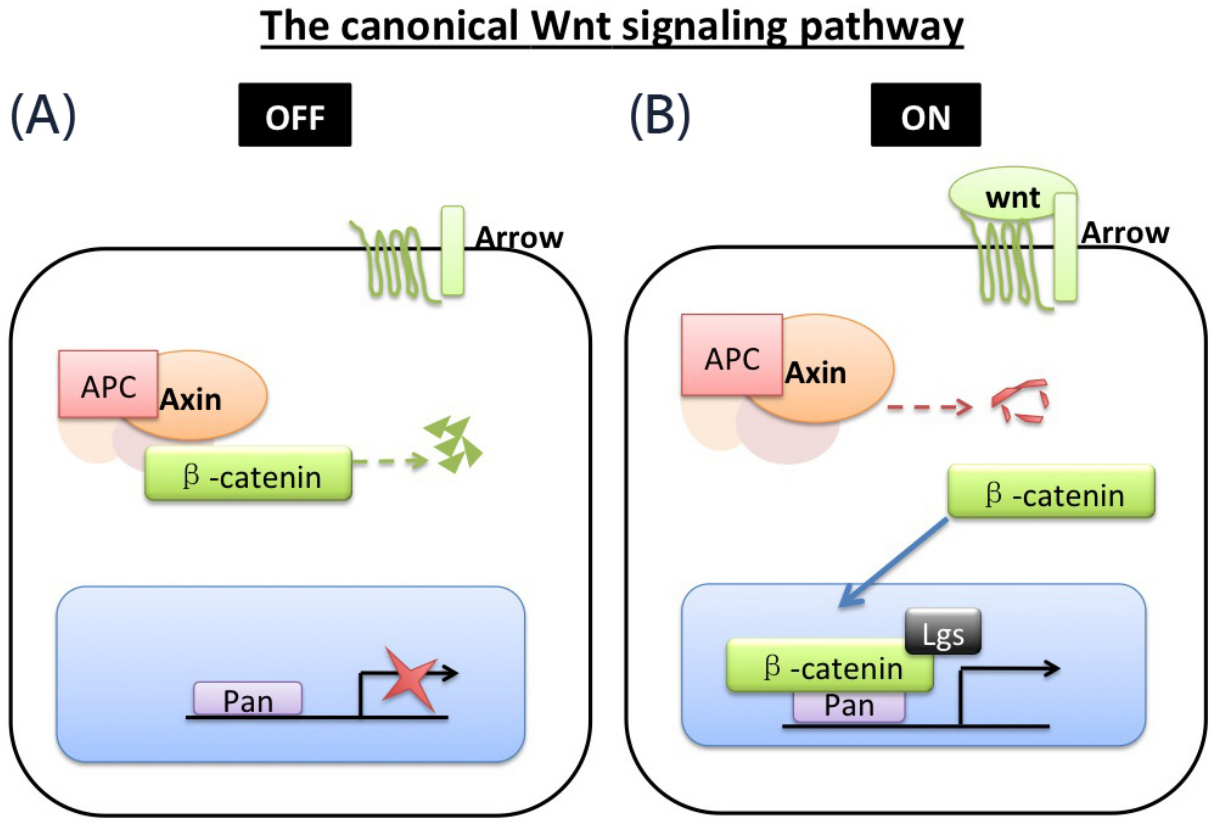

Figure 1.1: *The canonical Wnt signaling pathway. (A) Wnt signal is off, β-catenin is degraded in the cytosol by the destruction complex composed of Axin, GSK3β/Shaggy and APC. Without β-catenin, downstream target genes are not transcribed in the nucleus. (B) Wnt signal is on, the Wnt ligand binds to the receptor and initiates the degradation of the destruction complex. This allows rescued β-catenin to accumulate and transfer to the nucleus and subsequently activate target genes alongside other transcription factors including TCF/LEF/Pan and BCL9/Lgs.*

1.2 Anterior-posterior (AP) axis patterning

How animals break the symmetry and establish the anterior-posterior(AP) polarity during early embryogenesis is one of the most fascinating mysteries in nature. Molecular methods and resources, including RNA interference (RNAi), genome sequencing, and expression profiling, allow the search for mechanisms underlying axis patterning in an unprecedented range of representatives of many phyla across the animal kingdom. This enables a comparative approach that could allow the identification of common principles underlying axis

formation. Observations in most metazoans reveal the effects of the canonical Wnt signal on establishment of the AP axis polarity [2].

In the following, I will briefly review comparative studies in varisou model organisms from Deuterostomia, Ecodysozoans and Lophotrochozoa, all of which compose most of the Bilateria (Fig. 1.2).

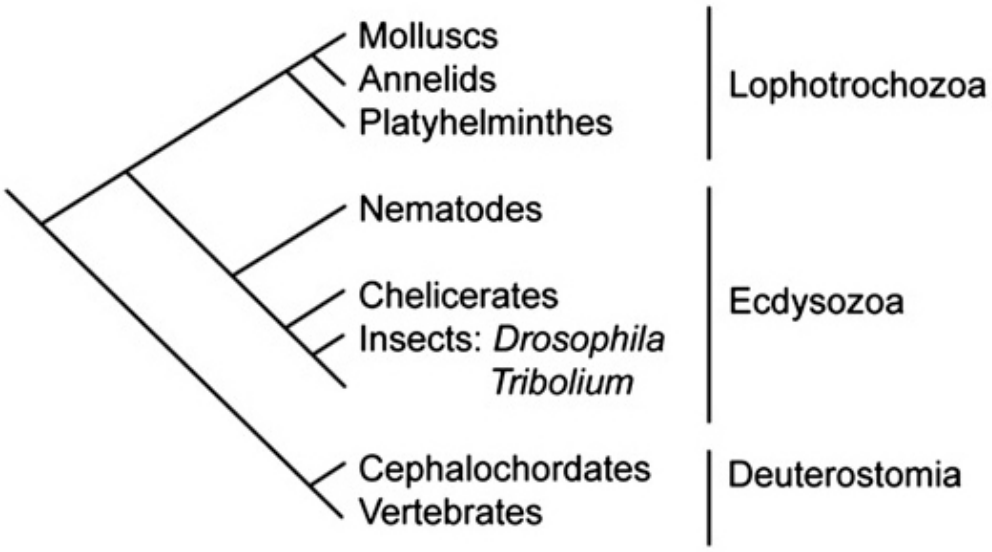

Figure 1.2: *Phylogenetic tree for Bilateria*

1.3 The canonical Wnt pathway and AP axis patterning in Deuterostomia

In vertebrates, canonical Wnt activity has an early role in establishing the AP axis [6]. In both mouse and zebrafish, active Wnt signal in posterior and Wnt repression in anterior are essentail for proper development. In other vertebrates, including frog and chicken [7], several Wnt ligands are expressed in the posterior growth zone suggesting that most likely this mechanism is utilized for axis patterning by all vertebrates.

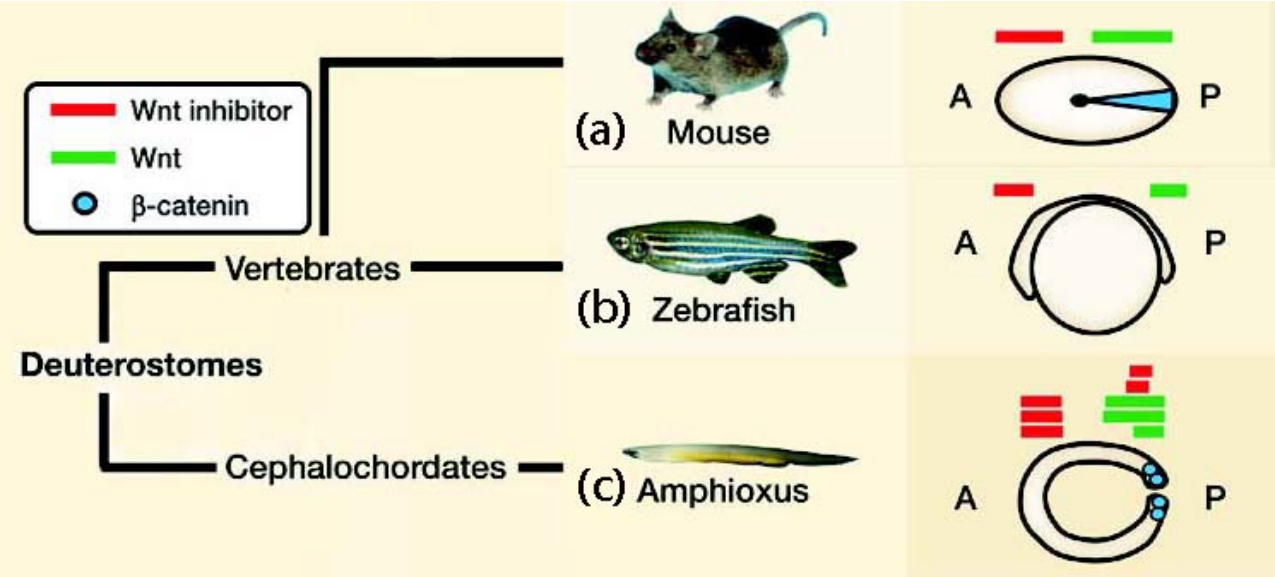

Figure 1.3: *Posterior Wnt signal and anterior Wnt repression in the Deuterostomia. Nuclear β-catenin proteins (blue) and Wnt gene expression domains (green) tend to be posteriorly localized, while Wnt inhibitor gene expression domains (red) tend to be anteriorly localized. (a) Mouse early gastrulation stage. β-catenin proteins (blue triangle) and Wnt3 expression domain are at the prospective primitive streak, whereas Dkk1, a Wnt inhibitor, is expressed in the anterior visceral endoderm [8–10]. (b) Zebrafish tailbud stage. Wnt8 and Wnt3a expression domains are restricted at the posterior pole and sFRP3/frzb, a Wnt inhibitor, is anteriorly expressed [11–14]. (c) Amphioxus late gastrula stage: Wnt3a and Wnt8 expression domains are at posterior region, while Dkk3, Dkk1/2/4,sFRP3/4 and sFRP2-like expression domains are at anterior region [15]. This figure is modified from Ref.[2]*

Mouse

During early gastrulation stage, the Wnt inhibitor Dkk1 is localized at the anterior visceral endoderm [8]. Contrarily, expression domains for Wnt3 and TCF-responsive promoter, together with abundanct β-catenin proteins, are detected at the site of primitive streak formation in the posterior region of the embryo [9, 10]. Knockout of Wnt3 and β-catenin produced severely truncated embryos which formed only the head and anterior trunk [9, 16, 17]. Wnt inhibitor Dkk1 knockout mice lost anterior structures [18]. Further experiments indicated that ectopic Wnt activity caused anterior loss and expansion or bifurcations of the primitive streak, producing partial axial structure duplications [19–22].

Zebrafish

In zebrafish, Wnts including Wnt8 and Wnt3a are posteriorly expressed in early gastrula, tailbud, and somite stages and a Wnt inhibitor sFRP3/frzb is expressed in the anterior neurectoderm from the tailbud stage [7, 12–14]. Ectopic Wnt activity in the zebrafish headless mutant lacking Tcf3 function, resulted in anterior loss — an absence of eyes, forebrain, and midbrain [23]. Contrarily, deletion of Wnt genes after morpholinos treatment caused posterior defects, including head enlargement, failure to form posterior mesoderm and maintain the growing tail bud [7, 12, 13, 24, 25].

Amphioxus

Cephalochordates (amphioxus) are basal chordates. The study of AP patterning in amphioxus can help determine whether the axial roles of canonical Wnt signal as seen in vertebrates, are the result of conservation from the common ancestor or are independently derived. In this species, the blastopore, locating at the vegetal pole, represents the prospective posterior end of the embryo. Expression domains for several Wnts and nuclear β-catenin proteins are localized posteriorly around the blastopore (Fig. 1.3 c) [15, 26]. In contrast, Wnt antagonists expression domains are found at the anterior pole [15]. Ectopic Wnt activity after lithium chloride treatment in amphioxus resulted in anterior loss and posteriorization [26, 27].

1.4 The canonical Wnt pathway and AP axis patterning in Ecdysozoans

Nematodes

Different from many other organisms, development in the nematode *Caenorhabditis elegans* (*C.elegans*) happens via highly reproducible cell lineages rather than establishment

of tissue domains. Despite of this feature during embryogenesis, posteriorly expressed Wnt genes control the AP polarity throughout *C. elegans* embryonic development. During most embryonic AP asymmetric cell divisions, two β-catenins, WRM-1 and SYS-1, are localized in the posterior daughter cell [28–30] (Fig. 1.4 a). Loss of Wnt signal made the cell with prospective posterior fate adopt anterior fate [31, 32]. Contrarily, loss of function of the *pop-1/Tcf* repressor caused the anterior cell to adopt the posterior fate [33].

Arthropods

Embryonic axis formation is one of the most well studied phenomena in *Drosophila melanogaster*, where canonical Wnt signal is not required for the global AP formation. However, the long germ mode of embryogenesis employed in *Drosophila*, where axis establishment occurs in a syncytial environment, is highly derived and not typical of most arthropods [34]. In this case, in order to search for general mechanisms for typical arthropods, people transfered attention to short germ-band embryogenesis which is the ancestral mode within the arthropod phylum. In short germ mode, the embryonic anlage is much small compared to the egg, only the anterior segments including head and thorax are formed before gastrulation stage, and the posterior segments are added sequentially in a cellular environment from a posterior region named the growth zone.

Recent studies provide exciting conclusion that active canonical Wnt, like in vertebrates, is required for posterior development in arthropods. *Tribolium* Wnt genes (WntA, Wnt1, and Wnt8) are expressed at the posterior pole in the early blastoderm stage [35] (Fig. 1.4). In addition, Wnt genes are expressed in the posterior growth zone in *Gryllus* [36], *Tribolium* [35], and *Achaearanea* [37] (Fig. 1.4). Knockdown of β-catenin in *Gryllus*, Wnt8 in *Tribolium*, or Wnt8 in *Achaearanea*, resulted in posterior truncation [36–38]. Therefore, canonical Wnt signal can control posterior patterning in arthropods. However before my study, described in Chapter 2, there was no evidence from any arthropod about requirement of Wnt repression for anterior development.

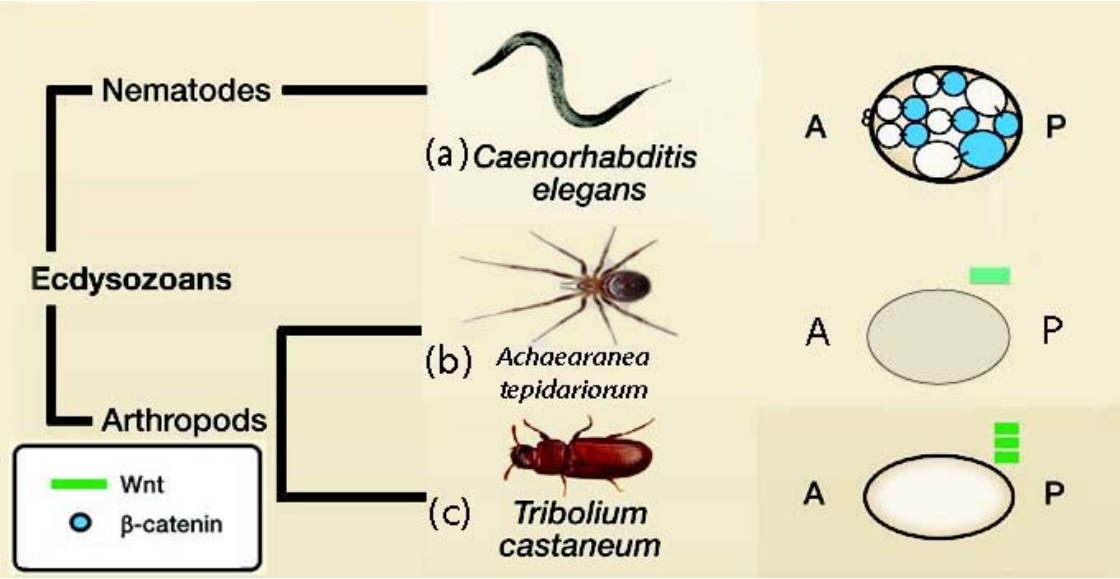

Figure 1.4: *Posterior Wnt signal in the Ecdysozoans. (a) C. elegan cleavage stage. WRM-1/-catenin and SYS- 1/-catenin are asymmetrically localized in the posterior daughter of each axial cell division [28–32]. (b) Achaearanea germband stage. At-Wnt8 expression domain is at the posterior region of the germband, in the ectoderm of the growth zone. (c) Tribolium blastoderm stage. WntA, Wnt1, and Wnt8 are posteriorly expressed [35]. This figure is modified from Ref.[2]*

1.5 The canonical Wnt pathway and AP axis patterning in Lophotrochozoa

Platyhelminthes

As member of the Lophotrochozoa, planarians are freshwater flatworms and are famous for their ability to regenerate a head or a tail or both after transection [39]. Three planarian Wnts are posteriorly expressed, whereas a Wnt inhibitor-like gene is expressed at the anterior pole [40] (Fig. 1.5 a). Depletion of β-catenin transcripts with RNAi in the planarian *Schmidtea mediterranea* produced a two-head phenotype after regeneration, suggesting that planarian canonical Wnt signal is required for tail formation at posterior-facing wounds [41–43]. Contrarily, ectopic Wnt activity after APC-like gene RNAi produced a two-tail phenotype after regeneration [41], suggesting that Wnt signal has to be repressed for proper

head formation at anterior-facing wounds. Together, data above suggests posterior Wnt signal and anterior Wnt repression are required for proper establishment of AP polarity during planarian regeneration.

Annelids

Similar to the case in *C.elegans*, canonical Wnt signal is also required for the axial asymmetric cell divisions in the annelid *Platynereis dumerilii*. β-catenin is asymmetrically localized in the vegetal daughter cell of each early division [44] (Fig. 1.5 b). Overactivation of β-catenin made animal daughter cells adopt vegetal fates after axial cell divisions, indicating that canonical Wnt activity promotes vegetal fates during axial asymmetric cell divisions. Considering the animal pole is aligned with head formation and head-like cells are formed in the animal pole of *Platynereis* larvae [44], the role of the canonical Wnt activity in animal-vegetal cell division polarity might be similar to its role in anterior-posterior cell division polarity in *C.elegans*.

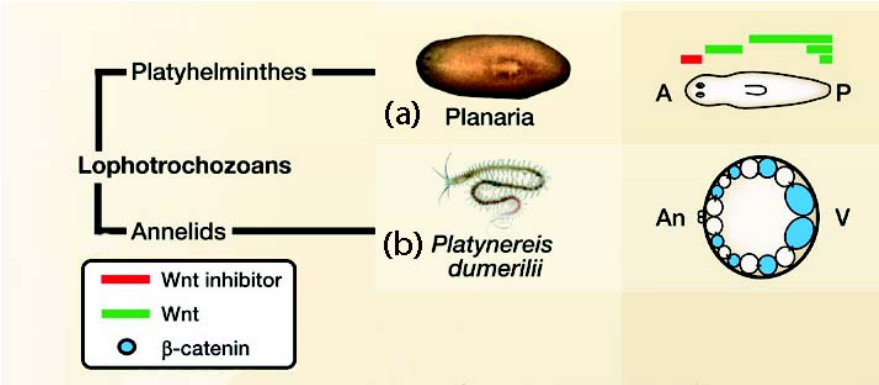

Figure 1.5: *Posterior Wnt signal and anterior Wnt repression in Lophotrochozoa. (a) In planarian, Smed-wntP-1, Smed-wntP-2, Smed-wnt11-1 are expressed at the posterior pole, Smed-wnt2-1 is expressed in the pre-pharyngeal region, whereas Smed-sFRP-1 is restricted at anterior pole [43]. (b) Platynereis dumerilii cleavage stage. β-catenin is localized to the vegetal cell during each axial division [44]. This figure is modified from Ref.[2]*

1.6 *Tribolium castaneum* as a model organism

The red flour beetle, *Tribolium castaneum*, has been selected as a model organism for several reasons. Compared with *Drosophila*, a highly derived long-germ insect in which all segments are formed simultaneously

1.7 Asymmetric distribution of *Tc-axin* transcripts in early stages of *Tribolium* embryogenesis

As described in the subsection 1.4, posterior Wnt activity is required for *Tribolium* posterior formation. However, limited evidence was found either in *Tribolium* or any other arthropod that anterior Wnt repression is required for anterior formation, like the case in Deuterostomia.

In situ hybridization revealed *Tc-axin* transcripts initially localized at the anterior pole of freshly laid eggs containing only the pronuclei [45] (Fig. 1.6 A and A′). During cleavage stages the *Tc-axin* expression domain extended more posteriorly [45] (Fig. 1.6 B, B′, C and C′). At the differentiated blastoderm stage, *Tc-axin* was expressed ubiquitously, at somewhat higher levels in the embryo (posterior) than in the serosa (anterior) [45] (Fig. 1.6 D and D′). This anterior localization of negative Wnt regulator is strongly reminiscent of the expression patterns of *dkk* in mouse and *axin* in zebrafish. One exciting hypothesis that anterior Wnt repression might be required for *Tribolium* anterior patterning initiates my study in Chapter 2.

1.8 Thesis outline

In my thesis, there are four chapters and one appendix in total. Chapter 1, as above, provides a brief review about AP patterning role of the canonical Wnt signaling pathway

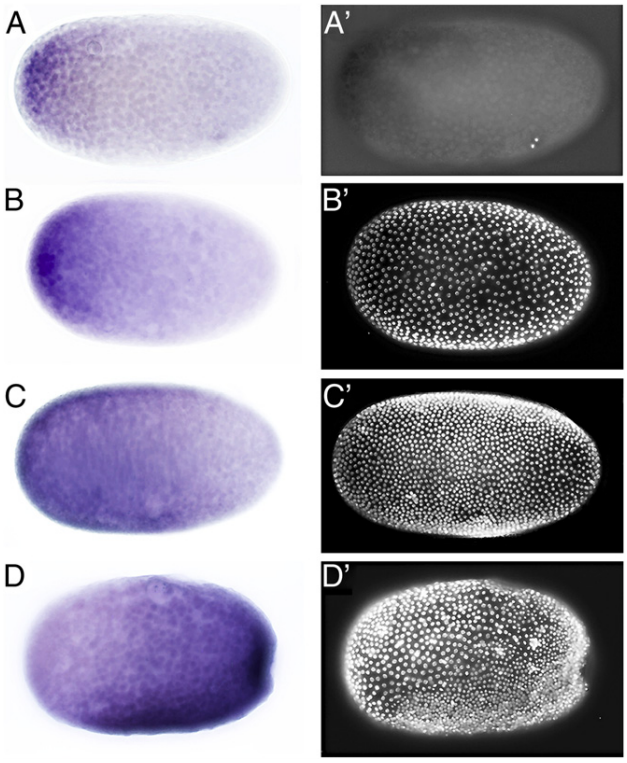

Figure 1.6: *Expression of Tc-axin in wildtype embryos. Embryos are oriented with anterior to the left. For the same embryos, both brightfield images (A-D) and DAPI (stained nuclei) staining images (A′-D′) are provided. Maternal Tc-axin transcripts were localized at the anterior pole in freshly laid eggs (A and A′). During cleavage and early blastoderm stages, the expression domain expanded posteriorly (B, B′, C and C′) until Tc-axin was expressed ubiquitously in the embryo in subsequent stages (D and D′). This figure is cited from Ref. [45]*

in various animal models. Chapter 2 talks about *Tc-axin* RNAi in *Tribolium*. Anterior loss phenotype, together with anterior expansion of posterior fate, is the first evidence in arthropod that canonical Wnt signal has to be repressed for proper anterior formation. Chapter 3 continues the analysis of anterior loss phenotype after Wnt component RNAi by focusing on serosa tissue. Using live imaging technique, some descriptive data comparing the early serosa formation in wildtype and *Tc-pangolin* RNAi mutant will be provided. This morphogenesis information will complement future study on genetic mechanisms underlying the serosa formation. Chapter 4 is a brief summary. Finally in the Appendix A, I will show a survey for the contribution of PCP and JNK pathways in *Tribolium* embryogenesis.

Chapter 2

Asymmetrically expressed *Tc-axin* is required for anterior development in *Tribolium*

2.1 Introduction

There is a huge diversity among Bilateria. They have different features, different morphologies and different habitats. However, almost all of them have to solve one essential problem during their early embryogenesis — The fertilized egg needs to establish two primary axes, anterior-posterior (AP) axis and dorsal-ventral (DV) axis. In the case of AP axis, for proper anterior patterning, some factor or factors should be localized in the anterior pole of the embryo.

In mouse, which is a model organism of the vertebrates, a secreted antagonist named Dkk is restricted at the anterior pole in early embryogenesis [46]. Dkk is a negative regulator of the canonical Wnt signaling pathway in mouse. The anterior localization of Dkk represses anterior Wnt signal. Once this repression is removed in the Dkk knockout mouse, head was lost in progeny. The requirement of repression in canonical Wnt activity for proper anterior

development is also confirmed by the study in zebrafish in which mutation in Axin, a negative regulator of the pathway, led to reduced head and eyes [47]. However, in *Drosophila*, an invertebrate model organism, the canonical Wnt signaling pathway is not involved in the global AP axis development [48]. Ectopic activation of Wnt targets by loss of *axin* function resulted in segmental defects [49] but did not result in posteriorization or loss of anterior fate. Instead, a maternal transcription factor named Bicoid forms a gradient, high in anterior and low in posterior. Different concentrations of Bicoid activate different groups of target genes, called gap genes which would further activate various downstream targets genes, specifying body segments with different identities along the AP axis [50, 51]. Manipulations of Bicoid levels affected anterior fate in progeny, with lower level causing either anteriorly shift or as severe as anterior loss, and with higher level causing posteriorly expansion in which head tissue became abnormally large [50, 51].

However, as a long-germ insect, *Drosophila* is highly derived and turns out not a typical insect. In *Tribolium* and other short-germ arthropods, where segments are added sequentially during embryogenesis, posterior Wnt activities are required for posterior patterning including germband elongation and formation of abdominal segments [37, 38, 52]. Segments that form in the *Tribolium* blastoderm develop normally, indicating canonical Wnt activity is not necessary for anterior formation. However, it is not clear whether canonical Wnt signal is simply not relevant to anterior patterning, or has to be carefully regulated. Previous colleagues in the Brown lab studied *Tribolium* by searching for maternal factors localizing at the anterior pole during early embryogenesis. Interestingly, *Tc-axin* is one of them that were found [45] (Fig. 1.6). The molecular functions of the canonical Wnt pathway components are highly conserved between *Tribolium* and vertebrates [53]. Is it possible that arthropods regulate the anterior patterning by repressing the canonical Wnt signaling, just like the case in vertebrates? To test this question, I repressed the function of *Tc-axin* with RNAi technique in *Tribolium*. I will show that *Tc-axin* RNAi caused anterior loss in progeny and shifted the blastoderm fate map anteriorly. This study, for the first time, demonstrates that

in arthropods, the canonical Wnt signaling pathway is required to be repressed for proper anterior development. The function of canonical Wnt signal in AP axis is highly conserved among vertebrates and arthropods.

2.2 Materials and Methods

2.2.1 Strain and Maintenance

Tribolium castaneum GA-1 strain was used for gene expression and functional analysis. The beetles were cultured at 30 °C in whole-wheat flour supplemented with 5 % dried yeast.

2.2.2 Gene cloning

Tribolium total RNA was extracted from GA-1 pupae with the RNeasy Protect Mini Kit (Qiagen, Valencia, CA, USA). cDNA was synthesized with the SuperScript III kit (Invitrogen, Carlsbad, CA, USA). *Tribolium* homologs of the proteins were identified using reciprocal BLAST analysis of *Drosophila* homologs. Primers were designed with the Primer3Plus (http://www.bioinformatics.nl/cgi-bin/primer3plus/primer3plus.cgi/). PCR amplified fragments were cloned into pCR4-TOPO with the TOPO TA Cloning Kit (Invitrogen).

2.2.3 Primers used to clone fragments of *Tribolium* genes

Tc-axin specific primers designed previously (forward: TCGCCCGTAATAAAGTAAACA; reverse: TCTTTGAACTGGCGTAGGGTAA) were used to amplify an approximately 1 kb fragment, which was cloned into TOPO (Invitrogen). A 588 bp fragment of *Tc-legless* was amplified from cDNA (forward primer: GTAAATAGCAGTAACACCGAACC; reverse: AGGACTCGGAGTAGGAAATAAGT) and cloned into TOPO. A 531 bp fragment of *Tc-basket* was amplified from cDNA (forward primer: GTGATGGAATTAATGGACGCG; re-

verse: GTCGGAGGGAAACAGCACAT) and cloned into TOPO. A 3.6 kb *Tc-shaggy* cDNA identified previously was subcloned into pCMV Sport4 (Invitrogen). All clones were sequenced to confirm their identity (*Tc-axin* = NCBI LOC655873 and HE608844, Beetlebase TC006314; *Tc-shaggy* = NCBI LOC664299, Beetlebase TC08141; *Tc-basket*= NCBI LCO 663836, Beetlebase TC006810). T7-tagged TOPO primer sequence [54] was used to amplify *Tc-axin* and *Tc-basket* templates for dsRNA production. For *Tc-shaggy*, T7-tagged primers (forward: TAATACGACTCACTATAGGGATTTGCAATGAGC; reverse TAATACGACTCACTATAGGGAGACGTTCGGTTCG) were used to amplify a 650 bp template for dsRNA production. For *Tc-pan*, T7-tagged primer sequences (forward: TAATACGACTCACTATAGGGAGATGCGAGCG; reverse: TAATACGACTCACTATAGGGAGATGGACTGG) were used to amplify a 550 bp template for dsRNA from a previously identified cDNA clone [55]. *Tc-arrow* dsRNA was produced as previously described [52].

2.2.4 RNA interference (RNAi) and *in situ* Hybridization

dsRNA was synthesized with the T7 megascript kit (Ambion) and purified with the Megaclear kit (Ambion). dsRNA was mixed with injection buffer (5 mM KCl, 0.1 mM KPO4, pH 6.8) before injection. Adult females were injected and embryos were analyzed as previously described [56] with some modification. Since the eggs layed by the injected females during the next 3 to 4 days following injection are very possibly the fertilized eggs with impermeable membrane to dsRNA during the process of injection, to guarantee all collected eggs are the ones that successfully took up dsRNA, we let the injected females rest in whole wheat flour for 4 days at 30 °C before egg collection treatment. Eggs were collected every day, either fixed immediately for *in situ* hybridization or allowed to develop at 30 °C for four days before cuticle preparation. Off-target effects were excluded by injections of two nonoverlapping dsRNA fragments (base pairs 448 - 1091 and 1,168 - 1,617 of *Tc-axin* cds, respectively), which elicited the same phenotype as the injection of the long dsRNA fragments; *In situ* hybridization was performed as previously described [57].

2.2.5 Microscopy and Imaging

Cuticles and stained embryos were viewed with a Nikon Digital Camera DXM 1200F camera on an Olympus BX50 microscope and photographed using Nikon ACT-1 Version 2.62 software. Embryos were optically sectioned and images were assembled using MONTAGE software. Brightness and contrast were adjusted using Adobe Photoshop CS2 software.

2.3 Results

2.3.1 *Tc-axin* RNAi caused anterior loss in progeny

Progeny of the injected adult females with *Tc-axin* dsRNA (50 ng/μL) failed to hatch and showed a wide range of phenotypes. Eggs collected during 4-13 days post injection (dpi) did not contain any cuticles (Fig. 2.2 A), grouped as empty eggs. After DAPI (stained nuclei in the embryo) staining in those progeny during 24-36 hours old, at which age in wildype the embryo should be well developed with all segments formed (Fig. 2.5 A_4), highly condensed embryo without any definable structures was found in the posterior pole (Fig. 2.5 A_3 and A_4). This suggests the loss of function essential to early embryogenesis. RNAi effects began to wear off with dpi increased [56]. At 13-14 dpi, though most progeny were empty eggs, some embryos secreting cuticles were recovered. Careful examination after dissection revealed that they contained varying numbers of abdominal segments, but no head or thorax (Fig. 2.1 D and E). Later at 24-25 dpi, a wider range of phenotypes were observed in addition to empty eggs and those with partial abdomen only, others contained intact abdomen and partial thorax, or intact abdomen thorax and partial head structures (Fig. 2.1 B and C). When the concentration of injected dsRNA was decreased to 10 ng/μL, the RNAi effects wore off more quickly (Fig. 2.2 B-D). Only empty eggs were observed during 4-9 dpi, but cuticles displaying the same range of phenotypes described above were recovered thereafter. Close inspection of body segments, including abdomen thorax and head, revealed a graded

sensitivity to RNAi in which the most anterior structures were most often lost (Fig. 2.1 D). Thus, the severity of the response to *Tc-axin* RNAi was both dose-dependent and graded along the AP axis.

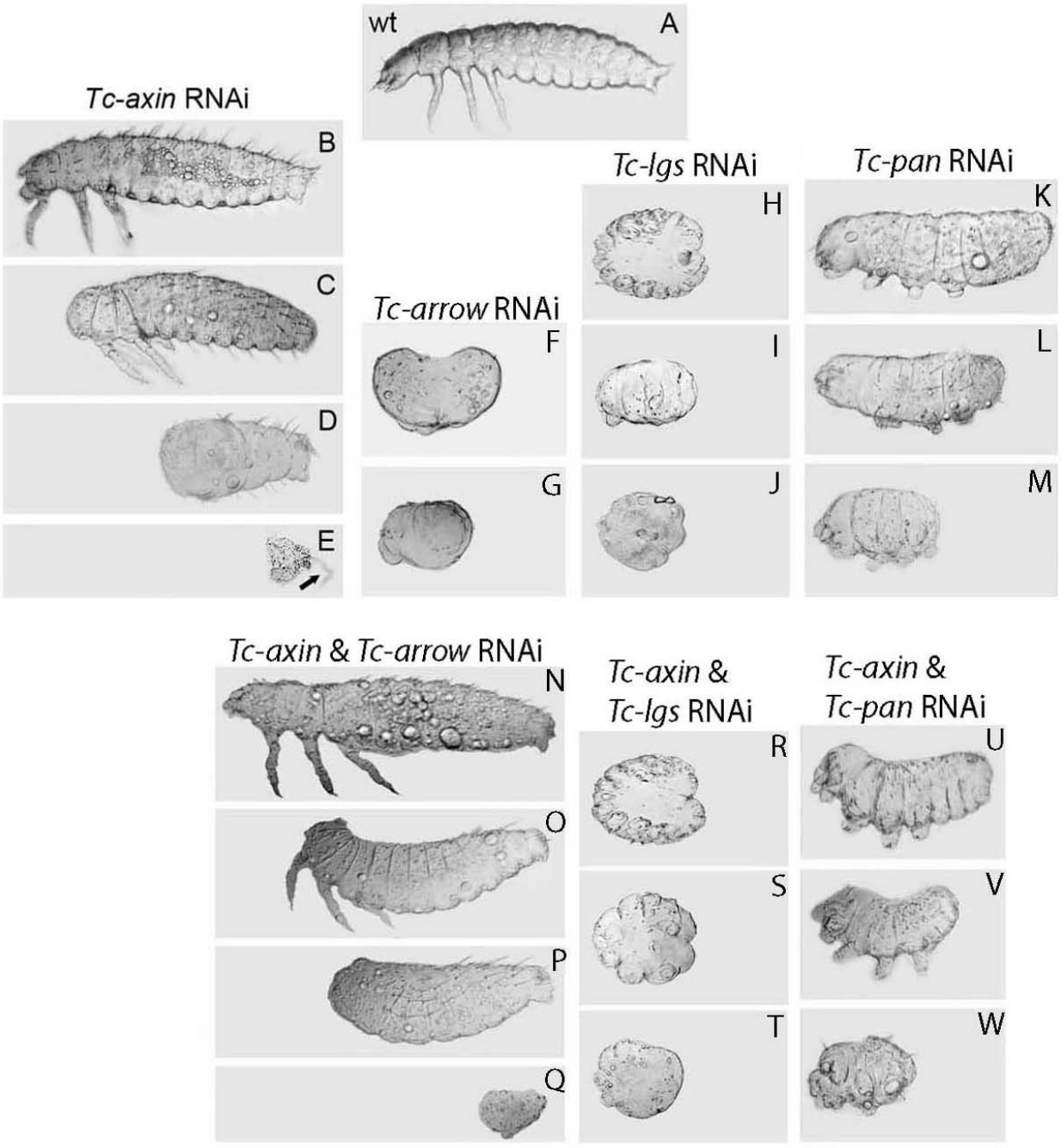

Figure 2.1: *(Caption next page.)*

Figure 2.1: *(Previous page.) Comparison of wildtype and RNAi (the Wnt components) cuticles. Embryos are oriented with anterior to the left. Except the embryos in H, J, R, S and T which are ventral view, the rest are all lateral view. After RNAi, all collected eggs failed to hatch and produced either no cuticule (empty eggs) or cuticular phenotypes as shown above. (A) Wildtype larvae contain head, thorax with three pairs of legs, and abdomen. (BE) After Tc-axin RNAi, a graded loss of anterior structures was observed in cuticles. (B) Weak phenotype with reduced anterior head structures. (C) Intermediate phenotype losing head and anterior thorax. (D) Stronger phenotype missing head, thorax, and anterior abdomen. (E) Severe cuticular phenotype in which only gut (arrow) and posterior terminus formed. (F-G) Tc-arrow RNAi produced embryos losing distal appendages in both head and thorax, with tiny and undefinable head structures and varying loss of posterior abdomen. (F) Mild phenotype missing several posterior abdominal segments. (G) Severe phenotype without whole abdomen. (H-J) After Tc-lgs RNAi, lack of distal appendages in both head and thorax, and severe truncation in abdomen were observed. (H) Mild phenotype with posterior abdomen truncation. (I) Intermediate phenotype with loss of whole abdomen. (J) Severe phenotype not only lacking whole abdomen but also forming undefinable thorax structures. (K-M) Tc-pan RNAi resulted in embryos lacking distal appendages, with small though intact head structures, and varying severities of posterior truncation. (K) Weak phenotype in lack of several posterior abdominal segments. (L) Intermediate pheontype with fewer abdominal segments. (M) Fully truncated embryo losing whole abdomen. (N-Q) Tc-axin, Tc-arrow double RNAi. A range of phenotypes, (N) Weak, (O) Intermediate, (P) Stronger and (Q) Severe, similar to Tc-axin single RNAi, indicates that Tc-axin functions epistatic to, or downstream of, Tc-arrow function. (R-T) Tc-axin, Tc-lgs double RNAi. A range of phenotypes, (R) Mild, (S) Intermediate and (T) Severe, similar to Tc-lgs single RNAi, suggests that Tc-lgs functions epistatic to, or downstream of, Tc-axin function. (U-W) Tc-axin, Tc-pan double RNAi. A range of phenotypes, (U) weak, (V) intermediate, and (W) strong, similar to Tc-pan single RNAi indicates that Tc-pan functions epistatic to, or downstream of, Tc-axin function.*

2.3.2 *Tc-axin* RNAi shifted blastoderm fate map anteriorly

To check how fate-map changed after *Tc-axin* RNAi during early embryogenesis in more details, I analyzed the expression patterns of early developmental markers including the anterior marker *Tc-zerknullt1* (*Tc-zen1*), which is expressed exclusively in serosa tissue and the posterior markers *Tc-caudal* (*Tc-cad*) and *Tc-even-skipped* (*Tc-eve*) in *Tc-axin* RNAi embryos at blastoderm stage. In wildtype, *Tc-zen1* is expressed as a dorsally titled cap in the large, widely spaced cells of the serosa (Fig. 2.3 A and A′) (see also Ref. [58]). In *Tc-axin* RNAi embryos, *Tc-zen1* expression was restricted to the anterior tip in the few

remaining serosal cells (Fig. 2.3 D and D′; compare black and red arrows in Fig. 2.3 A and D). *Tc-cad* is expressed in the posterior half of wildtype embryos (Fig. 2.3 B and B′) (see also Ref. [59]). In *Tc-axin* RNAi embryos, the *Tc-cad* expression domain was anteriorly expanded, and the anterior embryonic tissue free of *Tc-cad* expression, which is normally fated to develop into anterior head, was strongly reduced (Fig. 2.3 E and E; compare white bars in Fig. 2.3 B′ and E′). In wildtype, *Tc-eve* is expressed in the posterior half of the

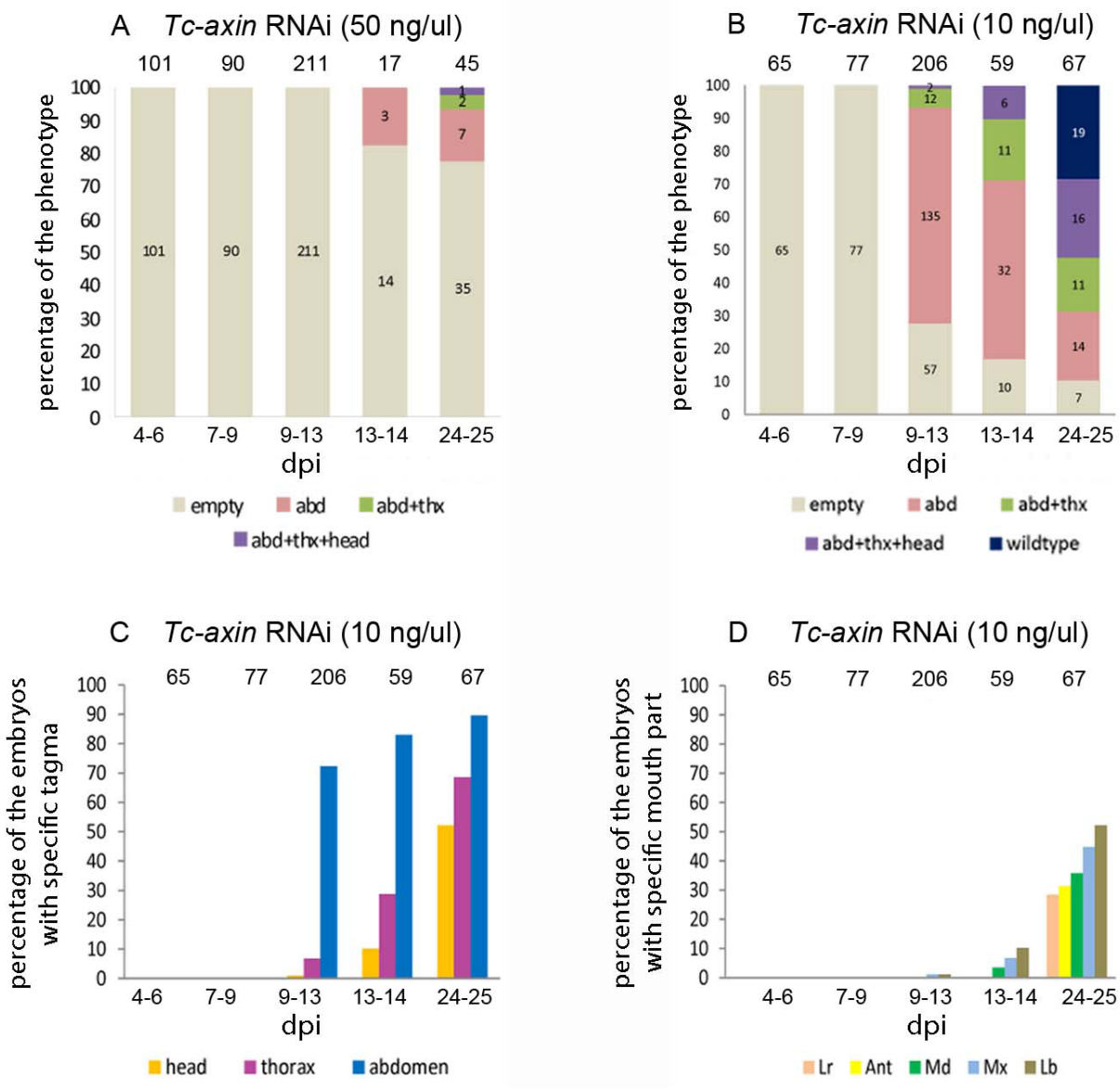

Figure 2.2: *(Caption next page.)*

Figure 2.2: *(Previous page.) Tc-axin RNAi quantitation. The RNAi effects wore off with time after parental dsRNA injection. Each column in the graph represents one collection of progeny in a range of days post injection (dpi). Total number of progeny in each collection is indicated at the top of each graph. Percentage of progeny in each class, which is indicated with specific color, is shown on the Y axis, and dpi on the X axis. (A) RNAi quantitation with Tc-axin dsRNA concentration at 50 ng/μL. The first three egg collections after injection resulted in empty eggs indicating severe phenotypes that did not produce cuticle, while the portion containing cuticles rose in subsequent collections. With dpi increased, more anterior structures survived. (B) RNAi quantitation with Tc-axin dsRNA concentration at 10 ng/μL. The first two egg collections after injection resulted in empty eggs indicating severe phenotypes that did not produce cuticle. In later dpi range, portion containing cuticles rose, similar to the case with dsRNA concentration at 50 ng/μL, though relatively milder. (C) Of those embryos showing cuticle structures, the severity of anterior loss decreased with time as judged by the presence of the main tagma (The main tagma from anterior to posterior are headthoraxabdomen). (D) In the weakest phenotypes, head was present but anterior segments were more sensitive than more posterior ones to Tc-axin RNAi (Head segments from anterior to posterior are LabrumAntennae MandiblesMaxillaeLabium). The following abbreviations were used: empty = empty eggs in cuticle preps; abd = cuticles containing varying numbers of abdominal segments only, see Fig. 2.1 D and E; abd+thx = cuticles containing intact abdomen and varying numbers of thoracic segments only, see Fig. 2.1 C; abd+thx+head = cuticles containing intact abdomen and intact thorax and some head segments, see Fig. 2.1 B; Lr = Labrum; Ant = Antennae; Md = Mandibles; Mx = Maxillae; Lb = Labium.*

embryos with the anterior edge of the first *Tc-eve* stripe in the center of the egg (Fig. 2.3 C and C′) (see also Ref. [60]). In *Tc-axin* RNAi embryos, the *Tc-eve* expression domain was shifted anteriorly (compare white arrowheads in Fig. 2.3 C and F). The anterior expansion of the expression domains for the posterior markers after *Tc-axin* RNAi is pretty consistent in all RNAi embryos throughout the early embryogenesis (quantified in Fig. 2.4). Anterior restriction of the *Tc-zen1* expression domain and anterior shifts in the expression domains of *Tc-cad* and *Tc-eve*, accompanied by the reduction of presumptive head region, indicate that in absence of *Tc-axin* function, posterior fate shifted at the expense of anterior fate.

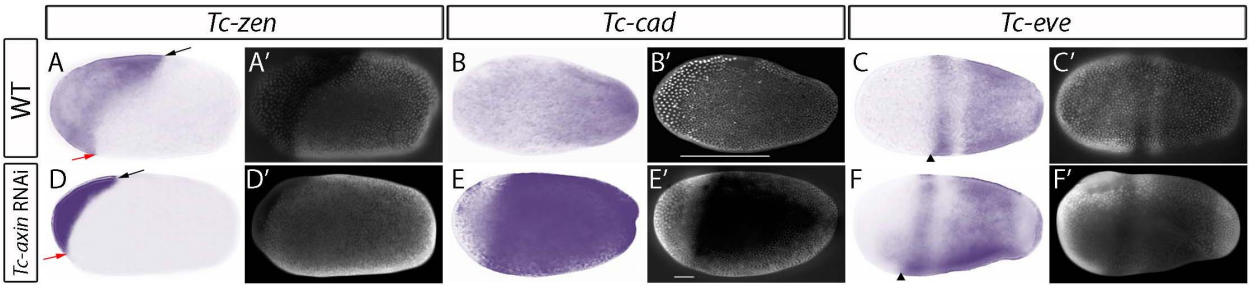

Figure 2.3: *Expression of Tc-zen, Tc-cad, and Tc-eve in wildtype and Tc-axin RNAi embryos. Embryos are oriented with anterior to the left and dorsal to the top. For the same embryos, both Brightfield images (AF) and DAPI nuclear counterstained images (A′F′) are provided. The Tc-axin RNAi images are shown immediately below their wildtype counterparts; gene is denoted at the top of the figure. (A and D) In wildtype, Tc-zen1 expression marks the serosa, which forms an asymmetric, dorsally tilted boundary with the embryonic tissue. After Tc-axin RNAi, Tc-zen1 expression was highly reduced at both ventral and dorsal borders (compare red and black arrows in A and D). (B and E) Blastodermal Tc-cad expression was expanded anteriorly after Tc-axin RNAi, leaving only few embryonic cells unstained (compare bars in B′ with E′). (C and F) The anterior expression boundary of Tc-eve (see arrowheads) was shifted toward the anterior in Tc-axin RNAi embryos (compare arrowheads in C and F).*

2.3.3 Epistasis analysis for the canonical Wnt pathway components

Tc-axin RNAi embryos developed normally during early cleavage stages (Fig. 2.5, compare C_1 and A_1), until at the differentiated blastoderm stage when serosa tissue was distinguishable from the embryonic tissue, more nuclei were allocated to the embryonic rudiment at the expense of serosal cells compared with wildtype (Fig. 2.5, compare C_2 and A_2). Later, in wildtype embryogenesis, the embryonic germ rudiment forms on the ventral side of the egg and elongates over the posterior pole as segments are added (Fig. 2.5 A_3 and A_4). In *Tc-axin* RNAi progeny, the embryonic cells contracted towards the posterior pole of the egg, and loss of the serosal membrane left most of the anterior yolk exposed (Fig. 2.5 C_3 and C_4). Similar effects were observed after *Tc-shaggy/GSK3* RNAi (Fig. 2.5 B_1 and B_4), suggesting the effects might be mediated through the canonical Wnt signaling pathway, since both *Tc-axin* and *Tc-shaggy* are homologs of the pathway components [62]. To test this

hypothesis, I did epistasis analysis for the canonical Wnt signaling pathway in *Tribolium*.

Epistasis analysis is a genetic method used to identify the group of genes controlling a particular pathway and to establish an order-of-function map that reflects the sequence of events in a pathway controlled by several genes [63, 64]. To apply the epistasis test for two components from one pathway, the loss-of-function phenotypes of two components

A. Quantitation of *Tc-cad* riboprobe staining

dosage and collection time		Type 1	Type 2	Type 3	Type 4	Type 5
50 ng/ul axin, 7-8 dpi	No cuticle formed	9	7	5	15	19
50 ng/ul axin, 9-10 dpi		18	2	2	4	31
50 ng/ul axin, 10-12 dpi		2	2	1	1	11
total number		29	11	8	20	61

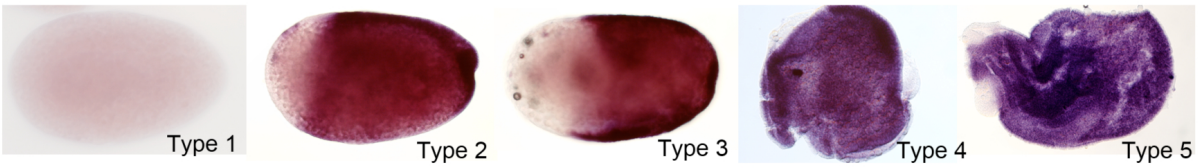

B. Quantitation of *Tc-eve* riboprobe

dosage and collection time		Type 1	Type 2	Type 3	Type4	Type 5
50 ng/ul axin, 5-7 dpi	no cuticle formed	17	5	-	3	30
50 ng/ul axin, 6-8 dpi		10	2	4	3	12
50 ng/ul axin, 10-13 dpi		70	2	5	6	84
Total number		97	9	9	12	126

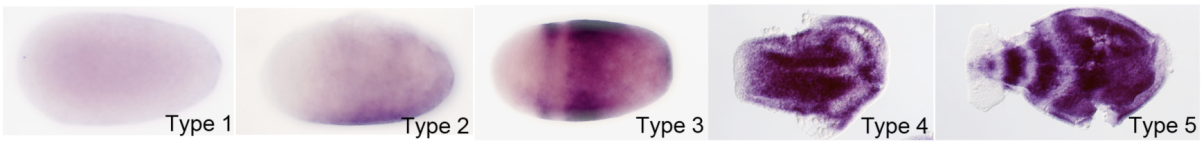

Figure 2.4: *(Caption next page.)*

Figure 2.4: *(Previous page.) Quantitation of Tc-cad and Tc-eve expression patterns in Tc-axin RNAi embryos. (A) Tc-cad expression in Tc-axin RNAi embryos. Embryos were collected over 48 hours. All embryos were stained, classified into types 1-5 and each type quantified. Type 1-3 are blastoderm stages from young to old, Types 4 and 5 are germband stages from young to old, but their exact ages were not determined. Type 1 is too young to show Tc-cad expression. In type 2 embryos the anterior boarder of the blastoderm Tc-cad expression moved anteriorly compared with wildtype (Fig. 2.3 B). In type 3 embryos the embryo was condensing toward the posterior pole. In type 4 and 5, the embryo were condensed at the posterior pole of the egg and after dissection as shown above, there was modulated Tc-cad staining throughout the embryos, it was not restricted to the posterior region as in wildtype [59]. No embryos displaying wildtype Tc-cad expression were observed. (B) Tc-eve expression in Tc-axin RNAi embryos. Embryos were collected over 48 hours. All embryos were stained, classified into types 1-5 and each type quantified. Type 1 was too young to show Tc-eve expression. In type 2 embryos the anterior boarder of the earliest Tc-eve expression was moved anteriorly, compared with wildtype [61]. In type 3 embryos the first two stripes formed in more anterior locations, compared with wildtype (Fig. 2.3 C). In type 4 embryos, Tc-eve was expressed throughout the embryo which condensed at the posterior pole and in type 5 embryos there was modulated Tc-eve expression but the stripes were not properly regulated (they did not split into two secondary stripes as the case in wildtype) and the most anterior stripe appeared at the ventral midline, in a more anterior location. Embryos displaying wildtype Tc-eve expression were not observed.*

must be different from each other. With this prerequirement, loss-of-double-component-function phenotype would be compared with loss-of-function phentype for each component. For the regulation pathway, downstream regulator masks upstream regulator [63, 64]. In other words, the loss-of-double-component-function phenotype should be same to the loss-of-function for the component that functions downstream. Based on the comparison, the order-of-function map would be determined.

The canonical Wnt signaling pathway is highly conserved among different organisms. The core component is a transcription factor named β-catenin. When Wnt signal is off (Fig. 1.1 A), β-catenin would be degraded in the cytosol by a three-member destruction complex composed of Axin, Shaggy/GSK3 and APC. Without β-catenin, downstream target genes are not transcribed in the nucleus. When Wnt signal is on (Fig. 1.1 B), the Wnt ligand binds to the receptor and initiates the degradation of the destruction complex. This allows rescued β-catenin to accumulate and translocate to the nucleus and subsequently activate

target genes alongside other transcription factors including TCF/LEF/Pan and BCL9/Lgs. *Tc-arrow* is a *Tribolium* homolog of the Wnt receptor and its inhibition after RNAi caused posterior truncation in progeny [52] (Fig. 2.1 F and G). *Tc-legless* (*Tc-lgs*) is a *Tribolium* homolog of the *BCL9* transcription factor and initiates transcription together with β-catenin when the canonical Wnt signal is on. Similar to the case of *Tc-arrow*, depletion of *Tc-lgs* transcripts after RNAi resulted in posteriorly truncated embryos, ranging from head and thorax only to head thorax and partial abdomen (Fig. 2.1 H-J). *Tc-pangolin* (*Tc-pan*), a *Tribolium* homolog of *TCL/LEF* transcription factor, represses transcription when not bound by β-catenin, but it is also required for target genes activation when β-catenin is present (Fig. 1.1). Depletion of *Tc-pan* transcripts derepresses the Wnt pathway targets but at the same time does not allow full activation of them, producing mild *Tc-lgs*-like phenotypes [65]. *Tc-pan* RNAi resulted in a range of cuticular phenotypes, including loss of distal appendages and posterior truncations ((Fig. 2.1 K-M)) that were not as severe as RNAi phenotypes of Wnt ligands [38]. Since *Tc-axin* RNAi caused loss of anterior fate, which is opposite to the effects described above for the *Tc-arrow*, *Tc-lgs* and *Tc-pan*, I did double RNAi for *Tc-axin/Tc-arrow*, *Tc-axin/Tc-lgs* and *Tc-axin/Tc-pan* to test whether *Tc-axin* functions through the canonical Wnt signaling pathway.

Tc-axin/Tc-arrow double RNAi resulted in progeny with different severities of anterior loss (Fig. 2.1 N-Q), similar to *Tc-axin* RNAi(Fig. 2.1 B-E). This indicates that *Tc-axin* functions downstream of *Tc-arrow*. *Tc-axin/Tc-lgs* double RNAi resulted in the same phenotypes (Fig. 2.1 R-T) as that in *Tc-lgs* RNAi (Fig. 2.1 H-J), suggesting *Tc-lgs* masks *Tc-axin*. Similarly, *Tc-pan* masks *Tc-axin* since *Tc-axin/Tc-pan* double RNAi caused *Tc-pan*-like effects (compare Fig. 2.1 U and K, V and L, W and M). So, both *Tc-lgs* and *Tc-pan* function downstream of *Tc-axin*, which is confirmed by similar epistasis results obtained from DAPI stainings for early embryogenesis in RNAi embryos (Fig. 2.5).

In double RNAi for *Tc-axin* and *Tc-pan*, the phenotype was same as the single RNAi for *Tc-pan*. This could be due to the epistasis relationship between *Tc-axin* and *Tc-pan* or

simply due to some technique problem that *Tc-axin* dsRNA did not work efficiently when it mixed with the dsRNA of other genes. To exclude the latter possibility, I did double RNAi for *Tc-axin* and *Tc-basket*. *Tc-basket* is one component from the JNK pathway [66]. Depletion of *Tc-basket* transcripts after RNAi produced late effects that interrupt hatch process while leave early embryogenesis as normal as wildtype. I observed *Tc-axin*-like phenotype in the double RNAi, which suggest *Tc-axin* dsRNA worked well in the mixture with dsRNA of other genes.

Based on the epistasis analysis above, most likely, *Tc-axin* mediates through the canonical Wnt pathway to regulate *Tribilium* anterior patterning.

2.4 Discussion

Analysis of genes expressed during the blastoderm stage revealed that interference with *Tc-axin* function resulted in an anterior shift of the blastodermal fate-map. The similar effects of *Tc-axin* and *Tc-shaggy* RNAi, combined with the epistatic relationships of *Tc-axin* to *Tc-arrow*, *Tc-lgs* to *Tc-axin* and *Tc-pan* to *Tc-axin* strongly implicate the canonical Wnt pathway in mediating the effects of *Tc-axin* RNAi. Furthermore, the expression domain of *Tc-cad*, a target of the canonical Wnt pathway in *Gryllus* [67] and *Tribolium* [45, 68], expanded more anteriorly in *Tc-axin* RNAi embryos, suggesting increased levels of Wnt activity there. Thus, anteriorly localized *Tc-axin* appears to be playing an important role in regulating canonical Wnt signaling. However, Wnt ligands are not expressed in freshly laid eggs; the first detectable Wnt ligands, with *in situ* staining, are found in the head lobes and at the posterior pole during the blastoderm stage, and depletion of Wnt ligands after RNAi does not affect segmentation in the blastoderm [38]. Thus, any Wnt activity in the preblastoderm embryo must be ligand-independent. The expression pattern of *Tc-axin*, maternally localized at the anterior pole, implicates a mechanism to produce graded levels of Wnt activity during early embryognesis. The early asymmetry of *Tc-axin* expression

represses Wnt activity anteriorly, resulting in a gradient with highest levels in the posterior region. Later, Wnt ligands expressed at the posterior pole maintain Wnt activity there as *Tc-axin* expression becomes ubiquitous throughout the embryo. Though Wnt activity is apparently not involved in *Drosophila* global AP patterning, a wingless domain in the posterior blastoderm has recently been reconsidered as a legacy of such a function [69].

Axin and Shaggy are components of the β-catenin destruction complex. Anterior localization of *Tc-axin* suggests higher activity of the complex at the anterior pole, which results in lower levels of β-catenin. However, there are two β-catenin homologs in *Tribolium* that function during the cleavage stages [70], obscuring the ability to test what roles, if any, they might play in regulating the blastoderm fate-map. An additional level of *Tc-cad* regulation, required for head formation in *Tribolium*, involves translational repression of *Tc-cad* activity by *Tc-mex3* in the differentiated blastoderm stage [71]. The earlier asymmetry of *Tc-axin*, combined with the more extensive phenotypes induced by *Tc-axin* RNAi, suggests that Wnt signaling functions upstream of *Tc-mex3* or that both mechanisms cooperate to modulate the anterior *Tc-cad* gradient. Importantly, neither system appears to be involved in *Drosophila* axis patterning although they are clearly conserved during evolution; the Mex3/Pal1-Cad system is also found in *Caenorhabditis elegans* [72, 73], and the posteriorizing effect of Wnt activity is known from the vertebrate neural plate and planarian regeneration [3]. Thus, in contrast to *Drosophila*, *Tribolium* has retained a more ancestral mode of anterior-posterior (AP) axis formation. In vertebrates, Wnt antagonists, such as Dkk, are expressed anteriorly to inhibit Wnt activity in the head [46]. Before my study, in insects, such antagonizing factors have yet to be found, and inhibition of Wnt activity has not been implicated in anterior development.

In contrast, *Drosophila* bicoid (bcd) transcripts are maternally localized to the anterior pole of the egg. Upon fertilization, the resulting protein gradient provides positional information in a concentration-dependent manner [74]. However, bcd appears to be restricted to Dipterans and is not found in other insects, including *Tribolium* [75]. It has been proposed

that orthologs of gap genes including orthologs of Orthodenticle (otd), a more conserved homeodomain protein with similar target specificity, provide anterior morphogen function in *Tribolium* and other short-germ insects [76, 77]. However, *Tc-orthodenticle1* (*Tc-otd1*) is ubiquitously expressed in preblastoderm stages in *Tribolium* [76] and *Tc-mex3* expression arises zygotically in the blastoderm [71], leaving in question the earliest asymmetric signal in the embryo. Data in this chapter indicate that maternal anterior localization of *Tc-axin* transcripts (similar to bicoid in *Drosophila*) is one of the first asymmetric signals in the *Tribolium* embryo. Furthermore, it is shown that inhibition of Wnt signaling is required for embryonic head development in arthropods, as it is in vertebrate embryogenesis and in planarian regeneration (summarized in Fig. 2.6), supporting the hypothesis that Wnt signaling is an integral part of an ancestral metazoan mechanism that polarizes and patterns the AP axis early in development. Finally, anterior localization of β-catenin destruction complex activity is a previously undescribed mechanism in arthropods by which to confer positional information.

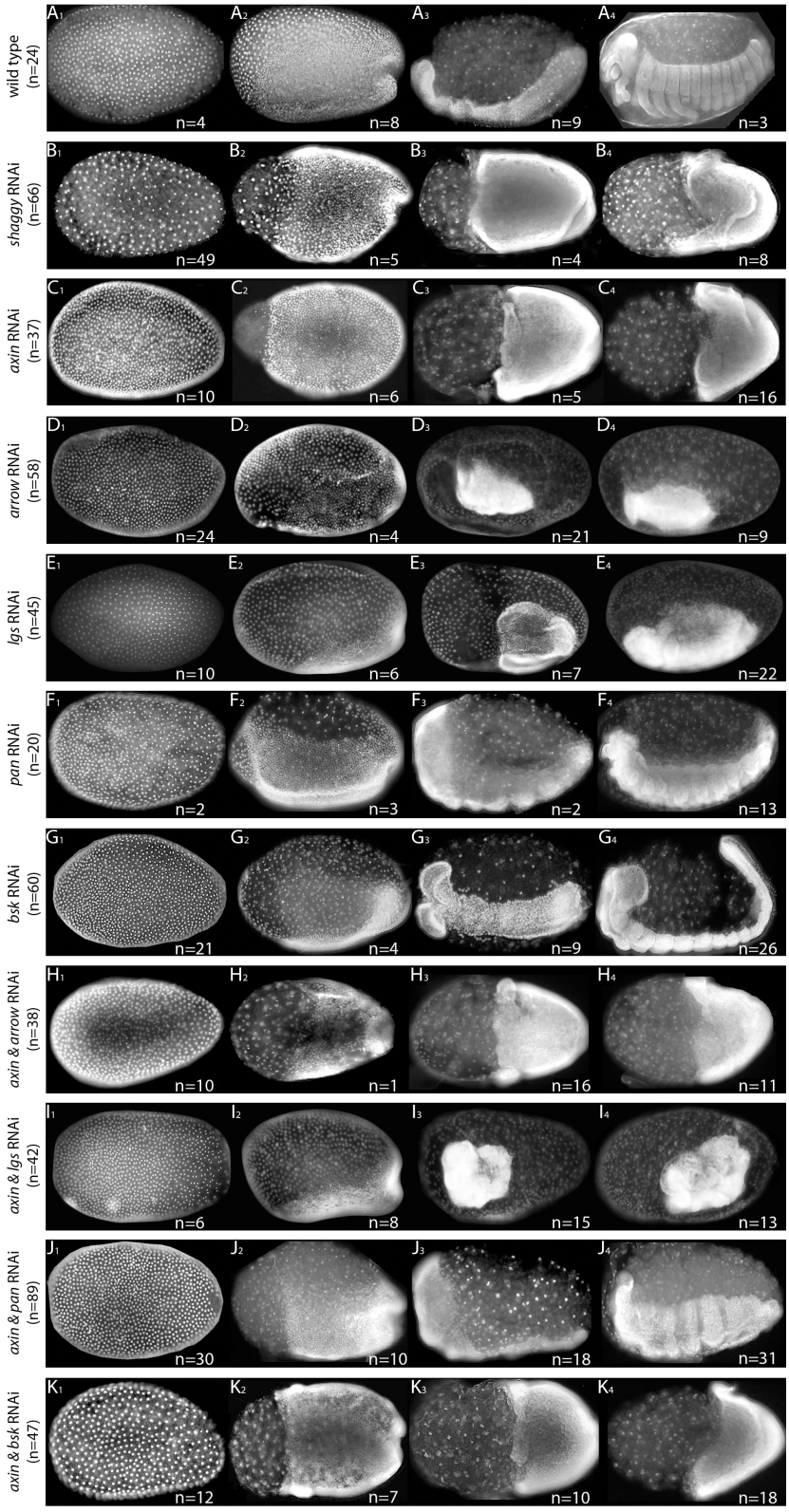

Figure 2.5: *(Caption next page.)*

Figure 2.5: *(Previous page.) Early development in wildtype and RNAi embyros. DAPI stained embryos, anterior to the left, dorsal up (if known). Early cleavage, differentiated blastoderm, early germband, and a later stage (equivalent to germband elongation in wildtype) are shown from left to right for each RNAi experiment. The total number of embryos examined and the number in each class are also shown: (A_1-A_4) wildtype; (B_1-B_4)* Tc-shaggy *RNAi embryos had early develomental defects, similar to Tc-axin RNAi embryos; (C_1-C_4)* Tc-axin *RNAi; (D_1-D_4)* Tc-arrow *RNAi embryos displayed typical Wnt$^-$ phenoptypes; (E_1-E_4)* Tc-legless *RANi embryos, similar to* Tc-arrow *RNAi embryos, displayed typical Wnt$^-$ phenoptypes; (F_1-F_4) (Tc-pangolin) RNAi embryos displayed* pangolin*-specific early developmental defects including division of serosa to distinct anterior and dorsal serosa domains by dorsally extended headlobe-like tissue, different from* Tc-axin *RNAi; (G_1-G_4)* Tc-basket *RNAi embryos (negative control) developed similarly to wildtype; (H_1-H_4)* Tc-axin/Tc-arrow *double RNAi embryos resembled* Tc-axin *RNAi embryos; (I_1-I_4)* Tc-axin/Tc-legless *double RNAi embryos resembled* Tc-legless *RNAi embryos; (J_1-J_4)* Tc-axin/Tc-pangolin *double RNAi embryos resembled* Tc-pangolin *RNAi embryos; (K_1-K_4)* Tc-axin/Tc-basket *double RNAi embryos (negative control) resembled* Tc-basket *RNAi embryos.*

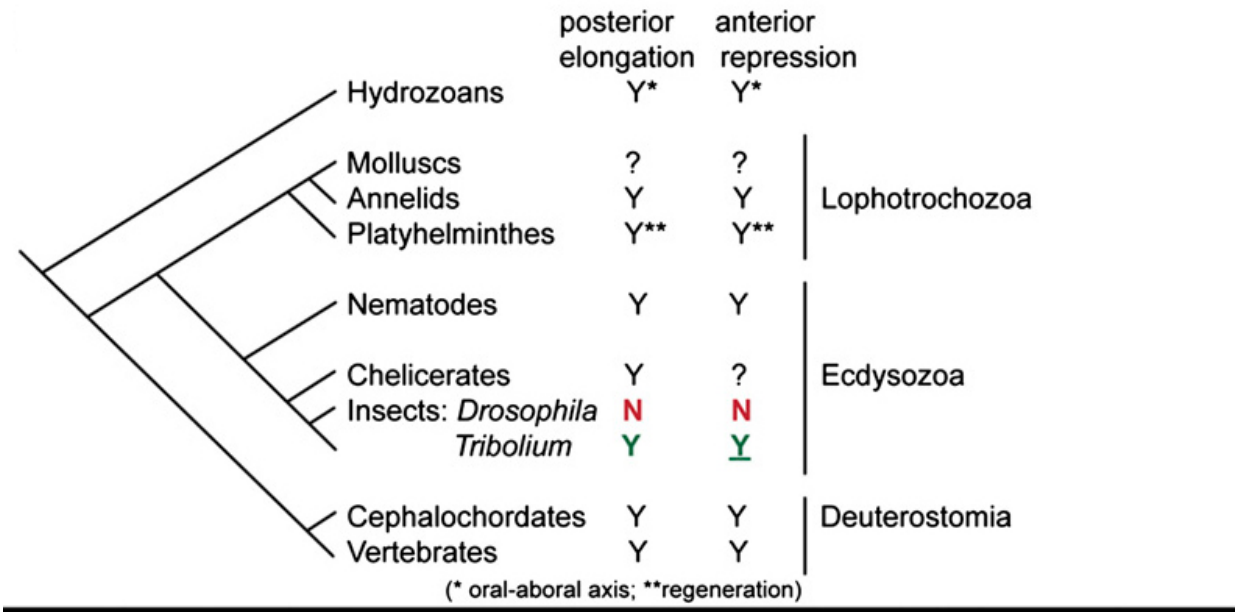

Figure 2.6: *Role of the canonical Wnt pathway in axis formation in the bilateria. Throughout Bilateria, posterior activity, and anterior repression of canonical Wnt signaling have been shown to be essential for AP axis patterning. Based on Drosophila data, insects had been regarded as an exception since Wnt activity is not required for AP axis patterning. Previous data from Tribolium, together with data in this chapter (RNAi experiments for positive regulator of the canonical Wnt pathway, including Tc-arrow, Tc-legless and Tc-pan) showed that it is required for posterior formation. Here, we show that canonical Wnt signaling has to be repressed for proper anterior patterning. Y, functional or expression data suggesting involvement of the canonical Wnt pathway; N, data not supporting involvement of the canonical Wnt pathway; ?, no data. This figure is modified from Ref. [45]. Figure information is based on Refs. [2, 4] and references therein.*

Chapter 3

Survey of the *Tc-zen* expression pattern at *Tribolium* blastoderm stage

3.1 Introduction

In most insects including *Tribolium*, an intact extraembryonic membrane, the serosa (marked as red in Fig. 4.1 A), lies just beneath the chorion (eggshell) and envelops the embryo, amnion and yolk in the egg. The presence of this membrane is one of the major characteristics that make insects extraordinarily successful in occupying earth habitats, since the serosa membrane not only provides physical protection [78–83] including desiccation resistance [83–88], but also seems to function in the innate immune system against bacteria infections [78, 89]. The amnion (marked as blue in Fig. 4.1 A), another extraembryonic membrane, is located ventrally beneath serosa membrane. However in *Drosophila*, a highly derived insect, instead of two separate extraembryonic membranes, only one, the amnioserosa, exists (see the dot line with both blue and red colors in Fig. 4.1 B). How the two extraembryonic epithelia evolved into one is unclear.

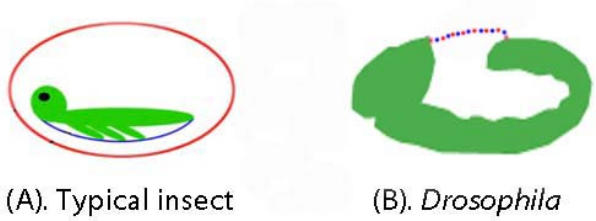

Figure 3.1: *Extraembryonic membranes in a typical insect and Drosophila. Green marks embryo, red marks serosa, blue marks amnion and dot line with both blue and red colors marks amnioserosa. (A) In a typical insect, an intact serosa membrane envelopes embryo, amnion, and yolk in the egg. Amnion, another extraembryonic membrane locates ventrally. (B) In Drosophila, a highly derived epithelium named amnioserosa locates dorsally.*

Serosa formation in *Tribolium* starts at blastoderm stage [90]. After gastrulation, during the process of germband retraction, the intact serosa membrane retracts dorsally and is finally absorbed by yolk before dorsal closure is completed. To provide a brief description, embryos at different stages are displayed in Fig. 3.2. At a very early stage, nuclei are dividing deep inside the yolk (Fig. 3.2 A). After several divisions, most of the nuclei move out and ubiquitously locate at the surface of the egg, forming the syncitial blastoderm (Fig. 3.2 B). After cellularization, the serosa-fated cells are first distinguishable in the differentiated blastoderm (Fig. 3.2 C) [90, 91], as large-nuclei are widely positioned in a dorsally tilted anterior cap. Cells fated to form the embryo are evident as smaller and more densely packed nuclei. During early gastrulation, coincident with the ventral movement of germ rudiment cells, presumptive serosa cells move ventrally and posteriorly to cover the embryo proper at the posterior pole, forming the posterior amniotic fold. Meanwhile, similar but less extensive movement occurs at the anterior edge of the embryonic head forming the anterior amniotic fold. As the posterior and anterior serosal folds move over the ventral surface of the embryo, they form a round serosal window. Finally the window closes and a continuous serosal membrane is formed [90]. The embryo, located ventrally in the egg, beneath the serosa and amnion completes germband elongation, with abdominal segments added sequentially in the posterior-to-anterior direction from the posterior growth zone (Fig. 3.2 D). This sequential formation of posterior segments during gastrulation is a typical process in the short germ-band mode, a mode utilized by other insects and most arthropods

[34, 92]. Comparatively, in *Drosophila*, which is a highly derived insect, a long germ-band mode is utilized. All segments of whole body are almost simultaneously specified in a syncitial blastoderm, based on a blastoderm fate map for the entire future body plan in approximately natural proportions [34, 92].

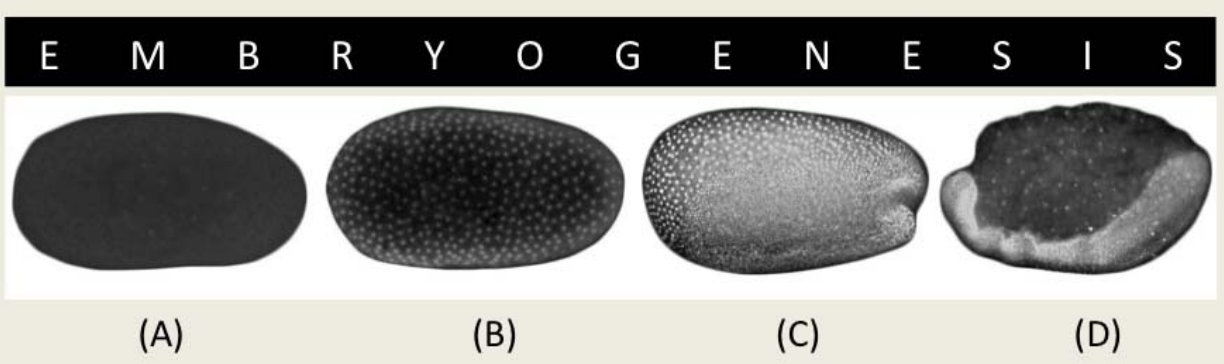

Figure 3.2: *Tribolium embryogenesis. Embryos at different stages are stained with DAPI so that each nucleus is visible at the black background. (A) Early cleavage stage. (B) Uniform blastoderm stage. (C) Differentiated blastoderm stage. (D) Germband elongation stage.*

Different from typical insects in which there are two extraembryonic membranes including serosa and amnion, in *Drosophila*, these membranes underwent an evolutionary reduction from two to one membrane that covers only the dorsal side of the egg. *Drosophila* amnioserosa membrane originates from a small portion of the dorsal blastoderm and remains dorsal throughout embryogenesis. Similar to the fate of the extraembryonic membranes in *Tribolium* and other insects, at the end of germband retraction and dorsal closure, some of the amnioserosa cells are absorbed by the yolk, while most cells invaginate before degradation, transiently forming a tube-shaped dorsal organ [93, 94].

In *Drosophila*, a hox gene named *zerknüllt* (*zen*) is expressed predominantly in the amnioserosa [95], and is required for all aspects of amnioserosa formation that have been examined to date [96, 97]. Functional studies suggest *zen* is also required for serosa formation in *Tribolium* [58]. This indicates that the function of *zen* in the formation of extraembryonic membranes is highly conserved throughout the evolution. In the absence of *Tc-zen* transcripts after RNA interference (RNAi), the presumptive serosa cells are transformed to

germ rudiment cells [58]. *Tc-zen* expression pattern in early embryogenesis during serosa formation has been examined previously [98, 99]. It was reported that *Tc-zen* transcripts appear in an anterior cap during early blastoderm stage, also called uniform blastoderm stage, before serosa cells become distinguishable. Later its expression pattern changes to a dorsally tilted anterior cap. However, it is not clear whether the change in *Tc-zen* expression pattern from anterior cap to dorsally tilted cap is due to cell movement or due to the initiation of *Tc-zen* transcription in the dorsal region. In the latter case, it would suggest in the dorsal blastoderm portion some upstream factor or factors activate *Tc-zen* transcription at some later time to shift the expression pattern. Also it is not clear whether cell division provides any contribution to this process. To address this question, I examined the *Tc-zen* expression pattern in carefully staged *Tribolium* embryos during blastoderm stage. Meanwhile, with a *Tribolium* transgenic line [100] that expresses GFP in each nucleus driven by a *Tribolium* ubiquitous promoter (EFA-nGFP line), I performed live imaging experiments to track any possible nuclei movement.

Different from the dorsally originated amnioserosa in *Drosophila*, the serosa in *Tribolium* originates from the cells located in a dorsally tilted anterior cap at the blastoderm stage. It is most likely under the regulations of both Anterior-Posterior and Dorsal-Ventral patterning systems. The canonical Wnt signaling pathway has a conserved role in the patterning of A-P body axes in metazoan development [2, 5]. Though one notable exception is *Drosophila* in which canonical Wnt signaling is not required for either global axes formation or amnioserosa formation [48]. In *Tribolium*, Wnt signaling has to be activated for successful posterior development and be inhibited for proper anterior formation [38, 45, 52]. As a homolog of the Wnt downstream component, *Tc-pangolin* (*Tc-pan*) functions as an activator with nuclear β-catenin and as an inhibitor without nuclear β-catenin. Once *Tc-pan* transcripts are depleted after RNAi, anterior Wnt would be higher while posterior Wnt would be lower relative to wildtype levels. In this case, anterior and posterior development were both affected as described in Chapter 2. Anteriorly, the extraembryonic serosa was reduced

in *Tc-pan* RNAi embryos. Unlike the phenotypes after RNAi with other Wnt pathway components, in *Tc-pan* RNAi embryos, dorsally extended embryonic tissue divided the serosa into distinct anterior and posterior domains. To test how serosa fate determination is affected by Wnt signal, I used the EFA nGFP transgenic line and carefully checked the expression pattern of *Tc-zen* in staged *Tc-pan* RNAi embryos and performed live imaging for the same stages.

3.2 Materials and Methods

3.2.1 Beetle strains of *Tribolium castaneum*

GA1 wildtype and EFA nGFP transgenic [100] lines were used for gene expression and functional analysis. Live imaging was carried out using the EFA-nGFP line. Beetles were reared at 30 °C in whole-wheat flour supplemented with 5% yeast.

3.2.2 RNA interference (RNAi)

Tc-pan double-stranded RNA (dsRNA) was synthesized using the T7 megascript kit (Ambion) and purified using the Megaclear kit (Ambion). Adult females were injected with 200 ng/μL *Tc-pan* dsRNA, and allowed to recover in the whole-wheat flour for four days. After that, injected beetles were transferred to the triple-sifted flour for egg laying. One batch of eggs were collected and allowed to develop at 30 °C for four days before cuticle preparation. By checking the cuticle prep phenotypes, which are expected to be same as the ones described in Fig. 2.1 K-M, I made sure the *Tc-pan* RNAi worked efficiently.

3.2.3 Egg collections for desired stages

Beetles, either GA1 or EFA-nGFP line or *Tc-pan* RNAi of EFA-nGFP line, were incubated in the triple sifted flour (TSF) for one hour at 24 °C . Collected eggs were allowed to further

grow at 24 °C for another specified time: 12, 13, 14, 15, 16, 17, 18, 19, 20 hours (hr), resulting in sequentially aged groups as following: 12-13 hr, 13-14 hr, 14-15 hr, 15-16 hr, 16-17 hr, 17-18 hr, 18-19 hr, 19-20 hr, 20-21 hr.

3.2.4 In situ hybridization

In situ hybridization was performed using digoxigenin (DIG)-labeled RNA probes and an anti-DIG::alkaline phosphatase (AP) antibody (Roche). Signal was developed using NBT/BCIP (BM Purple, Roche).

3.2.5 Microscopy and Imaging

Cuticles and stained embryos were viewed with a Nikon Digital Camera DXM 1200F camera on an Olympus BX50 microscope and photographed using Nikon ACT-1 Version 2.62 software. Embryos were optically sectioned and images were assembled using MONTAGE software. Brightness and contrast were adjusted using Adobe Photoshop CS2 software.

3.2.6 Live imaging and nuclei tracking

EFA-nGFP eggs collected after 15 min incubation at 24 °C were kept at 24 °C and allowed to develop for another either 12 hours for the experiment of "live imaging during the age of 14-18 hours" or 17 hours for the experiment of "live imaging during the age of 18-20 hours". Later, embryos were dechorionated by washing in 1% bleach for 30 seconds, followed by rinsing in distilled water for two minutes. Embryos were then immediately transferred to a small petri dish filled with halocarbon oil 700 (Sigma). One multiple-well microscope glass slide was prepared by filling each well with proper amount of halocarbon oil. One embryo was placed in each well. No coverslip was required. The time-lapse movie was taken by either manually capturing 5 focal planes every 15 minutes followed by montage treatment afterward with Automontage software (Movie 1), or capturing single focal plane every 5

minutes (Movie 2) or every 20 minutes (Movie 3), at room temperature (24-25 °C) on a Leica M205 FA stereoscope at 200x magnification. Movie 1 was produced at a speed of 7 frames (105 minutes real time) per second. Movie 2 was produced at a speed of 3 frames (15 minutes real time) per second. Movie 3 was produced at a speed of 3 frames (60 minutes real time) per second.

Using ImageJ plugin MTrackJ tool, I manually tracked the GFP-marked nuclei of blastoderm embryo through time [101].

3.3 Results

3.3.1 Dynamics of *Tc-zen* expression at *Tribolium* blastoderm stage

In the EFA-nGFP line, the *Tc-zen* expression pattern went through three stages of dynamics during early blastoderm stage. At first stage (13-14 hr, see Fig. 3.3 D-F), near the end of the 11th synchronous nuclear division which occurred during approximately 12.5 hr-13.25 hr (Fig. 3.3 C-D), *Tc-zen* transcripts were firstly detected at the anterior pole of the egg (Fig. 3.3 D,D′). After the 11th and before the 12th nuclear division, more anterior *Tc-zen* transcripts were detected (compare Fig. 3.3 E and D). Soon, the occurrence of the 12th synchronous nuclear division during approximately 12.25 hr-14 hr (Fig. 3.3 F,F′) resulted in further more anterior *Tc-zen* transcripts (Fig. 3.3 F,F′). Most likely, cell divisions contribute to this dynamic. Followed is the second stage (14-18 hr, see Fig. 3.3 G-J) during which the expression pattern of *Tc-zen* started expanding dorsally (Fig. 3.3 H,H′) with age until reached the approximately 55% egg length from the posterior pole (Fig. 3.3 K,K′). No cell division was observed. It is likely that either cell movement or initiation of new *Tc-zen* transcription in the dorsal part of the egg contributes to this expression pattern dynamic from anterior cap to dorsally tilted region. At third stage (18-20 hr, see Fig. 3.3 K and L), *Tc-*

Table 3.1: *Quantitation data of Tc-zen early expression pattern in nGFP line. "n" indicates the total number of embryos in each aged group. As described in the subsection 3.2.3, one hour egg collections were incubated for different hours resulting in sequentially aged groups as shown in the left column. After In situ staining with* Tc-zen *ribo probe, embryos in each aged group were carefully examined one by one and classifed to different* Tc-zen *staining types with number counted. Orange color indicates the dominant type(s) in each aged group.*

age \ type	B	C	D	E	F	G	H	I	J	K	L	M	N
12-13h (n=36)	19	17											
13-14h (n=41)		1	9	14	15	2							
14-15h (n=39)					3	31	5						
15-16h (n=52)					1	4	40	3	4				
16-17h (n=32)							3	27	2				
17-18h (n=47)								2	39	4	2		
18-19h (n=31)									5	24	1	1	
19-20h (n=55)									3	8	37	7	
20-21h (n=43)											5	14	24

zen expression expanded posteriorly a little further concurrent with the asynchronous 13th cell division which exclusively occurred in the *Tc-zen* transcripts free region. No cell division was observed in the region with *Tc-zen* expression, which is consistent with previous studies [90, 102] and also confirmed by a current study with live imaging technique[103]. After that, serosa cells became distinguishable from germ rudiment cells at both morphological level and molecular level (Fig. 3.3 M,M′). Morphologically, serosa cells were large and loosely positioned while germ rudiment cells were small and condensed. Molecularly, *Tc-zen* transcripts were exclusively detected in serosa cells. This stage is called differentiated/late blastoderm stage. Quantitation data of *Tc-zen* expression pattern is shown in table. 3.1.

As a control, I performed the same experiments using GA1 line (Fig. 3.4). After careful comparison, the expression patterns in both lines at each same age range look very similar. This suggests the nGFP transgenic line develops at the same rate as GA1 and thus it serves as a reliable reporter of events in early *Tribolium* embryogenesis.

3.3.2 Live imaging during the age of 14-18 hours

As described in the subsection 3.3.1 above, *Tc-zen* expression pattern went through an apparent change from anterior cap to dorsally titled region during the second stage of expression dynamics, during the age range of 14-18 hr. No cell division was observed. In order to test whether any cell movement contributed to this dynamic process, I performed live imaging using EFA-nGFP transgenic embryo (see methods in subsection 3.2.6) to track nuclei movement (Movie1 and Fig. 3.5 A). Nuclei randomly and slightly moved around their original positions (Fig. 3.5 A). There is no cell movement with oriented direction that could possibly contribute to the shift of nuclei from anterior to dorsal. Also, no cell division was observed.

To exclude the possibility that UV exposure during the live imaging experiment might affect *Tribolium* embryogenesis, I checked and compared the treated embryo with control after 24 hours. Both looked similar (compare Fig. 3.5 B and C), which indicates UV exposure did not affect embryogenesis and the live imaging experiment provides reliable result.

Data above suggests that the second stage of *Tc-zen* expression pattern dynamics is not caused by either cell division or cell movement. Most likely, it is caused by the initiation of transcription in the dorsal region.

3.3.3 Live imaging during the age of 18-20 hours

Tc-zen expression pattern, combined with DAPI stainings, during the age of 18-20 hours (Fig. 3.3 K,K′,L,L′ and Fig. 3.4 K,K′,L,L′) suggests that it is the asynchronous 13th cell division, which exclusively occurred in the *Tc-zen* transcripts free region, that resulted in differentiated blastoderm. To confirm this hypothesis, I performed live imaging using a EFA-nGFP transgenic embryo (see methods in subsection /refliveimage) to track nuclei morphology (movie2 and Fig. 3.6 A). Cell movement with posterior-dorsal direction in the presumptive serosa explains the slight posterior expansion of *Tc-zen* expression pattern (compare Fig. 3.3 K and L). Consistent with the data from *Tc-zen* expression pattern as

described in the subsection 3.3.1, the asynchronous 13th cell division exclusively occurred in the germ rudiment region, resulting in the morphological differences between presumptive serosa tissue and germ rudiment tissue.

To exclude the possibility that UV exposure during the live imaging experiment might affect *Tribolium* embryogenesis, I checked and compared the treated embryo with control after 24 hours. Both developed similarly (compare Fig. 3.6 B and C).

3.3.4 Different markers on *Tc-pan* RNAi embryos

As mentioned in Fig. 2.5 from Chapter 2, serosa tissue in *Tc-pan* RNAi embryos was divided into distinct anterior and dorsal domains by dorsally extended head-lobe-like tissue. This separation is confirmed by *Tc-zen* expression pattern (Fig. 3.7 J,J′,M,M′,P,P′,S,S′). To test whether this dorsally extended tissue is head lobe or not, I checked the *Tc-wg* expression pattern in *Tc-pan* RNAi embryos. *Tc-wg* is the ortholog of *wnt1* in human and *wingless* in *Drosophila*. The expression pattern of *wg* is widely conserved among insects. In *Drosophila*, *wg* gene expression in the presumptive head region and in a caudal ring is detected in the early blastoderm [104]. While in *Tribolium* early blastoderm, *Tc-wg* is seen as stripes in the presumptive head lobes, and also detected at the posterior pole [105] (Fig. 3.8 A,A′). Dorsally extended anterior domains of *Tc-wg* in *Tc-pan* RNAi embryos confirm that the tissue between anterior and dorsal serosa domains is head lobe (Fig. 3.8 B,B′). In wildtype, *Tc-doc* marks the dorsal serosa [106–108] (Fig. 3.9 B,B′,D,D′,F,F′). The staining domain of *Tc-doc* in the dorsal part of the *Tc-pan* RNAi embryos (Fig. 3.9 H,H′,J,J′,L,L′) confirms that the remaining serosa is dorsal serosa.

In *Tc-pan* RNAi embryos, compared with the case in wildtype at similar age ranges, both anterior and dorsal serosa were reduced with decreased *Tc-zen* expression (Fig. 3.7 A-T, A′-T′). In severe mutants, dorsal serosa was completely gone without any dorsal *Tc-zen* expression detected (Fig. 3.7 H,H′,K,K′,N,N′,Q,Q′,T,T′), while anterior serosa is still maintained with very few *Tc-zen* transcripts in the anterior tip. Loss of the dorsal serosa

was also confirmed with *Tc-doc* stainings in *Tc-pan* RNAi progeny (Fig. 3.9 N,N′,P,P′,R,R′). Almost all the cells locating on the surface of the RNAi progeny were germ rudiment cells, while at the similar age in wildtype the embryo should be a differentiated blastoderm with both large and loosely positioned serosa cells versus small and condensed germ rudiment cells (Fig. 3.9 R,R′).

3.3.5 Live imaging of the *Tc-pan* RNAi embryo during the age of 18-20 hours

After *Tc-pan* RNAi, at uniform blastoderm stage, all the nuclei were uniformly positioned (Fig. 3.7 A-N,A′-N′), just like the case in wildtype (Fig. 3.7 a-e,a′-e′). Later at the differentiated blastoderm stage, the serosa was divided into distinct anterior and dorsal domains by germ rudiment tissue (the dorsally extended head lobes, to be specific). To determine whether this transformation process, from presumptive serosa tissue to head lobe tissue, involves any cell movement or cell division, I performed live imaging of an EFA-nGFP transgenic embryo (see methods in the subsection 3.2.6) to track nuclear morphology (Movie 3 and Fig. 3.10). Cell divisions were detected in the region between the separated anterior and dorsal serosa domains, resulting in small and condensed germ rudiment cells. No obvious cell movements were observed.

3.4 Discussion

3.4.1 *Tc-zen* expression pattern dynamics are caused by transcription shift rather than cell movement

During early embryogenesis, many genes are expressed in dynamic patterns at different stages [109]. *Tc-zen* is one of those genes. Zen is homologous to Hox 3 genes in vertebrates. Different from typical hox genes, at some point during insect evolution, zen/Hox3 lost its

function in AP axial patterning and contributed in the development of extraembryonic tissues [110].

Functional studies suggest *Tc-zen* is required for serosa formation and its expression is exclusively observed in the serosa-fated cells during differentiated blastoderm stage when serosa cells are firstly distinguishable from germ rudiment cells [58, 98]. Early at the uniform blastoderm stage, *Tc-zen* expression pattern shifts from anterior cap to dorsally titled anterior region. No one ever checked how this expression pattern shift happened. In this study, based on the live imaging during this process, no cell division or cell movement was observed. So most likely, initiation of new *Tc-zen* transcription in the dorsal part of the egg is the major reason that transforms the *Tc-zen* expression pattern from anterior cap to dorsally tilted anterior region.

3.4.2 Cell division initiates the transformation from the uniform blastoderm to the differentiated blastoderm

During the transition from the uniform to the differentiated blastoderm stage, cell divisions exclusively occurred in the *Tc-zen* transcripts free region, resulting in relatively small and condensed germ rudiment cells. By tracking the cell movement, it is obvious that no presumptive serosa cells move ventrally contributing to the germ rudiment tissue. Lack of *Tc-zen* coincides with occurrence of cell divisions. In *Tc-pan* RNAi embryos, abnormal cell divisions were recorded in the *Tc-zen* transcripts free region between anterior and dorsal *Tc-zen* expression domains, resulting in dorsally extended head lobe tissue. Presence of *Tc-zen* transcripts represses cell division in *Tribolium*, which is consistent with the case for *zen* in *Drosophila*. *Drosophila* studies suggest *zen* repressed cell division by repressing the transcription of *string*, which is an essential factor for cell division [111, 112]. String functions through positively regulating Cdk1/cdc2 complex to push cell cycle from G2 phase to M phase. Though mechanism is not clear for the case in *Tribolium*, as a future direction, we could test the hypothesis that *Tc-zen* represses cell division by repressing *Tc-string*, by

checking the expression pattern of *Tc-string* in *Tc-pan* RNAi progeny to see whether extra *Tc-string* transcripts exist between the separated dorsal and anterior serosa domains.

3.4.3 Evolution of the mechanisms underlying serosa formation

In *Tc-pan* RNAi progeny, serosa tissue was divided by dorsally extended head lobes into distinct anterior and dorsal serosa domains (see Fig. 4.2 A). In the most severe phenotype there was only anterior serosa domain left, indicating different sensitivities of the serosa domains to modulated Wnt signal. This implicates independent mechanisms underlying anterior and dorsal serosa domains in *Tribolium* (see Fig. 4.2 B). The mechanism regulating anterior serosa domain might be lost in *Drosophila* such that the serosa was restricted to the dorsal region (see Fig. 4.2 C). And the dorsal serosa mechanism is possibly modified though maintained throughout the evolution. One notable modification is the absence of the involvement of canonical Wnt activity, though the expression pattern of *wingless*, the main *Drosophila wnt* homologue, is similar to that in *Tribolium*. To which extent the dorsal serosa mechanism was modified in *Drosophila* is not clear, though some conservation aspects do exist. For example, *zen* is required for serosa formation in *Tribolium* as well as amnioserosa formation in *Drosophila*. *Zen* inhibits cell divisions in the prospective amnioserosa region in *Drosophila* as well as the prospective serosa region in *Tribolium*.

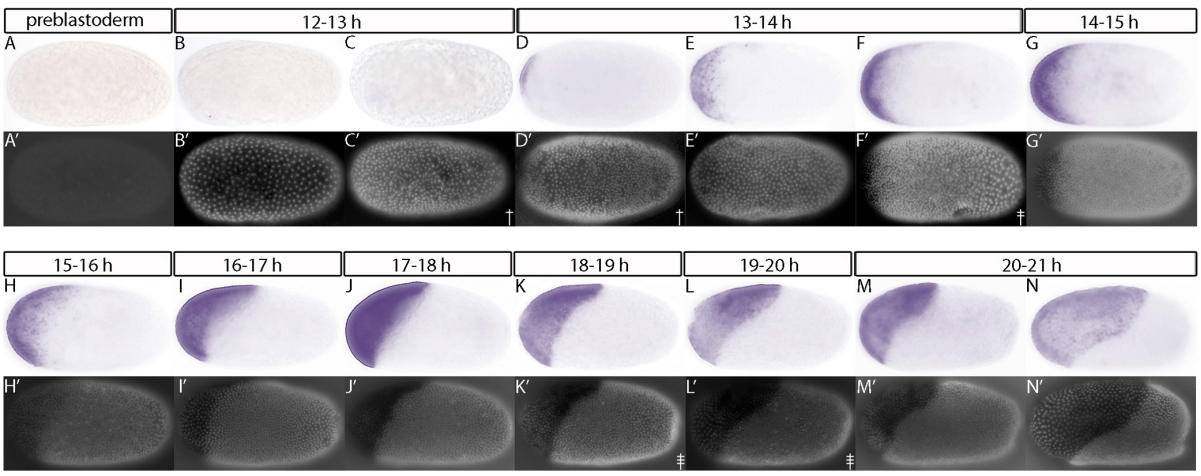

Figure 3.3: *Tc-zen early expression pattern in nGFP line. Embryos are oriented with anterior to the left and dorsal to the top, if known. As described in the subsection 3.2.3, one hour egg collections were incubated for different hours so that sequentially aged groups were produced. In some aged groups, embryos with slightly different ages based on nuclei numbers were displayed, with younger one at left. Quantitation data for each aged group were shown in Fig. 3.1. For the same embryos, both Bright field images (A-N) and DAPI (stained each nucleus) images (A′-N′) were shown. (A-C, A′-C′) Early embryonic stages without Tc-zen expression. (A, A′) Preblastoderm stage when nuclei are dividing deep inside the egg. (B, B′) Early uniform blastoderm stage when nuclei are moving and ubiquitously locating on the surface of the egg. (C, C′) The 11th nuclear division occurred, and most of the nuclei were at the metaphase with the existence of metaphase plates. (D-F, D′-F′) The first stage of Tc-zen early expression dynamics, with initiation and gradual increase of anterior Tc-zen transcripts. (D, D′) At the end of 11th nuclear division, for the first time, Tc-zen transcripts appeared at the aterior pole. (E, E′) More anterior Te-zen transcripts appeared (compare E and D). (F, F′) With the occurrence of the 12th nuclear division, more Tc-zen transcripts were detected (compare F and E). (G-J, G′-J′) The second stage of Tc-zen early expression dynamics, with pattern transformation from anterior cap to dorsally tilted anterior region. (G, G′) After the second stage of Tc-zen early expression dynamics, anteior Tc-zen transcripts accumulated to the maximum level (compare G and F). (H, H′) The expression pattern started to be slightly dorsally tilted. (I, I′) The pattern asymmetry became apparent (compare I and H). (J, J′) The dorsal Tc-zen transcripts reached the approximately 55% egg length from the posterior pole. (K-L, K′-L′) The third stage of Tc-zen early expression dynamics, slight expansion towards the posterior pole. (K, K′) The 13th asynchronous cell division started. (L, L′) Near the end of the 13th asynchronous cell division, dorsal Tc-zen expression further extended posteriorly (compare L and K). (M, M′) Differentiated blastoderm stage, with distinguishable serosa tissue. (N, N′) Gastrulation stage started , with the existence of pit at the posterior pole. Serosa cells moved posteriorly and ventrally.*

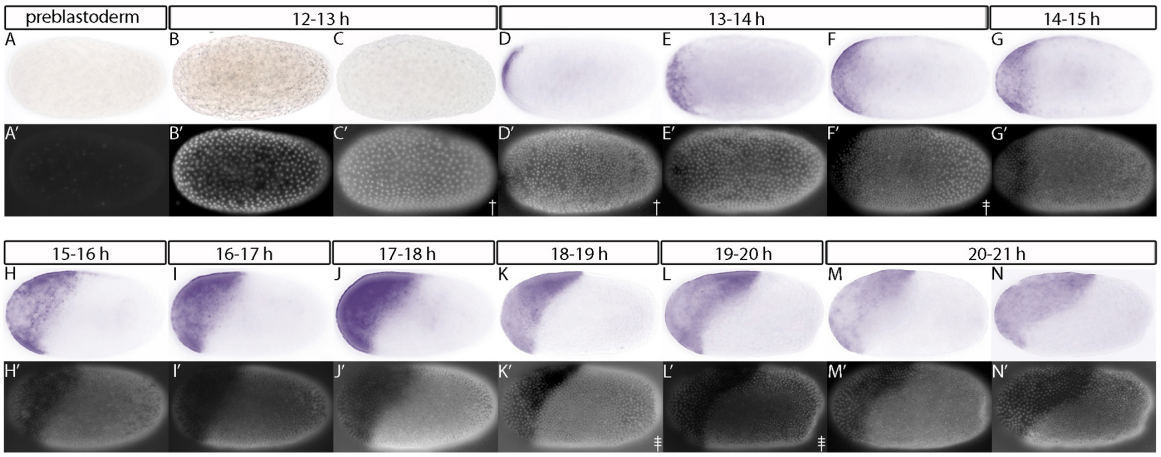

Figure 3.4: *Tc-zen early expression pattern in GA1. Embryos are oriented with anterior to the left and dorsal to the top, if known. This is a control experiment. After careful comparison with Fig. 3.3, the expression patterns in both lines at each same age range look most likely same, suggesting the nGFP transgenic line develops at the same rate as GA1 and thus it serves as a reliable reporter of events in early Tribolium embryogenesis.*

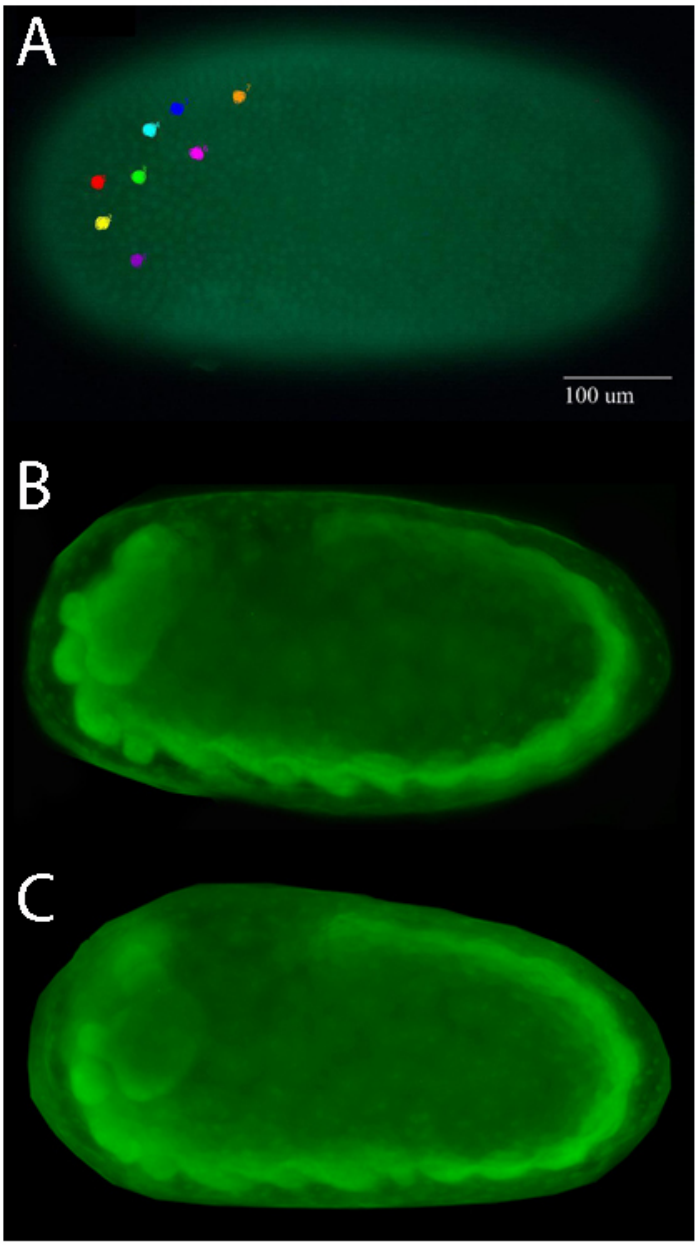

Figure 3.5: *No nuclei movement is involved in Tc-zen expression pattern dynamic stage during 14-18 hours. Embryos are oriented with anterior to the left and dorsal to the top. (A) Stills from live imaging of an EFA-nGFP transgenic Tribolium embryo (Movie 1) in the second stage of Tc-zen expression dynamic during the age of 14-18 hours at room temperature (24-25 °C). Colored circles track the movement of nuclei, implicating no movement involved. (B-C) Comparison of DAPI stainings for control and treated embryo after 24 hours incubation at room temperature following live imaging experiment. (B) The same EFA-nGFP transgenic Tribolium embryo from the live imaging experiment. (C) Control, another EFA-nGFP transgenic Tribolium embryo that underwent same treatments as the embryo in (B) except the UV exposure.*

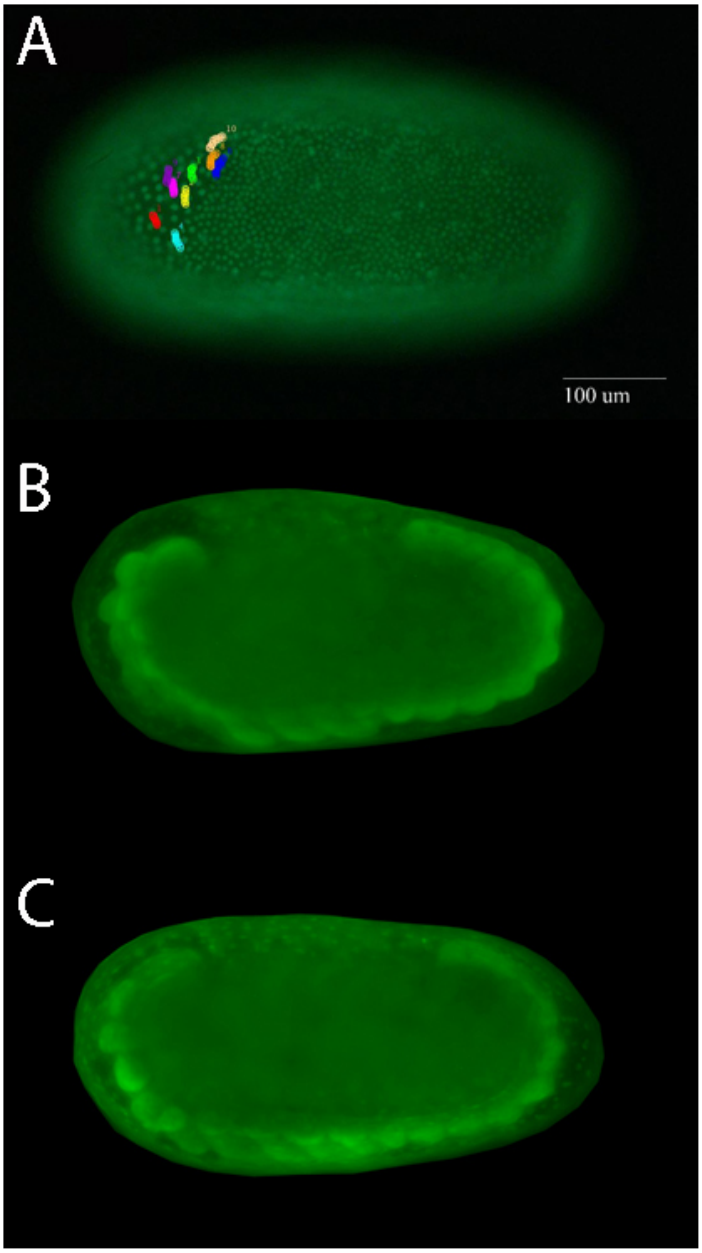

Figure 3.6: *Cell movement with posterior-dorsal direction in the presumptive serosa not only explains the slight posterior extension of Tc-zen expression pattern, but also excludes the contribution of serosa cells to germ rudiment tissue by cell movement towards ventral part of the embryo. (A) Stills from live imaging of an EFA-nGFP transgenic Tribolium embryo (Movie 2) in the third stage of Tc-zen expression dynamic during the age of 18-20 hours at room temperature (24-25 °C). Colored circles track the movement of cell. (B-C) Comparison of DAPI stainings for control and treated embryo after 24 hours incubation at room temperature following live imaging experiment. (B) The same EFA-nGFP transgenic Tribolium embryo from the live imaging experiment. (C) Control, another EFA-nGFP transgenic Tribolium embryo that underwent same treatments as the embryo in (B) except the UV exposure.*

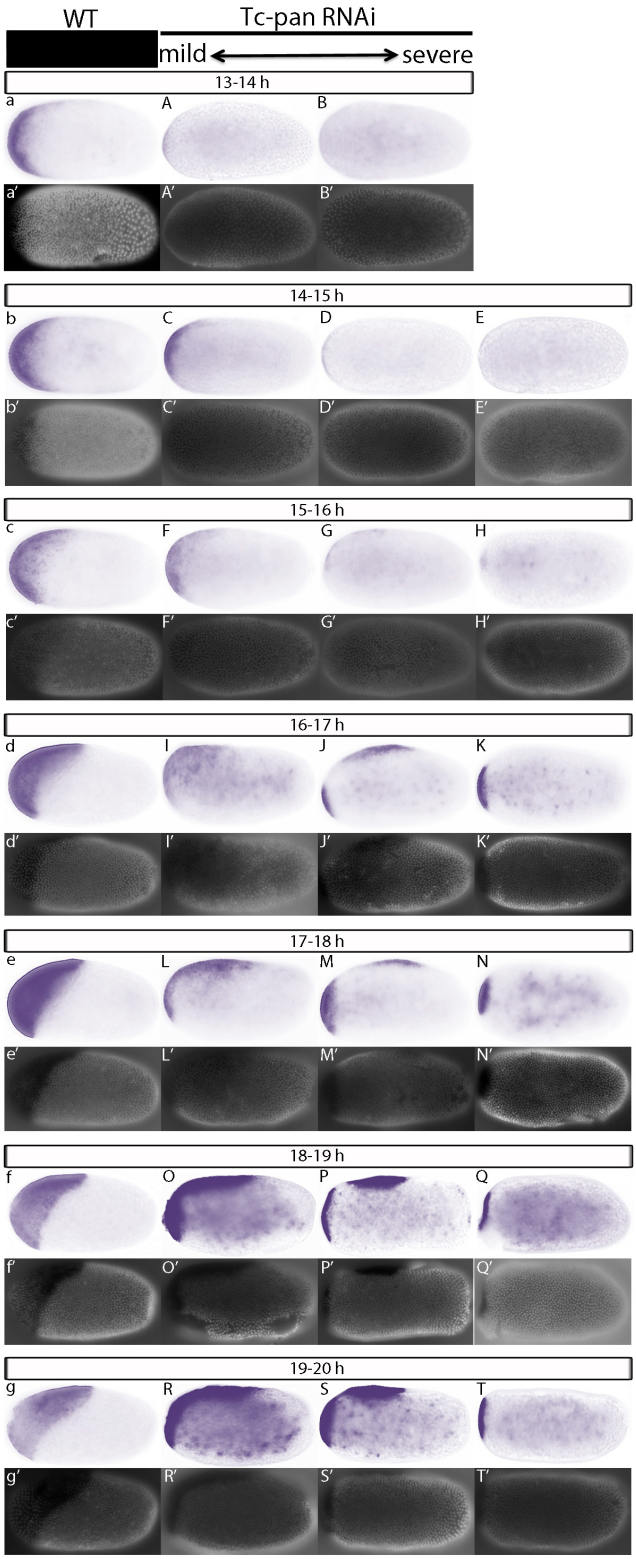

Figure 3.7: *(Caption next page.)*

Figure 3.7: *(Previous page.) Tc-zen early expression pattern in Tc-pan RNAi embryos. Embryos are oriented with anterior to the left and dorsal to the top, if known. Embryos at different age ranges are displayed one row by one row with youngest on top row. For the same embryos, Bright field images (a-g, A-T) and DAPI (stained each nuclei) images (a′-g′, A′-T′) are provided. (a-g, a′-g′) Tc-zen early expression pattern in wildtype embryos, as control. (A,A′,C,C′,F,F′,I,I′,L,L′,O,O′,R,R′) Mild mutant. Compared with the case in wildtype, at each aged group, Tc-zen transcripts in Tc-pan RNAi mild mutant progeny were highly reduced. (B,B′,D,D′,G,G′,J,J′,M,M′,P,P′,S,S′) Median mutant. Tc-zen transcripts in Tc-pan RNAi median mutant progeny were not only reduced but also divided to distinct anterior and dorsal domains. (E,E′,H,H′,K,K′,N,N′,Q,Q′,T,T′) Severe mutant. Dorsal Tc-zen transcripts were lost in Tc-pan RNAi severe mutant progeny.*

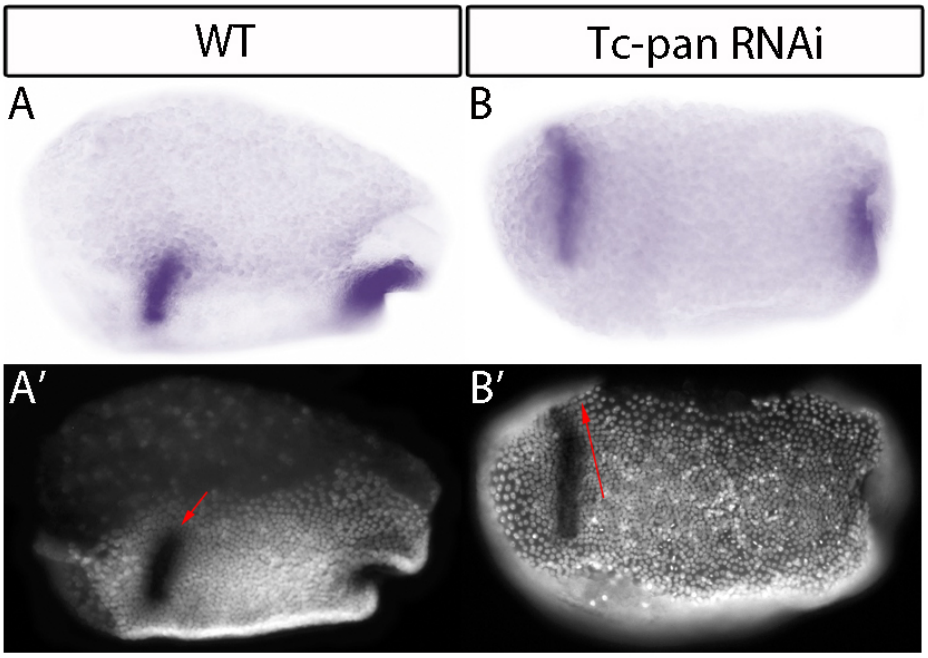

Figure 3.8: *Tc-wg stainings suggest the dorsal extension of head lobes in the Tc-pan RNAi embryos. Embryos are oriented with anterior to the left and dorsal to the top. (A) In wildtype, Tc-wg is expressed in the head lobes. (B) In Tc-pan mutant progeny, Tc-wg expression extended dorsally, implicating the dorsal extension of the head lobe tissue. (See the red arrows in A and B)*

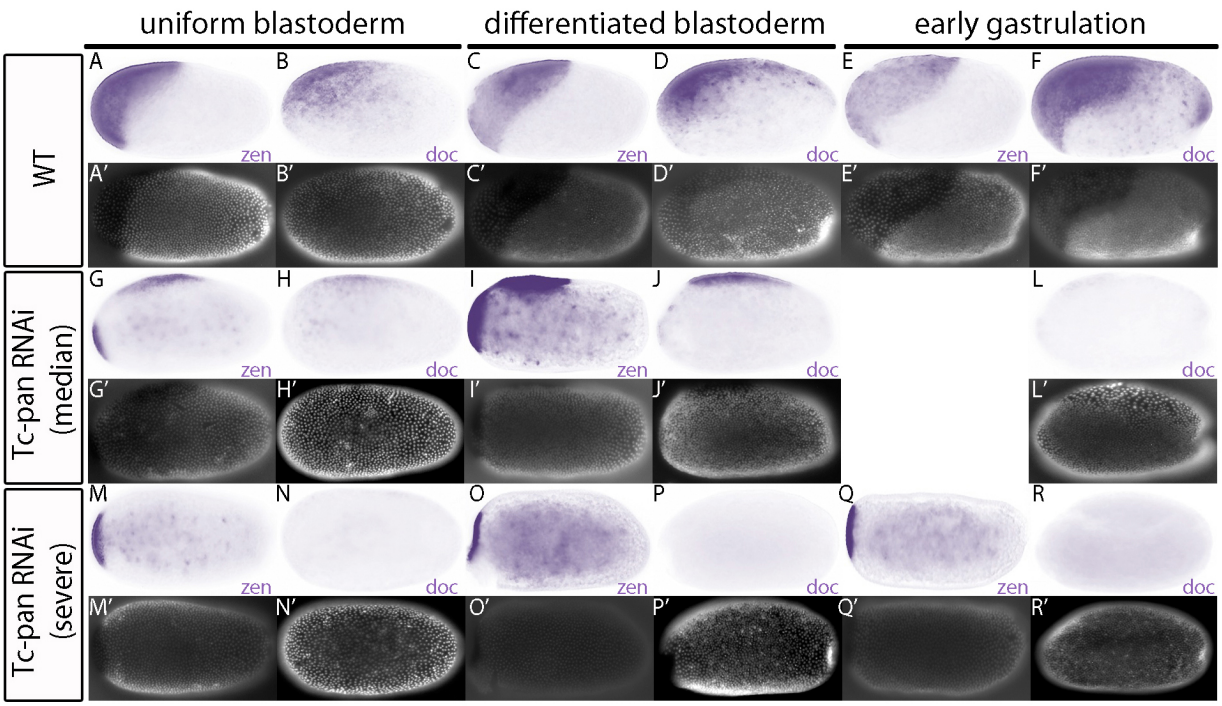

Figure 3.9: *Tc-doc stainings in Tc-pan RNAi embryos. Embryos are oriented with anterior to the left and dorsal to the top, if known. Each column at specific developmental stage, including uniform blstoderm, differentiated blastoderm and early gastrulation. Bright field images and DAPI staining images for the same embryos are shown. (A-F, A′-F′) Stainings in wildtype embryos for Tc-zen (A,A′,C,C′,E,E′), as comparison, and Tc-doc (B,B′,D,D′,F,F′). (G-L, G′-L′) Stainings in median Tc-pan RNAi mutant progeny for Tc-zen (G,G′,I,I′), as comparison, and Tc-doc (H,H′,J,J′,L,L′). (M-R, M′-R′) Stainings in severe Tc-pan RNAi mutant progeny for Tc-zen (M,M′,O,O′,Q,Q′), as comparison, and Tc-doc (N,N′,P,P′,R,R′)*

.

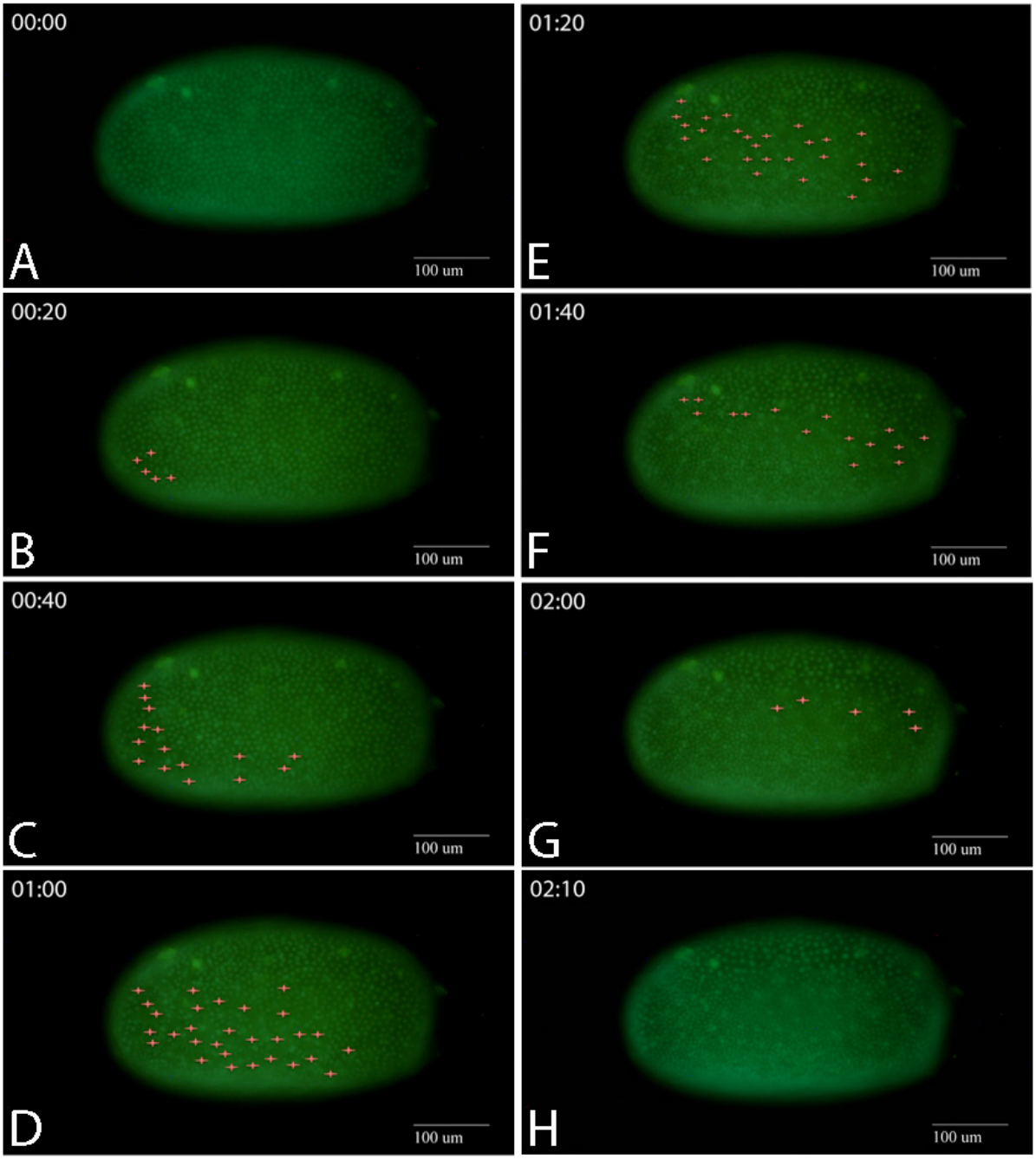

Figure 3.10: *Cell division contributes to the dorsally extended head lobe formation in the Tc-pan RNAi embryo. (A-H) Stills from Movie 3. Embryos are oriented with anterior to the left and dorsal to the top. Red star marks the cell division.*

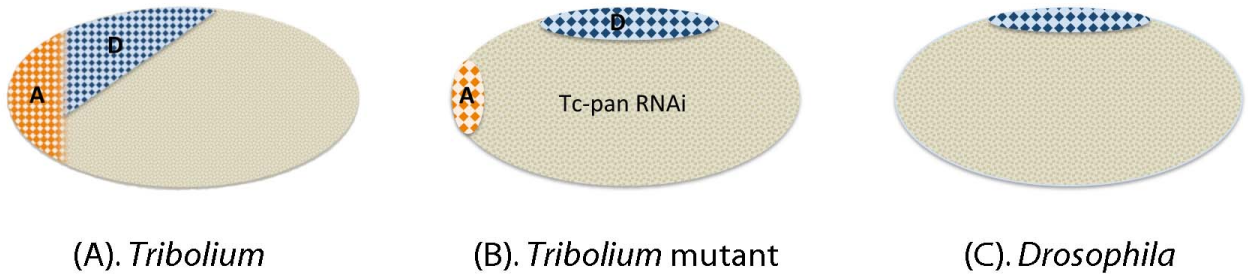

Figure 3.11: *Comparison of serosa domains among Tribolium and Drosophila. Orange dotted pattern marks anterior serosa, blue dotted pattern marks either dorsal serosa in Tribolium or amnioserosa in Drosophila. (A) Tribolium wildtype. (B) Tribolium mutant after Tc-pan RNAi. (C) Drosophila wildtype. Abbreviation used: A - anterior serosa domain; D - dorsal serosa domain.*

Chapter 4

Summary

Comparative studies in different model organisms suggest that the canonical Wnt siganling pathway is highly conserved and most likely a widely used Anterior-Posterior patterning mechanism throughout the evolution. In vertebrates, Wnt signal is requird for posterior development and has to be repressed for proper anterior formation. In arthropods, Wnt signal is also essential for posterior patterning, however, limited evidence about the contribution of Wnt signal in anterior development was ever found. The studies in this thesis have provided the first evidence that anterior canonical Wnt signal has to be repressed for proper anterior development in an arthropod.

4.1 Evolution of the segmentation mode

In arthropods, the body plan is divided into series of repetitive segments along the anterior-posterior axis. This segmental organization allow organisms much more flexibility in adaptation to new tasks and might be of huge benefit for morphological and functional evolution. The segmentation modes in different organisms could be quite different. In long-germ mode, with the representative of *Drosophila*, all segments of whole body are almost simultaneously specified in a syncitial blastoderm [34, 92]. At this stage, cellularization has not yet occurred

and proteins could freely diffuse throughout the whole egg. Transcription factors, such as Bicoid, function as morphogens by forming graidients along the AP axis and concentration-dependently activating different groups of downstream target genes that efficiently set up a blastoderm fate map for the entire future body plan in approximately natural proportions [113]. While in short-germ mode, which is the same mode utilized by another big group of segmented animals — vertebrates, only anterior segments, including either head only or both head and thorax, are formed in blastoderm stage before cellularization, leaving posterior segments sequentially patterned from the posterior growth zone after gastrulation, in an anterior to posterior progression. The cellularized environment prevents the entirely dependence on the diffusable morphogen gradient mechanism, as the case in long-germ mode.

Long-germ segmentation mode has been very well studied in *Drosophila*. However, Bicoid, an essential morphogen that specifies anterior structures in a concentration-dependent way in long-germ mode, was only found in high Diptera flies and it turned out that *Drosophila* is a highly derived insect utilizing the highly derived segmentation mode. Comparatively less is known about the mechanism underlying short-germ mode, which is widely found in most other arthropods including *Tribolium*[34, 92] and most likely the ancestral mode for both vertebrates and arthropods. Studies in this thesis provide the first evidence that an arthropod utilizes Axin, a negative regulator of the canonical Wnt pathway, as an alternative mechanism to pattern anterior development. It is indicated that arthropods require anterior Wnt repression and posterior Wnt siganl for AP patterning, just like the case in vertebrates, suggesting a conserved AP patterning mechanism along the evolution. It supports the hypothesis that, most likely, the common ancestor of vertebrates and arthropods is a short-germ organism and pattern its AP axis by carefully regulating Wnt activity along the main axis.

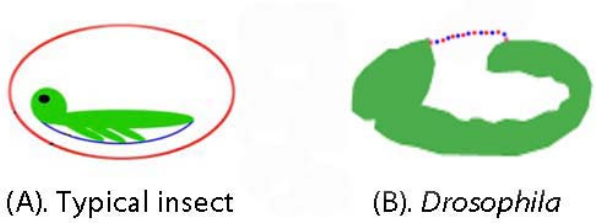

Figure 4.1: *Extraembryonic membranes in a typical insect and Drosophila. Green marks embryo, red marks serosa, blue marks amnion and dot line with both blue and red colors marks amnionserosa. (A) In a typical insect, an intact serosa membrane envelopes embryo, amnion, and yolk in the egg. Amnion, another extraembryonic membrane locates ventrally. (B) In Drosophila, a highly derived epithelium named amnionserosa locates dorsally.*

4.2 Evolution of the mechanisms underlying serosa formation

In most insects including *Tribolium*, an intact extraembryonic membrane named serosa (see red in Fig. 4.1 A) lies just under the chorion (eggshell) and envelopes embryo, amnion, and yolk in the egg. Amnion, another extraembryonic membrane locates ventrally (see blue in Fig. 4.1 A). However in *Drosophila*, a highly derived insect, the serosa tissue has been highly restricted and evolved as a dorsal epithelium called amionserosa (see the dot line with both blue and red colors in Fig. 4.1 B). How the two extraembryonic epithelia evolved into one is unclear.

In chapter 3 of this thesis, it is shown that in *Tc-pan* RNAi mutant progeny, serosa tissue was divided by dorsally extended head lobes into distinct anterior and dorsal serosa domains (see Fig. 4.2 A). In most severe mutant progeny there was even only anterior serosa domain left, indicating differen sensitivities of the serosa domains to modulated Wnt signal. Taken together, these data implicates independent mechanisms underlying anterior and dorsal serosa domains in *Tribolium* (see Fig. 4.2 B). Throughout the evolution, the mechanism regulating anterior serosa domain might be lost in *Drosophila* so that serosa was highly restricted into dorsal region (see Fig. 4.2 C) with a possibly modified dorsal serosa mechanism maintained. To which extent the dorsal serosa mechanism was modified in *Drosophila* is not clear, though some conservations do exist. For example, *zen* is required

for serosa formation in *Tribolium* as well as amnionserosa formation in *Drosophila*. *Zen* expressions inhibit cell division in the prespective amnionserosa region in *Drosophila* as well as the presepctive serosa region in *Tribolium*. It was reported that in *Drosophila*, Zen represses cell division by repressing the transcription of a cell division component named String [111, 112]. For future work, It would be interesting to test whether in *Tribolium*, *Tc-zen* also inhibits the 13th asynchronous cell division in the prespective serosa tissue by repressing transcription of any cell division components such as *Tc-string* or *Tc-cyclin D*.

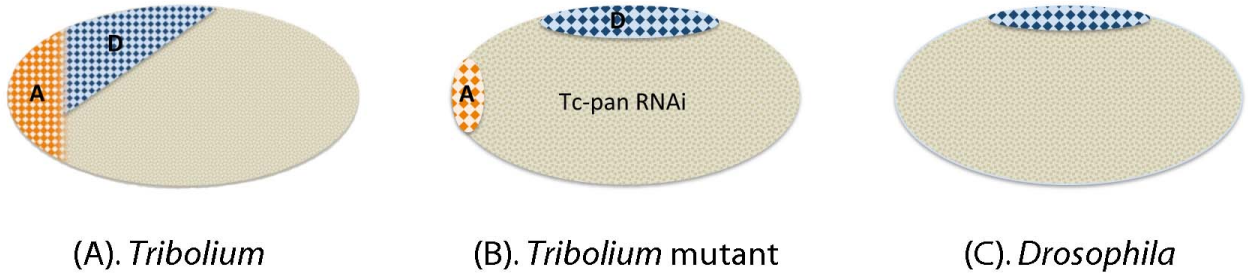

Figure 4.2: *Comparison of serosa domains among Tribolium and Drosophila. Orange dotted pattern marks anterior serosa, blue dotted pattern marks either dorsal serosa in Tribolium or amnionserosa in Drosophila. (A) Tribolium wildtype. (B) Tribolium mutant after Tc-pan RNAi. (C) Drosophila wildtype. Abbreviation used: A - anterior serosa domain; D - dorsal serosa domain.*

Bibliography

[1] J. F. Ryan and A. D. Baxevanis. Hox, wnt, and the evolution of the primary body axis: insights from the early-divergent phyla. *Biol Direct*, 2:37, 2007.

[2] C. P. Petersen and P. W. Reddien. Wnt signaling and the polarity of the primary body axis. *Cell*, 139(6):1056–68, 2009.

[3] C. Niehrs. On growth and form: a cartesian coordinate system of wnt and bmp signaling specifies bilaterian body axes. *Development*, 137(6):845–57, 2010.

[4] B. L. Martin and D. Kimelman. Wnt signaling and the evolution of embryonic posterior development. *Curr Biol*, 19(5):R215–9, 2009.

[5] G. H. Qian and Y. Q. Wang. Wnt signaling pathway and the evo-devo of deuterostome axis. *Yi Chuan*, 33(7):684–94, 2011.

[6] A. F. Schier and W. S. Talbot. Molecular genetics of axis formation in zebrafish. *Annu Rev Genet*, 39:561–613, 2005.

[7] C. Kiecker and C. Niehrs. A morphogen gradient of wnt/beta-catenin signalling regulates anteroposterior neural patterning in xenopus. *Development*, 128(21):4189–201, 2001.

[8] A. Glinka, W. Wu, H. Delius, A. P. Monaghan, C. Blumenstock, and C. Niehrs. Dickkopf-1 is a member of a new family of secreted proteins and functions in head induction. *Nature*, 391(6665):357–62, 1998.

[9] P. Liu, M. Wakamiya, M. J. Shea, U. Albrecht, R. R. Behringer, and A. Bradley. Requirement for wnt3 in vertebrate axis formation. *Nat Genet*, 22(4):361–5, 1999.

[10] O. A. Mohamed, H. J. Clarke, and D. Dufort. Beta-catenin signaling marks the prospective site of primitive streak formation in the mouse embryo. *Dev Dyn*, 231(2):416–24, 2004.

[11] A. C. Lekven, C. J. Thorpe, J. S. Waxman, and R. T. Moon. Zebrafish wnt8 encodes two wnt8 proteins on a bicistronic transcript and is required for mesoderm and neurectoderm patterning. *Dev Cell*, 1(1):103–14, 2001.

[12] T. Shimizu, Y. K. Bae, O. Muraoka, and M. Hibi. Interaction of wnt and caudal-related genes in zebrafish posterior body formation. *Dev Biol*, 279(1):125–41, 2005.

[13] C. J. Thorpe, G. Weidinger, and R. T. Moon. Wnt/beta-catenin regulation of the sp1-related transcription factor sp5l promotes tail development in zebrafish. *Development*, 132(8):1763–72, 2005.

[14] C. Tendeng and C. Houart. Cloning and embryonic expression of five distinct sfrp genes in the zebrafish danio rerio. *Gene Expr Patterns*, 6(8):761–71, 2006.

[15] J. K. Yu, Y. Satou, N. D. Holland, I. T. Shin, Y. Kohara, N. Satoh, M. Bronner-Fraser, and L. Z. Holland. Axial patterning in cephalochordates and the evolution of the organizer. *Nature*, 445(7128):613–7, 2007.

[16] H. Haegel, L. Larue, M. Ohsugi, L. Fedorov, K. Herrenknecht, and R. Kemler. Lack of beta-catenin affects mouse development at gastrulation. *Development*, 121(11):3529–37, 1995.

[17] J. Huelsken, R. Vogel, V. Brinkmann, B. Erdmann, C. Birchmeier, and W. Birchmeier. Requirement for beta-catenin in anterior-posterior axis formation in mice. *J Cell Biol*, 148(3):567–78, 2000.

[18] M. Mukhopadhyay, S. Shtrom, C. Rodriguez-Esteban, L. Chen, T. Tsukui, L. Gomer, D. W. Dorward, A. Glinka, A. Grinberg, S. P. Huang, C. Niehrs, J. C. Izpisua Bel-

monte, and H. Westphal. Dickkopf1 is required for embryonic head induction and limb morphogenesis in the mouse. *Dev Cell*, 1(3):423–34, 2001.

[19] H. Popperl, C. Schmidt, V. Wilson, C. R. Hume, J. Dodd, R. Krumlauf, and R. S. Beddington. Misexpression of cwnt8c in the mouse induces an ectopic embryonic axis and causes a truncation of the anterior neuroectoderm. *Development*, 124(15):2997–3005, 1997.

[20] L. Zeng, F. Fagotto, T. Zhang, W. Hsu, T. J. Vasicek, 3rd Perry, W. L., J. J. Lee, S. M. Tilghman, B. M. Gumbiner, and F. Costantini. The mouse fused locus encodes axin, an inhibitor of the wnt signaling pathway that regulates embryonic axis formation. *Cell*, 90(1):181–92, 1997.

[21] T. O. Ishikawa, Y. Tamai, Q. Li, M. Oshima, and M. M. Taketo. Requirement for tumor suppressor apc in the morphogenesis of anterior and ventral mouse embryo. *Dev Biol*, 253(2):230–46, 2003.

[22] B. J. Merrill, H. A. Pasolli, L. Polak, M. Rendl, M. J. Garcia-Garcia, K. V. Anderson, and E. Fuchs. Tcf3: a transcriptional regulator of axis induction in the early embryo. *Development*, 131(2):263–74, 2004.

[23] C. H. Kim, T. Oda, M. Itoh, D. Jiang, K. B. Artinger, S. C. Chandrasekharappa, W. Driever, and A. B. Chitnis. Repressor activity of headless/tcf3 is essential for vertebrate head formation. *Nature*, 407(6806):913–6, 2000.

[24] C. E. Erter, T. P. Wilm, N. Basler, C. V. Wright, and L. Solnica-Krezel. Wnt8 is required in lateral mesendodermal precursors for neural posteriorization in vivo. *Development*, 128(18):3571–83, 2001.

[25] M. Rhinn, K. Lun, M. Luz, M. Werner, and M. Brand. Positioning of the midbrain-hindbrain boundary organizer through global posteriorization of the neuroectoderm mediated by wnt8 signaling. *Development*, 132(6):1261–72, 2005.

[26] L. Z. Holland, K. A. Panfilio, R. Chastain, M. Schubert, and N. D. Holland. Nuclear beta-catenin promotes non-neural ectoderm and posterior cell fates in amphioxus embryos. *Dev Dyn*, 233(4):1430–43, 2005.

[27] T. Onai, H. C. Lin, M. Schubert, D. Koop, P. W. Osborne, S. Alvarez, R. Alvarez, N. D. Holland, and L. Z. Holland. Retinoic acid and wnt/beta-catenin have complementary roles in anterior/posterior patterning embryos of the basal chordate amphioxus. *Dev Biol*, 332(2):223–33, 2009.

[28] K. Nakamura, S. Kim, T. Ishidate, Y. Bei, K. Pang, M. Shirayama, C. Trzepacz, D. R. Brownell, and C. C. Mello. Wnt signaling drives wrm-1/beta-catenin asymmetries in early c. elegans embryos. *Genes Dev*, 19(15):1749–54, 2005.

[29] H. Takeshita and H. Sawa. Asymmetric cortical and nuclear localizations of wrm-1/beta-catenin during asymmetric cell division in c. elegans. *Genes Dev*, 19(15):1743–8, 2005.

[30] S. Huang, P. Shetty, S. M. Robertson, and R. Lin. Binary cell fate specification during c. elegans embryogenesis driven by reiterated reciprocal asymmetry of tcf pop-1 and its coactivator beta-catenin sys-1. *Development*, 134(14):2685–95, 2007.

[31] C. E. Rocheleau, W. D. Downs, R. Lin, C. Wittmann, Y. Bei, Y. H. Cha, M. Ali, J. R. Priess, and C. C. Mello. Wnt signaling and an apc-related gene specify endoderm in early c. elegans embryos. *Cell*, 90(4):707–16, 1997.

[32] C. J. Thorpe, A. Schlesinger, J. C. Carter, and B. Bowerman. Wnt signaling polarizes an early c. elegans blastomere to distinguish endoderm from mesoderm. *Cell*, 90(4):695–705, 1997.

[33] R. Lin, S. Thompson, and J. R. Priess. pop-1 encodes an hmg box protein required for the specification of a mesoderm precursor in early c. elegans embryos. *Cell*, 83(4):599–609, 1995.

[34] G. K. Davis and N. H. Patel. Short, long, and beyond: molecular and embryological approaches to insect segmentation. *Annu Rev Entomol*, 47:669–99, 2002.

[35] R. Bolognesi, A. Beermann, L. Farzana, N. Wittkopp, R. Lutz, G. Balavoine, S. J. Brown, and R. Schroder. Tribolium wnts: evidence for a larger repertoire in insects with overlapping expression patterns that suggest multiple redundant functions in embryogenesis. *Dev Genes Evol*, 218(3-4):193–202, 2008.

[36] K. Miyawaki, T. Mito, I. Sarashina, H. Zhang, Y. Shinmyo, H. Ohuchi, and S. Noji. Involvement of wingless/armadillo signaling in the posterior sequential segmentation in the cricket, gryllus bimaculatus (orthoptera), as revealed by rnai analysis. *Mech Dev*, 121(2):119–30, 2004.

[37] A. P. McGregor, M. Pechmann, E. E. Schwager, N. M. Feitosa, S. Kruck, M. Aranda, and W. G. Damen. Wnt8 is required for growth-zone establishment and development of opisthosomal segments in a spider. *Curr Biol*, 18(20):1619–23, 2008.

[38] R. Bolognesi, L. Farzana, T. D. Fischer, and S. J. Brown. Multiple wnt genes are required for segmentation in the short-germ embryo of tribolium castaneum. *Curr Biol*, 18(20):1624–9, 2008.

[39] P. W. Reddien and A. Sanchez Alvarado. Fundamentals of planarian regeneration. *Annu Rev Cell Dev Biol*, 20:725–57, 2004.

[40] C. P. Petersen and P. W. Reddien. A wound-induced wnt expression program controls planarian regeneration polarity. *Proc Natl Acad Sci U S A*, 106(40):17061–6, 2009.

[41] K. A. Gurley, J. C. Rink, and A. Sanchez Alvarado. Beta-catenin defines head versus tail identity during planarian regeneration and homeostasis. *Science*, 319(5861):323–7, 2008.

[42] M. Iglesias, J. L. Gomez-Skarmeta, E. Salo, and T. Adell. Silencing of smed-betacatenin1 generates radial-like hypercephalized planarians. *Development*, 135(7):1215–21, 2008.

[43] C. P. Petersen and P. W. Reddien. Smed-betacatenin-1 is required for anteroposterior blastema polarity in planarian regeneration. *Science*, 319(5861):327–30, 2008.

[44] S. Q. Schneider and B. Bowerman. beta-catenin asymmetries after all animal/vegetal-oriented cell divisions in platynereis dumerilii embryos mediate binary cell-fate specification. *Dev Cell*, 13(1):73–86, 2007.

[45] J. Fu, N. Posnien, R. Bolognesi, T. D. Fischer, P. Rayl, G. Oberhofer, P. Kitzmann, S. J. Brown, and G. Bucher. Asymmetrically expressed axin required for anterior development in tribolium. *Proc Natl Acad Sci U S A*, 109(20):7782–6, 2012.

[46] S. L. Lewis, P. L. Khoo, R. A. De Young, K. Steiner, C. Wilcock, M. Mukhopadhyay, H. Westphal, R. V. Jamieson, L. Robb, and P. P. Tam. Dkk1 and wnt3 interact to control head morphogenesis in the mouse. *Development*, 135(10):1791–801, 2008.

[47] C. P. Heisenberg, C. Houart, M. Take-Uchi, G. J. Rauch, N. Young, P. Coutinho, I. Masai, L. Caneparo, M. L. Concha, R. Geisler, T. C. Dale, S. W. Wilson, and D. L. Stemple. A mutation in the gsk3-binding domain of zebrafish masterblind/axin1 leads to a fate transformation of telencephalon and eyes to diencephalon. *Genes Dev*, 15(11):1427–34, 2001.

[48] A. Bejsovec and A. Martinez Arias. Roles of wingless in patterning the larval epidermis of drosophila. *Development*, 113(2):471–85, 1991.

[49] K. Willert, C. Y. Logan, A. Arora, M. Fish, and R. Nusse. A drosophila axin homolog, daxin, inhibits wnt signaling. *Development*, 126(18):4165–73, 1999.

[50] P. Francois, V. Hakim, and E. D. Siggia. Deriving structure from evolution: metazoan segmentation. *Mol Syst Biol*, 3:154, 2007.

[51] K. Fujimoto, S. Ishihara, and K. Kaneko. Network evolution of body plans. *PLoS One*, 3(7):e2772, 2008.

[52] R. Bolognesi, T. D. Fischer, and S. J. Brown. Loss of tc-arrow and canonical wnt signaling alters posterior morphology and pair-rule gene expression in the short-germ insect, tribolium castaneum. *Dev Genes Evol*, 219(7):369–75, 2009.

[53] K. M. Cadigan and M. Peifer. Wnt signaling from development to disease: insights from model systems. *Cold Spring Harb Perspect Biol*, 1(2):a002881, 2009.

[54] S. C. Miller, S. J. Brown, and Y. Tomoyasu. Larval rnai in drosophila? *Dev Genes Evol*, 218(9):505–10, 2008.

[55] G. Bucher, L. Farzana, S. J. Brown, and M. Klingler. Anterior localization of maternal mrnas in a short germ insect lacking bicoid. *Evol Dev*, 7(2):142–9, 2005.

[56] G. Bucher, J. Scholten, and M. Klingler. Parental rnai in tribolium (coleoptera). *Curr Biol*, 12(3):R85–6, 2002.

[57] J. Schinko, N. Posnien, S. Kittelmann, N. Koniszewski, and G. Bucher. Single and double whole-mount in situ hybridization in red flour beetle (tribolium) embryos. *Cold Spring Harb Protoc*, 2009(8):pdb prot5258, 2009.

[58] M. van der Zee, N. Berns, and S. Roth. Distinct functions of the tribolium zerknullt genes in serosa specification and dorsal closure. *Curr Biol*, 15(7):624–36, 2005.

[59] C. Schulz, R. Schroder, B. Hausdorf, C. Wolff, and D. Tautz. A caudal homologue in the short germ band beetle tribolium shows similarities to both, the drosophila and the vertebrate caudal expression patterns. *Dev Genes Evol*, 208(5):283–9, 1998.

[60] S. J. Brown, J. K. Parrish, R. W. Beeman, and R. E. Denell. Molecular characterization and embryonic expression of the even-skipped ortholog of tribolium castaneum. *Mech Dev*, 61(1-2):165–73, 1997.

[61] E. El-Sherif, M. Averof, and S. J. Brown. A segmentation clock operating in blastoderm and germband stages of tribolium development. *Development*, 139(23):4341–6, 2012.

[62] E. Heeg-Truesdell and C. LaBonne. Wnt signaling: a shaggy dogma tale. *Curr Biol*, 16(2):R62–4, 2006.

[63] F. P. Roth, H. D. Lipshitz, and B. J. Andrews. Epistasis. *J Biol*, 8(4):35, 2009.

[64] D. Fiedler, H. Braberg, M. Mehta, G. Chechik, G. Cagney, P. Mukherjee, A. C. Silva, M. Shales, S. R. Collins, S. van Wageningen, P. Kemmeren, F. C. Holstege, J. S. Weissman, M. C. Keogh, D. Koller, K. M. Shokat, and N. J. Krogan. Functional organization of the s. cerevisiae phosphorylation network. *Cell*, 136(5):952–63, 2009.

[65] E. Brunner, O. Peter, L. Schweizer, and K. Basler. pangolin encodes a lef-1 homologue that acts downstream of armadillo to transduce the wingless signal in drosophila. *Nature*, 385(6619):829–33, 1997.

[66] Anning Lin. *The JNK Signaling Pathway*. Landes Bioscience, USA, 2006.

[67] Y. Shinmyo, T. Mito, T. Matsushita, I. Sarashina, K. Miyawaki, H. Ohuchi, and S. Noji. caudal is required for gnathal and thoracic patterning and for posterior elongation in the intermediate-germband cricket gryllus bimaculatus. *Mech Dev*, 122(2):231–9, 2005.

[68] T. Copf, R. Schroder, and M. Averof. Ancestral role of caudal genes in axis elongation and segmentation. *Proc Natl Acad Sci U S A*, 101(51):17711–5, 2004.

[69] P. P. Vorwald-Denholtz and E. M. De Robertis. Temporal pattern of the posterior expression of wingless in drosophila blastoderm. *Gene Expr Patterns*, 11(7):456–63, 2011.

[70] R. Bao, T. Fischer, R. Bolognesi, S. J. Brown, and M. Friedrich. Parallel duplication and partial subfunctionalization of beta-catenin/armadillo during insect evolution. *Mol Biol Evol*, 29(2):647–62, 2012.

[71] M. Schoppmeier, S. Fischer, C. Schmitt-Engel, U. Lohr, and M. Klingler. An ancient anterior patterning system promotes caudal repression and head formation in ecdysozoa. *Curr Biol*, 19(21):1811–5, 2009.

[72] B. W. Draper, C. C. Mello, B. Bowerman, J. Hardin, and J. R. Priess. Mex-3 is a kh domain protein that regulates blastomere identity in early c. elegans embryos. *Cell*, 87(2):205–16, 1996.

[73] C. P. Hunter and C. Kenyon. Spatial and temporal controls target pal-1 blastomere-specification activity to a single blastomere lineage in c. elegans embryos. *Cell*, 87(2):217–26, 1996.

[74] W. Driever and C. Nusslein-Volhard. The bicoid protein determines position in the drosophila embryo in a concentration-dependent manner. *Cell*, 54(1):95–104, 1988.

[75] S. Brown, J. Fellers, T. Shippy, R. Denell, M. Stauber, and U. Schmidt-Ott. A strategy for mapping bicoid on the phylogenetic tree. *Curr Biol*, 11(2):R43–4, 2001.

[76] R. Schroder. The genes orthodenticle and hunchback substitute for bicoid in the beetle tribolium. *Nature*, 422(6932):621–5, 2003.

[77] J. A. Lynch, A. E. Brent, D. S. Leaf, M. A. Pultz, and C. Desplan. Localized maternal orthodenticle patterns anterior and posterior in the long germ wasp nasonia. *Nature*, 439(7077):728–32, 2006.

[78] G. Chen, K. Handel, and S. Roth. The maternal nf-kappab/dorsal gradient of tribolium castaneum: dynamics of early dorsoventral patterning in a short-germ beetle. *Development*, 127(23):5145–56, 2000.

[79] R. G. Gerrity, J. G. Rempel, P. R. Sweeny, and N. S. Church. The embryology of lytta viridana le conte (coleoptera: Meloidae). ii. the structure of the vitelline membrane. *Can J Zool*, 45(4):497–503, 1967.

[80] T. Miura, C. Braendle, A. Shingleton, G. Sisk, S. Kambhampati, and D. L. Stern. A comparison of parthenogenetic and sexual embryogenesis of the pea aphid acyrthosiphon pisum (hemiptera: Aphidoidea). *J Exp Zool B Mol Dev Evol*, 295(1):59–81, 2003.

[81] R. Rakshpal. Morphogenesis and embryonic membranes of gryllus assimilis (fabricius) (orthoptera: Gryllidae). *Proc. R. Entomol. Soc. Lond.*, A 37:1–12, 1962.

[82] Y. Kobayashi. Embryogenesis of the fairy moth, nemophora albiantennella issiki (lepidoptera, adelidae)adelidae), with special emphasis on its phylogenetic implications. *Int. J. Insect Morphol. Embryol.*, 27:157–166, 1998.

[83] E.H. Slifer. Insect development: Iii. blastokinesis in the living grasshopper egg. *Biol. Zbl.*, 52:223–229, 1932.

[84] R.H. Cobben. Evolutionary trends in the heteroptera: Part i. eggs, architecture of the shell, gross embryology and eclosion. centre for agricultural publishing and documentation, wageningen. 1968.

[85] H. Mori. Water absorption by the columnar serosa in the eggs of the waterstrider, gerris paludum insularis. *J. Insect Physiol.*, 18:675–681, 1972.

[86] A. Dorn. Ultrastructure of embryonic envelopes and integument of oncopeltus fasciatus

dallas (insecta, heteroptera): I. chorion, amnion, serosa, integument. *Zoomorphologie*, 85:111–131, 1976.

[87] D.W. Zeh, J.A. Zeh, and R.L. Smith. Ovipositors, amnions and eggshell architecture in the diversification of terrestrial arthropods. *Q. Rev. Biol.*, 64:147–168, 1989.

[88] C. G. Jacobs, G. L. Rezende, G. E. Lamers, and M. van der Zee. The extraembryonic serosa protects the insect egg against desiccation. *Proc Biol Sci*, 280(1764):20131082, 2013.

[89] P. Berger-Twelbeck, P. Hofmeister, S. Emmling, and A. Dorn. Ovicideinduced serosa degeneration and its impact on embryonic development in manduca sexta (insecta: Lepidoptera). *Tissue Cell*, 35:101–112, 2003.

[90] K. Handel, C. G. Grunfelder, S. Roth, and K. Sander. Tribolium embryogenesis: a sem study of cell shapes and movements from blastoderm to serosal closure. *Dev Genes Evol*, 210(4):167–79, 2000.

[91] D.T. Anderson. The development of hemimetabolous insects. *In Developmental Systems. Insects(ed. S.J.Counce and C.H.Waddington)*, 1:95–163, 1972.

[92] D. Tautz, M. Friedrich, and R. Schroder. Insect embryogenesis - what is ancesral and what is derived? *Development*, pages 193–199, 1994.

[93] Frieder Schöck Howard D Lipshitz Bruce H Reed, Ronit Wilk. Integrin-dependent apposition of drosophila extraembryonic membranes promotes morphogenesis and prevents anoikis. *Curr Biol*, 14(5):372–380, March 2004.

[94] Kevin A. Edwardsa Wayne L. Rickolla Daniel P. Kiehart, Catherine G. Galbraitha and Ruth A. Montaguea. Multiple forces contribute to cell sheet morphogenesis for dorsal closure in drosophila. *J Cell Biol*, 149(2):471–490, April 2000.

[95] Helen Doyle Christine Rushlow, Manfred Frasch and Michael Levine. Maternal regulation of zerknüllt: a homoeobox gene controlling differentiation of dorsal tissues in drosophila. *Nature*, 330:583–586, December 1987.

[96] Timothy Hoey Christine Rushlow, Helen Doyle and Michael Levine. Molecular characterization of the zerkniillt region of the antennapedia gene complex in drosophila molecular characterization of the zerkniillt region of the antennapedia gene complex in drosophila molecular characterization of the zerkniillt region of the antennapedia gene complex in drosophila. *Genes Dev*, 1:1268–1279, 1987.

[97] Michael Levine Christine Rushlow. Role of the zerknüllt gene in dorsal-ventral pattern formation in drosophila. *Advances in genetics*, 27:277–307, 1990.

[98] F. Falciani, B. Hausdorf, R. Schroder, M. Akam, D. Tautz, R. Denell, and S. Brown. Class 3 hox genes in insects and the origin of zen. *Proc Natl Acad Sci U S A*, 93(16):8479–84, 1996.

[99] Reinhard Schröder Rahul Sharmaa, Anke Beermannb. The dynamic expression of extraembryonic marker genes in the beetle tribolium castaneum reveals the complexity of serosa and amnion formation in a short germ insect. *Gene Expr Patterns*, 13(8):362–371, 2013.

[100] A. F. Sarrazin, A. D. Peel, and M. Averof. A segmentation clock with two-segment periodicity in insects. *Science*, 336(6079):338–41, 2012.

[101] E. Meijering, O. Dzyubachyk, and I. Smal. Methods for cell and particle tracking. *Methods Enzymol*, 504:183–200, 2012.

[102] K. Handel, A. Basal, X. Fan, and S. Roth. Tribolium castaneum twist: gastrulation and mesoderm formation in a short-germ beetle. *Dev Genes Evol*, 215(1):13–31, 2005.

[103] M. A. Benton, M. Akam, and A. Pavlopoulos. Cell and tissue dynamics during tribolium embryogenesis revealed by versatile fluorescence labeling approaches. *Development*, 140(15):3210–20, 2013.

[104] Nicholas E. Baker. Localization of transcripts from the wingless gene in whole drosophila embryos. *Development*, 103:289–298, 1988.

[105] Sean Carroll Lisa M. Nagy. Conservation of wingless patterning functions in the short-germ embryos of tribolium castaneum. *Nature*, 367:460–463, 1994.

[106] M. van der Zee, O. Stockhammer, C. von Levetzow, R. Nunes da Fonseca, and S. Roth. Sog/chordin is required for ventral-to-dorsal dpp/bmp transport and head formation in a short germ insect. *Proc Natl Acad Sci U S A*, 103(44):16307–12, 2006.

[107] Patrick Kalscheuer Abidin Basal Maurijn van der Zee Siegfried Roth Rodrigo Nunes da Fonseca, Cornelia von Levetzow. Self-regulatory circuits in dorsoventral axis formation of the short-germ beetle tribolium castaneum. *Dev Cell*, 2008.

[108] Robin E. Denell Yoshinori Tomoyasu, Scott R. Wheeler. Ultrabithorax is required for membranous wing identity in the beetle tribolium castaneum. *Nature*, 433:643–647, 2004.

[109] P. Tomancak, A. Beaton, R. Weiszmann, E. Kwan, S. Shu, S. E. Lewis, S. Richards, M. Ashburner, V. Hartenstein, S. E. Celniker, and G. M. Rubin. Systematic determination of patterns of gene expression during drosophila embryogenesis. *Genome Biol*, 3(12):RESEARCH0088, 2002.

[110] Thomas C. Kaufman Cynthia L. Hughes. Hox genes and the evolution of the arthropod body plan. *Evol Dev*, 4(6):459–499, 2002.

[111] B. A. Edgar and P. H. O'Farrell. The three postblastoderm cell cycles of drosophila embryogenesis are regulated in g2 by string. *Cell*, 62(3):469–80, 1990.

[112] B. A. Edgar, D. A. Lehman, and P. H. O'Farrell. Transcriptional regulation of string (cdc25): a link between developmental programming and the cell cycle. *Development*, 120(11):3131–43, 1994.

[113] M. D. Schroeder, M. Pearce, J. Fak, H. Fan, U. Unnerstall, E. Emberly, N. Rajewsky, E. D. Siggia, and U. Gaul. Transcriptional control in the segmentation gene network of drosophila. *PLoS Biol*, 2(9):E271, 2004.

[114] I. Palmeirim, D. Henrique, D. Ish-Horowicz, and O. Pourquie. Avian hairy gene expression identifies a molecular clock linked to vertebrate segmentation and somitogenesis. *Cell*, 91(5):639–48, 1997.

[115] M. L. Dequeant, E. Glynn, K. Gaudenz, M. Wahl, J. Chen, A. Mushegian, and O. Pourquie. A complex oscillating network of signaling genes underlies the mouse segmentation clock. *Science*, 314(5805):1595–8, 2006.

[116] C. Jouve, T. Iimura, and O. Pourquie. Onset of the segmentation clock in the chick embryo: evidence for oscillations in the somite precursors in the primitive streak. *Development*, 129(5):1107–17, 2002.

[117] E. M. Ozbudak and O. Pourquie. The vertebrate segmentation clock: the tip of the iceberg. *Curr Opin Genet Dev*, 18(4):317–23, 2008.

[118] A. Stollewerk, M. Schoppmeier, and W. G. Damen. Involvement of notch and delta genes in spider segmentation. *Nature*, 423(6942):863–5, 2003.

[119] D. Tautz. Segmentation. *Dev Cell*, 7(3):301–12, 2004.

[120] J. R. Finnerty, K. Pang, P. Burton, D. Paulson, and M. Q. Martindale. Origins of bilateral symmetry: Hox and dpp expression in a sea anemone. *Science*, 304(5675):1335–7, 2004.

[121] B. Benazeraf and O. Pourquie. Formation and segmentation of the vertebrate body axis. *Annu Rev Cell Dev Biol*, 29:1–26, 2013.

[122] L. Solnica-Krezel and S. Eaton. Embryo morphogenesis: getting down to cells and molecules. *Development*, 130(18):4229–33, 2003.

[123] P. N. Adler. The genetic control of tissue polarity in drosophila. *Bioessays*, 14(11):735–41, 1992.

[124] D. Gubb and A. Garcia-Bellido. A genetic analysis of the determination of cuticular polarity during development in drosophila melanogaster. *J Embryol Exp Morphol*, 68:37–57, 1982.

[125] C. R. Vinson and P. N. Adler. Directional non-cell autonomy and the transmission of polarity information by the frizzled gene of drosophila. *Nature*, 329(6139):549–51, 1987.

[126] J. D. Axelrod, J. R. Miller, J. M. Shulman, R. T. Moon, and N. Perrimon. Differential recruitment of dishevelled provides signaling specificity in the planar cell polarity and wingless signaling pathways. *Genes Dev*, 12(16):2610–22, 1998.

[127] J. D. Axelrod. Unipolar membrane association of dishevelled mediates frizzled planar cell polarity signaling. *Genes Dev*, 15(10):1182–7, 2001.

[128] D. R. Tree, J. M. Shulman, R. Rousset, M. P. Scott, D. Gubb, and J. D. Axelrod. Prickle mediates feedback amplification to generate asymmetric planar cell polarity signaling. *Cell*, 109(3):371–81, 2002.

[129] J. Wu, T. J. Klein, and M. Mlodzik. Subcellular localization of frizzled receptors, mediated by their cytoplasmic tails, regulates signaling pathway specificity. *PLoS Biol*, 2(7):E158, 2004.

[130] H. C. Wong, A. Bourdelas, A. Krauss, H. J. Lee, Y. Shao, D. Wu, M. Mlodzik, D. L. Shi, and J. Zheng. Direct binding of the pdz domain of dishevelled to a conserved internal sequence in the c-terminal region of frizzled. *Mol Cell*, 12(5):1251–60, 2003.

[131] R. Bastock, H. Strutt, and D. Strutt. Strabismus is asymmetrically localised and binds to prickle and dishevelled during drosophila planar polarity patterning. *Development*, 130(13):3007–14, 2003.

[132] A. Jenny, R. S. Darken, P. A. Wilson, and M. Mlodzik. Prickle and strabismus form a functional complex to generate a correct axis during planar cell polarity signaling. *EMBO J*, 22(17):4409–20, 2003.

[133] Y. Bellaiche, O. Beaudoin-Massiani, I. Stuttem, and F. Schweisguth. The planar cell polarity protein strabismus promotes pins anterior localization during asymmetric division of sensory organ precursor cells in drosophila. *Development*, 131(2):469–78, 2004.

[134] B. Ciruna, A. Jenny, D. Lee, M. Mlodzik, and A. F. Schier. Planar cell polarity signalling couples cell division and morphogenesis during neurulation. *Nature*, 439(7073):220–4, 2006.

[135] G. Das, A. Jenny, T. J. Klein, S. Eaton, and M. Mlodzik. Diego interacts with prickle and strabismus/van gogh to localize planar cell polarity complexes. *Development*, 131(18):4467–76, 2004.

[136] R. Keller. Shaping the vertebrate body plan by polarized embryonic cell movements. *Science*, 298(5600):1950–4, 2002.

[137] M. Mlodzik. Planar cell polarization: do the same mechanisms regulate drosophila tissue polarity and vertebrate gastrulation? *Trends Genet*, 18(11):564–71, 2002.

[138] D. C. Myers, D. S. Sepich, and L. Solnica-Krezel. Convergence and extension in vertebrate gastrulae: cell movements according to or in search of identity? *Trends Genet*, 18(9):447–55, 2002.

[139] D. R. Tree, D. Ma, and J. D. Axelrod. A three-tiered mechanism for regulation of planar cell polarity. *Semin Cell Dev Biol*, 13(3):217–24, 2002.

[140] M. T. Veeman, J. D. Axelrod, and R. T. Moon. A second canon. functions and mechanisms of beta-catenin-independent wnt signaling. *Dev Cell*, 5(3):367–77, 2003.

[141] J. B. Wallingford and R. M. Harland. Neural tube closure requires dishevelled-dependent convergent extension of the midline. *Development*, 129(24):5815–25, 2002.

[142] F. Carreira-Barbosa, M. L. Concha, M. Takeuchi, N. Ueno, S. W. Wilson, and M. Tada. Prickle 1 regulates cell movements during gastrulation and neuronal migration in zebrafish. *Development*, 130(17):4037–46, 2003.

[143] R. S. Darken, A. M. Scola, A. S. Rakeman, G. Das, M. Mlodzik, and P. A. Wilson. The planar polarity gene strabismus regulates convergent extension movements in xenopus. *EMBO J*, 21(5):976–85, 2002.

[144] T. Goto and R. Keller. The planar cell polarity gene strabismus regulates convergence and extension and neural fold closure in xenopus. *Dev Biol*, 247(1):165–81, 2002.

[145] N. Kinoshita, H. Iioka, A. Miyakoshi, and N. Ueno. Pkc delta is essential for dishevelled function in a noncanonical wnt pathway that regulates xenopus convergent extension movements. *Genes Dev*, 17(13):1663–76, 2003.

[146] M. Park and R. T. Moon. The planar cell-polarity gene stbm regulates cell behaviour and cell fate in vertebrate embryos. *Nat Cell Biol*, 4(1):20–5, 2002.

[147] M. Takeuchi, J. Nakabayashi, T. Sakaguchi, T. S. Yamamoto, H. Takahashi,

H. Takeda, and N. Ueno. The prickle-related gene in vertebrates is essential for gastrulation cell movements. *Curr Biol*, 13(8):674–9, 2003.

[148] J. B. Wallingford and R. M. Harland. Neural tube closure requires dishevelled-dependent convergent extension of the midline. *Development*, 129(24):5815–25, 2002.

[149] N. Perrimon and A. P. Mahowald. Multiple functions of segment polarity genes in drosophila. *Dev Biol*, 119(2):587–600, 1987.

[150] J. A. Zallen and E. Wieschaus. Patterned gene expression directs bipolar planar polarity in drosophila. *Dev Cell*, 6(3):343–55, 2004.

[151] S. Noselli. Jnk signaling and morphogenesis in drosophila. *Trends Genet*, 14(1):33–8, 1998.

[152] L. Zhang, W. Wang, Y. Hayashi, J. V. Jester, D. E. Birk, M. Gao, C. Y. Liu, W. W. Kao, M. Karin, and Y. Xia. A role for mek kinase 1 in tgf-beta/activin-induced epithelium movement and embryonic eyelid closure. *EMBO J*, 22(17):4443–54, 2003.

[153] X. Chen, S. W. Oh, Z. Zheng, H. W. Chen, H. H. Shin, and S. X. Hou. Cyclin d-cdk4 and cyclin e-cdk2 regulate the jak/stat signal transduction pathway in drosophila. *Dev Cell*, 4(2):179–90, 2003.

[154] B. A. Edgar and P. H. O'Farrell. The three postblastoderm cell cycles of drosophila embryogenesis are regulated in g2 by string. *Cell*, 62(3):469–80, 1990.

Publication List [1]

[1] **Jinping Fu**, Nico Posnien, Renata Bolognesia, Tamara D. Fischera, Parker Rayla, Georg Oberhofer, Peter Kitzmann, Susan J. Brown, and Gregor Bucher. Asymmetrically expressed *axin* required for anterior development in *Tribolium*. *Proc Natl Acad Sci* USA, 109(20):7782-6, 2012.

[2] **Jinping Fu**, Susan J. Brown. Survey of the *Tc-zen* expression pattern at *Tribolium* blastoderm stage. 2014. In preparation.

[3] Ezzat El-Sheri, Xin Zhu, **Jinping Fu**, Susan J. Brown. Caudal regulates the spatiotemporal dynamics of pair-rule waves in *Tribolium*. 2013. submitted.

[1] Most part of the Chapter 2 in this thesis has been published in [1]

Appendix A

RNAi survey for the contribution of cell movement and cell division in *Tribolium* segmentation

A.1 Introduction

Segmentation in biology refers to the division of body plans into a series of repetitive segments. It has been observed in three animal phyla: vertebrates, annelids and arthropods. Different mechanisms have been described to explain the segmentation process in vertebrates and arthropods. The clock and wavefront mechanism regulating segmentation in vertebrates [114–117] and the genetic hierarchy underlying segmentation in the model arthropod *Drosophila* [113] seemingly imply independent origins. However, comparative studies in other arthropods provide increasing molecular evidence for a common ancestry [68, 118–120]. In *Drosophila*, segments are formed simultaneously [34, 92]. In most other insects, including the red flour beetle *Tribolium castaneum*, other arthropods and vertebrates, segments are patterned sequentially in the posterior region of the embryo [34, 92].

As shown in Fig. A.1, the sequential segmented body plan contains three fundamental

processes — cell movement (named convergent extension in vertebrates), cell division and segmentation, all of which are required for metamerization in vertebrates [121].

During the whole process of embryogenesis in *Tribolium*, nuclei or cell movements should be involved. In the early cell proliferation stage, the nuclei divide and stay in the center of the egg. Later, most of the nuclei move towards the egg surface to form one single sheet which then undergoes cellularization indicating the blastoderm stage. Cell condensation towards ventral side marks the germband stage. The germband elongates during the segmentation and retracts once all segments are formed. Convergent extension is a specifically orchestrated series of cell shape changes and movements that contribute to germband elongation. The PCP and JNK (downstream of PCP) pathways are required for convergent extension in vertebrates, but not in *Drosophila*. To determine whether cell movement contributes to *Tribolium* germband elongation, I analyzed genes from the PCP and JNK pathways.

Additionally, to uncover how cell division is contributed to *Tribolium* segmentation, I also studied two genes, *cyclin D* and *string*, both of which are essential factors for cell cycle in almost all cells.

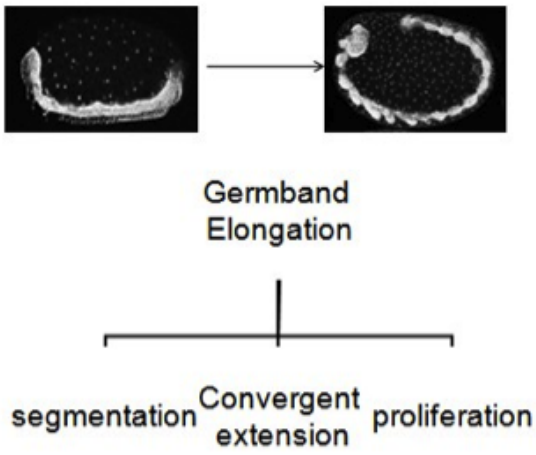

Figure A.1: *The sequential segmented body plan contains three fundamental processes.*

A.1.1 The PCP and JNK pathways

In tissues, cells show coordinated properties. For example in epithelia, cells are uniformly polarized along the apicalbasal axis. However, in addition to apicalbasal polarity, cells in most tissues also require positional information in the plane of the cell field to generate polarized structures or to move or orient themselves in a directed fashion. This type of polarization of a field of cells is referred to as Planar Cell Polarity (PCP).

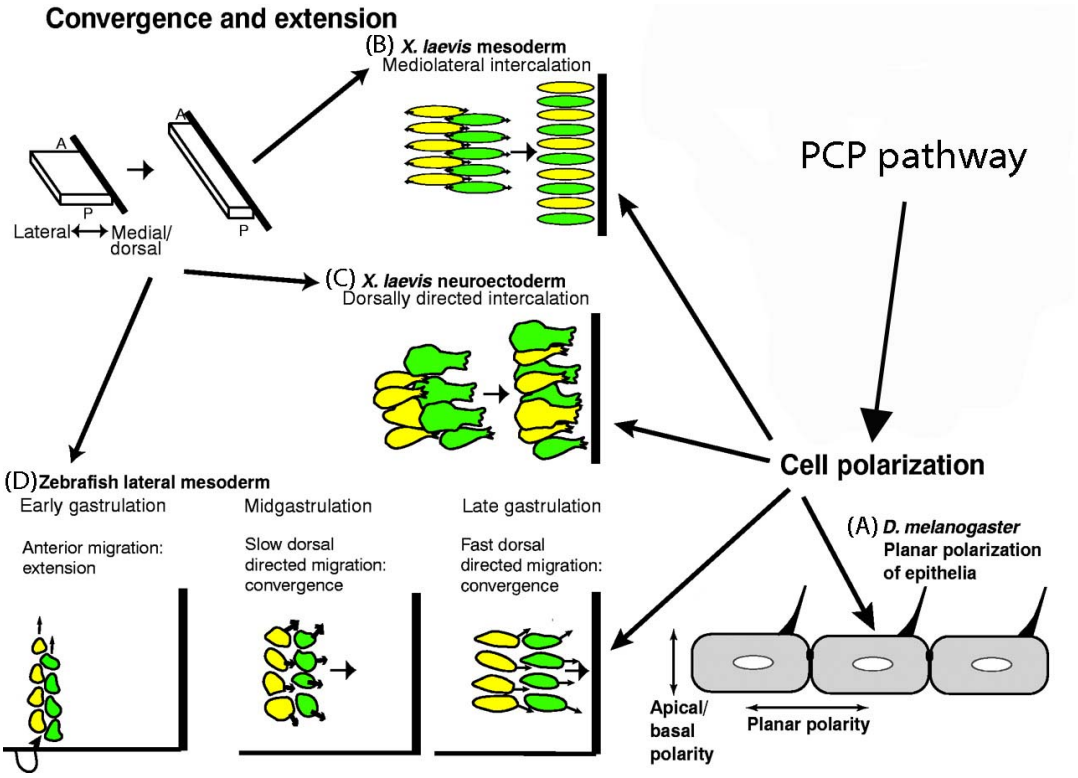

Figure A.2: *Evolutionarily conserved Planar Cell Polarity (PCP) signaling pathway controls various development events in invertebrates and vertebrates. (A) The D. melanogaster PCP pathway modulates cell polarity in the plane of epithelia. Convergence extension could be performed during gastrulation by distinct cellular activities: (B) In X. laevis mesoderm via mediolateral intercalation; (C) In X. laevis neuroectoderm via dorsally directed intercalation; and (D) In zebrafish lateral mesoderm via combined anterior and dorsally directed migration. This figure is adapted from Ref. [122].*

PCP was firstly recognized in *Drosophila melanogaster* [123–125]. Mutations of PCP genes caused disorganization of cuticular structures and the compound eye. Cellular hairs,

for example, showed swirls and wavy patterns instead of the characteristic proximaldistal orientation on the wing blade and show similar abnormalities on the body wall. In the compound eye, each ommatidium is precisely oriented in a nearly crystalline lattice. Moreover, each ommatidium exhibits one of two possible chiralities, as defined by the asymmetric packing of the eight photoreceptors. In the wildtype eye, ommatidia of differing chirality are segregated into two mirror image zones by a transverse equator. In PCP mutants, the ommatidia were variably oriented and the spatial segregation of ommatidial chirality was lost, with the result that individual ommatidia of the wrong chirality were found in each zone.

Based on these phenotypes, through genetic screen, *Drosophila* researchers discovered genes that are required for PCP and uncovered the evolutionarily conserved pathway - The Planar Cell Polarity (PCP) pathway. PCP pathway is one of the two noncanonical Wnt pathways that does not involve β-catenin (see Fig. A.4). It is not a simple, linear pathway and is best appreciated in a spatial context. Molecular interactions between the PCP core factors have been uncovered [126–135]. Cellular localization of PCP complexes is shown from an apical viewpoint in Fig. A.3. Two complexes, strabismus-prickle (STBM-PK) and frizzled-dishevelled-diego (FZ-DSH-DGO) with repressive effects on each other, are located on opposite sides of the cell. Though there is no biochemical data to confirm any physical interactions, genetic evidence puts flamingo (FMI) in both complexes. The asymmetric location of the FZ-DSH-DGO complex asymmetrically activates the downstream signaling pathway (Fig. A.4) and the subsequent changes in cytosekletal dynamics leading to development of correct planar polarity.

As shown in Fig. A.2 , the PCP pathway is conserved throughout evolution, but it mediates distinct developmental processes [136–141]. In zebrafish and *Xenopus* embryos, axis elongation involves cell intercalation and oriented cell divisions, and both processes are under the control of the PCP pathway. Indeed, no elongation took place in embryos in which the PCP pathway was disrupted [136, 141–148]. However, in *Drosophila*, mutations

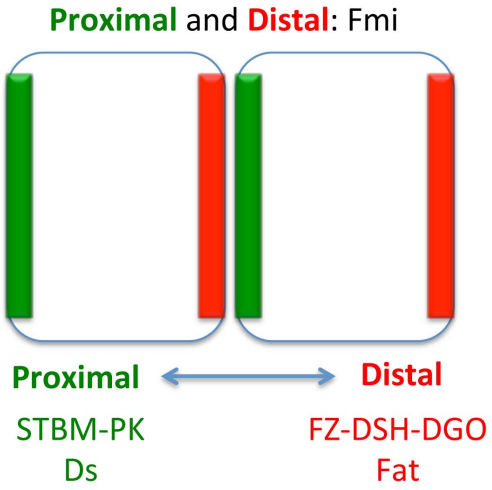

Figure A.3: *Cellular localization of the essential PCP components.*

in frizzled or disheveled, two genes involved in the classical PCP pathway, had no noticeable effects on extension [149, 150].

The JNK pathway functions downstream of the PCP pathway (see Fig. A.4) to regulate convergent extension movements in vertebrates [123]. Study in *Drosophila* shows that JNK pathway regulates embryonic dorsal closure [151], which is reminiscent of the JNK function in mammalian eyelid fusion during embryonic development [152].

Since *Tribolium* makes segments sequentially, as in vertebrates, I hypothesized that the PCP and JNK pathways would also be required for *Tribolium* germband elongation, though neither of these pathways appears to be required during germband extension in *Drosophila*. As part of this study, I cloned homologs of some essential components in the PCP and JNK pathways and surveyed their contributions in *Tribolium* embryogenesis with RNA interference technique.

A.1.2 Cyclin D and String

Cyclin D and String, both are essential factors for cell cycle in almost all cells. Cyclin D, also called G1-cyclin, initiates the transition from G1 phase to S phase. While, String helps cells go through the transition from G2 phase to M phase by positively regulating Cdk1/cdc2 complex.

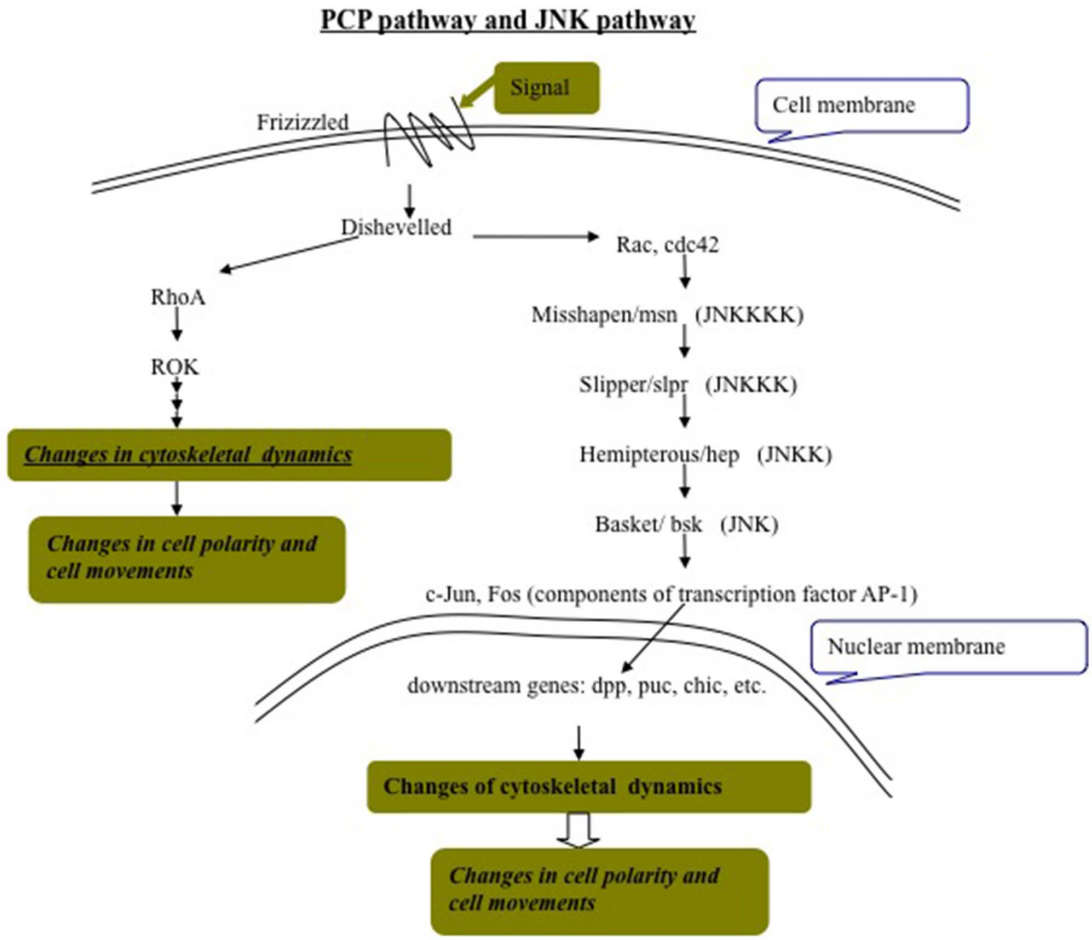

Figure A.4: *The JNK pathway is downstream part of the PCP pathway.*

Cyclin D, forming complex with Cdk4, has been shown to be the downstream part of JAK-STAT pathway in *Drosophila* [153]. Disruption of the function of Cyclin D-Cdk4 complex by the Cdk4 null mutant caused various developmental problems including deletion of the fifth abdominal segment and the posterior mid-ventral portion of the second thoracic and eighth abdominal denticle bands, fusion of the sixth and seventh band, and head defects [153].

In *Drosophila*, String is required for mitosis early in development and is transcribed in a dynamic pattern that anticipates the pattern of embryonic cell divisions [154]. It was shown that differential cell cycle regulation during postblastoderm development (cell cycles 14-16)

occurs in G2, which was controlled by String. *String* mutant got various problems including failure to involute the head region, head structure, few thoracic or abdominal denticles and only rudimentary tail structures.

Since cell proliferation is required in vertebrates, the pylum that also perform sequential segmentation as in *Tribolium*, I hypothesized that cell division is involved in *Tribolium* segmentation. So I expected that *Tc-cyclin D* RNAi and *string* RNAi should both cause truncation phenotype.

A.2 Materials and Methods

A.2.1 Strain and maintenance

The *Tribolium castaneum* GA1 strain, used for gene expression and functional analyses, was reared at 30 °C in whole wheat flour supplemented with 5% dried yeast at 30 °C.

A.2.2 Gene cloning

Using same methods as described in the subsection 2.2.2, I cloned *Tc-dachsous*, *Tc-fat* and *Tc-four-jointed*, from the PCP pathway; *Tc-basket* and *Tc-hemipterous* from the JNK pathway; *Tc-cyclin D* from cell division components. emphTc-string was cloned previously and I directly used dsRNA template for *Tc-string* dsRNA production from Brown Lab stock.

A.2.3 Primer sequences

Primers were designed with Vector NTI software.

Tc-dachsous forward: GGGCGGCGGAGTCAACACCT

Tc-dachsous reverse: GCAAGCCGGGCGTCACAG

Tc-fat forward: TGGGCGGGATCGACACAGGT

Tc-fat reverse: GGAACACGCCATTGAACGCATAGA

Tc-four-jointed forward: AATCTGCTCCCTGCCGCCATCC

Tc-four-jointed reverse: AGCCGCCCCACGTCCCTTTTC

Tc-basket forward: GTGATGGAATTAATGGACGCG

Tc-basket reverse: GTCGGAGGGAAACAGCACAT

Tc-hemipterous forward: AAGCGCCGAGCCCAACGATAGTC

Tc-hemipterous reverse: CGCGCCCTTAAATGTTGTGGAGAG

Tc-cyclin D forward: AGACCCCAACATCTTCAACGA

Tc-cyclin D reverse: ACAAACTGCTTTCGCCGC

A.2.4 RNA interference (RNAi)

T7-tagged TOPO primer sequence [54] was used to amplify templates for dsRNA production. dsRNA was synthesized with the T7 megascript kit (Ambion) and purified with the Megaclear kit (Ambion). dsRNA was mixed with injection buffer (5 mM KCl, 0.1 mM KPO4, pH 6.8) before injection.Female adults were injected with different concentrations of double-stranded RNA. For *Tc-dachsous*, concentrations between 0.01 μg/μL and 2 μg/μL were used; for *Tc-flamingo*, concentrations between 2 μg/μL and 6 μg/μL were used; for *Tc-fat*, the concentration of 2 μg/μL was used; for *Tc-four-jointed*, concentrations between 2 μg/μL and 12 μg/μL were used; for *Tc-basket*, concentrations between 2 μg/μL and 8 μg/μL were tested; for *Tc-hemipterous*, concentrations between 2 μg/μL and 12 μg/μL were used; For *Tc-cyclin D*, 2.0 μg/μL, 4.0 μg/μL and 6.0 μg/μL were used. For *Tc-string*, 1.0 μg/μL,3.0 μg/μL, 6.0 μg/μL and 8.0 μg/μL were used.

A.3 Results

A.3.1 RNAi survey for the PCP pathway

RNAi phenotypes are summaried in table A.1.

Table A.1: *RNAi results for the PCP and JNK pathways. For the last column "Adult lethal", "YES" means the injected female adults died within one or two month after injection (Lifespan of wildtype should be more than two years); "-" means RNAi had no effects on longevity. The possibility that the injection treatment itself might cause adult lethality was excluded by negative control that were injected with buffer only.*

genes		Conc. (ug/ul)	CP phenotype	Adult lethal
PCP	*dachsous*	1	Mostly empty eggs (death before germband, DAPI); remaining few with cuticles showing truncation and defects in dorsal closure, hair orientation and appendage formation.	YES
	Fat	2	Mostly empty eggs (death before germband, DAPI); some failed to hatch and some showed cuticle phenotypes with various problems including posterior truncation, fewer hairs and bristles, smooth non-segmented ventral surface, and defects in hair orientation, dorsal closure, and appendage formation.	-
	flamingo	4	79.9% larval lethality; 11.1% empty eggs; 10% containing cuticles with various abnormalities (1.5% truncation, 5.5% hair orientation defects, 4% dorsal closure defects and ventrally smooth, 2% appendage defects).	-
	four-jointed	12	wildtype	-
JNK	*basket*	8	With the concentration of 8 ug/ul, there was as high as 9.9% posterior truncation.	YES
	hemipterous	12	similar to *Tc-basket* but less penetrant.	-

Tc-dachsous has an early function before embryonic condensation

After RNAi, most progeny were empty eggs containing no cuticle, indicating early defects prior to cuticle deposition. A few eggs contained cuticles, and those cuticles showed defects in dorsal closure, hair orientation and appendage formation. In addition, very few were posteriorly truncated.

Most RNAi embryos stopped development before embryonic condensation suggesting an early function for *Tc-dachsous*. All injected female adults died within two months post-injection suggesting *Tc-dachsous* affects lifespan.

Since even lower concentrations (0.001 μg/μL) of *Tc-dachsous* dsRNA in parental RNAi also resulted in a high percentage of progeny that died prior to embryonic condensation, it may be necessary to inject embryos at late blastoderm stages to determine whether *Tc-dachsous* functions during germband elongation in *Tribolium*.

Tc-fat also functions prior to embryonic condensation

In cuticle preps, most eggs were empty, while some failed to hatch and some showed cuticle phenotypes with various problems including posterior truncation, smooth non-segmented ventral surfaces, fewer hairs and bristles, defects in hair orientation, dorsal closure and appendage formation. The posterior truncation indicates *Tc-fat* could possibly be required for *Tribolium* segmentation. DAPI staining for older progeny (24-48h embryos) as shown here suggest that most of the embryos died before germ band stage, which gave rise to the empty eggs containing no cuticle.

Tc-flamingo seems not essential for segmentation with the low penetrance of posterior truncation

Most progeny were survived until early larva stage suggesting the issue of gene redundancy. For the remaining progeny, the cuticle preps showed various problems including posterior truncation (1.5%), defects in hair orientation (5.5%), dorsal closure/ventral smooth (4%)

and appendage formation (2%). Together with DAPI staining, the cuticle preps explain that about 11% of the progeny died at early stage before blastoderm, indicating *Tc-flamingo* is required for early development before segmentation.

No matter what high concentration (as high as 12 μg/μL) was used, most progeny were survived until early larva stage. The possible issue of functional redundancy makes *Tc-flamingo* not a good candidate gene.

Tc-four-jointed **RNAi resulted in wildtype**

After RNAi, no non-wildtype phenotype was observed in the progeny, suggesting this gene has no essential function for embryogenesis or redundant components possibly exist.

A.3.2 RNAi survey for the JNK pathway

Tc-basket **RNAi produced posterior truncation**

Although *Tc-basket* RNAi resulted in various phenotypes, with the concentration of 8 μg/μL, we observed as high as 9.9% posterior truncation (Fig. A.5). This suggests that *Tc-basket* might be involved in *Tribolium* segmentation process.

Tc-hemipterous RNAi produced similar effects as Tc-basket RNAi

Most progeny had hatch defect though segmentation was fine. The remaining eggs obtained various problems including posterior truncation and defects in dorsal closure and appendage formation. Compared with *Tc-basket* RNAi, phenotypes of *Tc-hemipterous* were relatively mild. This could be probably caused by gene redundancy.

A.3.3 RNAi survey for cell division genes

Tc-cyclin D RNAi resulted in three apparent phenotypes: head defect(45.4%), abdomen truncation(26%) and thoracic defect(18.8%) (Fig. A.8 B-F). *Tc-string* RNAi produced

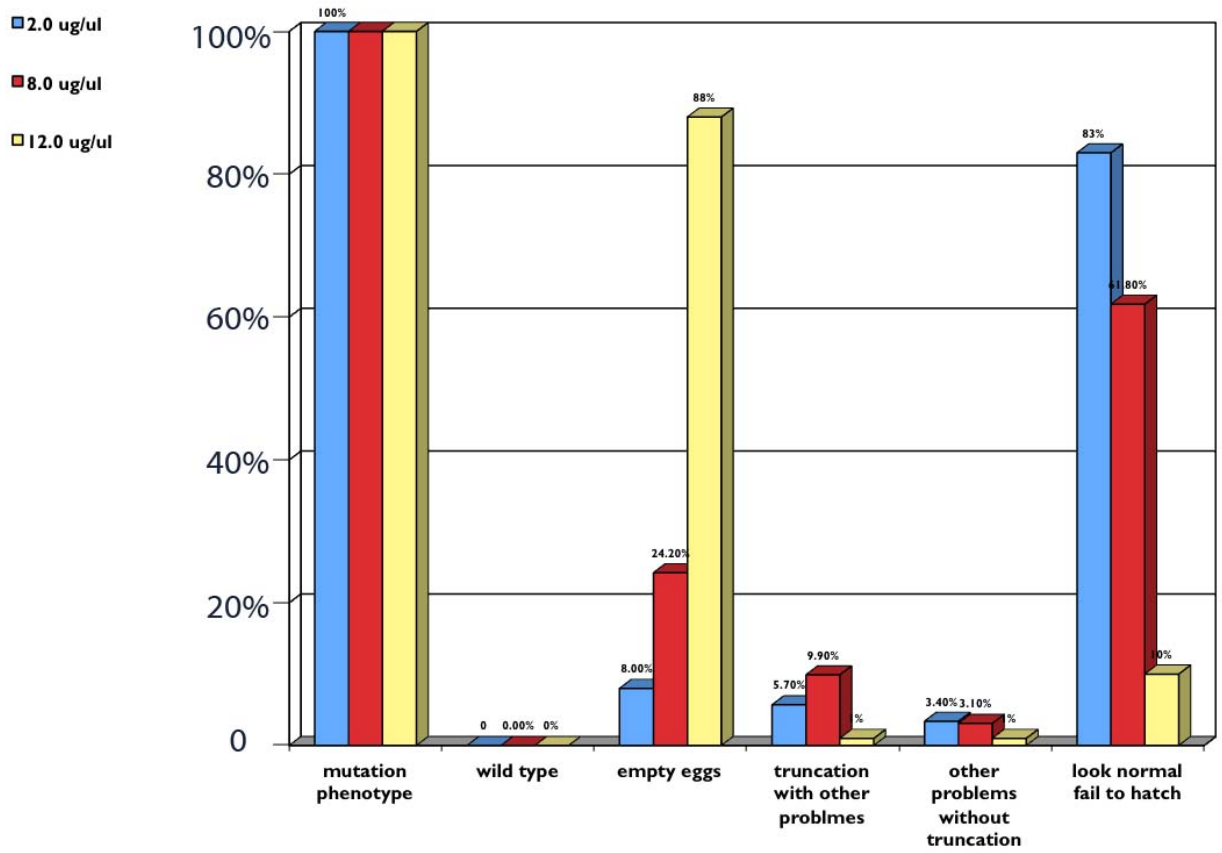

Figure A.5: *Quantitation data for the phenotypes after Tc-basket RNAi. There different concentrations of Tc-basket dsRNA were used: 2µg/µL, 8 µg/µL and 12 µg/µL. Y-axis is the percentage of specific phenotype, X-axis shows various phenotypes.*

same effects as *Tc-cyclin D* RNAi (Fig. A.8 G-K). Stainings with the segment marker, Tc-Engrailed, were consistent with the phenotypes in cuticle preparation (Fig. A.9). Data above suggest *Tc-cyclin D* and *Tc-string* might be required for correct cell division and the proliferation is most likely required for Tribolium segmentation.

A.4 Discussion

The diversity of phenotypes after RNAi for components from both PCP and JNK pathways suggest the numerous functions these pathways have during *Tribolium* embryogenesis. To specificly test their contributions in *Tribolium* segmentation, embryonic injection at blas-

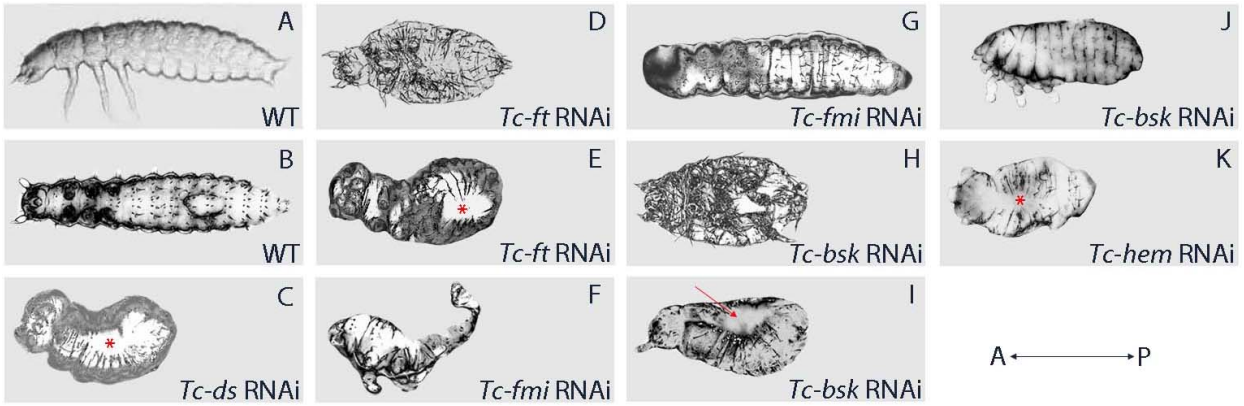

Figure A.6: *Comparison of wildtype and RNAi (the PCP componenets) cuticles. Cuticles are oriented with anterior to the left. (A-B) Wildtype, lateral view and dorsal view respectively. From anterior to posterior there are head, thorax with three pairs of legs and eight abdominal segments. (C) Tc-dachsous RNAi cuticle, dorsal view. Abdominal segments were truncated and dorsal was smooth without segmental grooves (see red star). (D-E) Tc-fat RNAi cuticles at venral views. (D) Abdominal segments were truncated. (E) Abdominal truncation and smooth ventral without segmental grooves (see red star). (F-G) Tc-flamingo RNAi cuticles. (F) Lateral view. Abdominal truncation. (G) Dorsal view. Defects in hair orientation (compare with wildtype in B). (H-J) Tc-fat RNAi cuticles. (H) Ventral view. Lack of abdominal segments. (I) Dorsal view. Posterior truncation and defect in dorsal closure (the red arrow points to the opened dorsal that failed in closure process). (J) Lateral view. Defect in appendage formation, including those in head and thorax. (K) Tc-hemipterous RNAi cuticle at dorsal view. Abdominal truncation and smooth dorsal without segmental grooves.*

toderm stage would be one option for future work. Two tables as following (table A.2 for the PCP pathway and table A.3 for the JNK pathway), by comparing with the cases in vertebrates and *Drosophila*, provide the possible functions that PCP and JNK pathways might contribute to *Tribolium*.

RNAi in cell division components produced truncated progeny, most likely, supporting the hypothesis that cell division is required for germband elongation. Though alternative explanation could be that defects in cell division during early blastoderm stage might affect later development including germband elongation, which make it hard to clarify the contribution of cell division in segmentation process. In this case, embryonic injection at early blastoderm stage would be the nice candidate as future work.

	Drosophila	*Tribolium*	Vertebrates
Convergent extension	no	Yes (guess)	yes
Body hair orientation	yes	Yes	yes
Nuclei clump Lifespan Appendage Dorsal formation	-	Yes	-

Table A.2: *Comparison of PCP functions among Drosophila, Tribolium and vertebrates.*

Table A.3: *Comparison of JNK functions among Drosophila, Tribolium and vertebrates. (solid line denotets conserved phenotype among different organism; dot line denotes that there might be similar mechanism between phenotypes in different organisms.)*

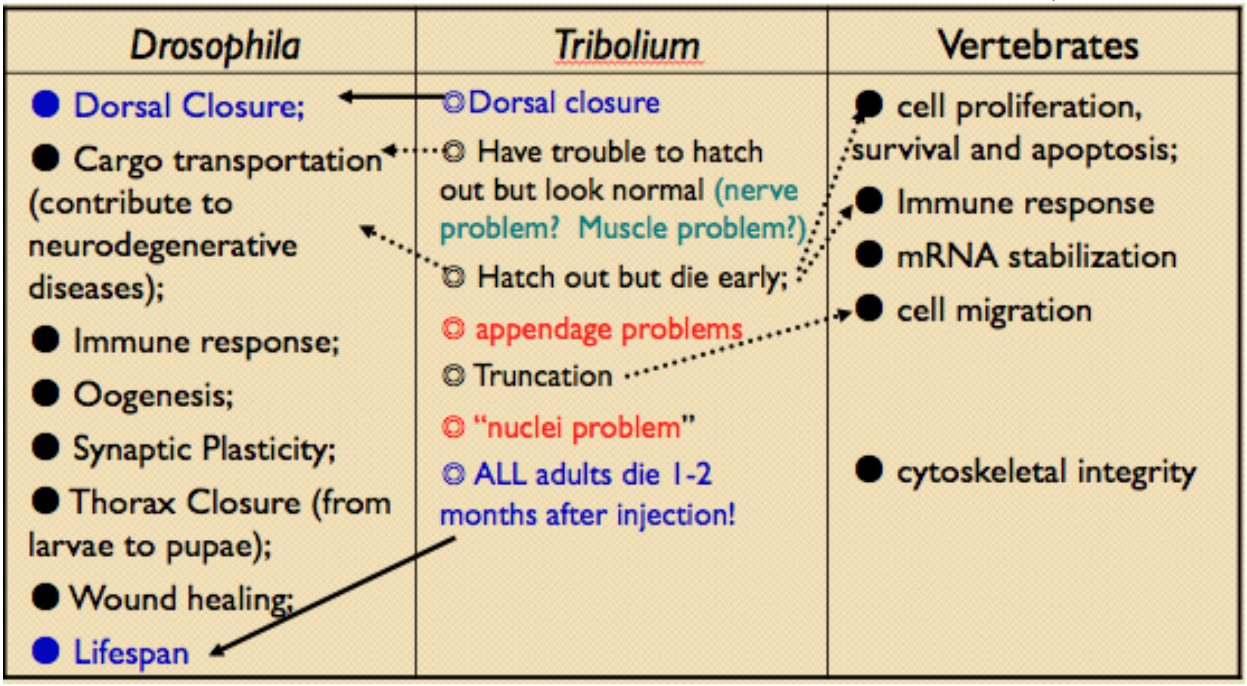

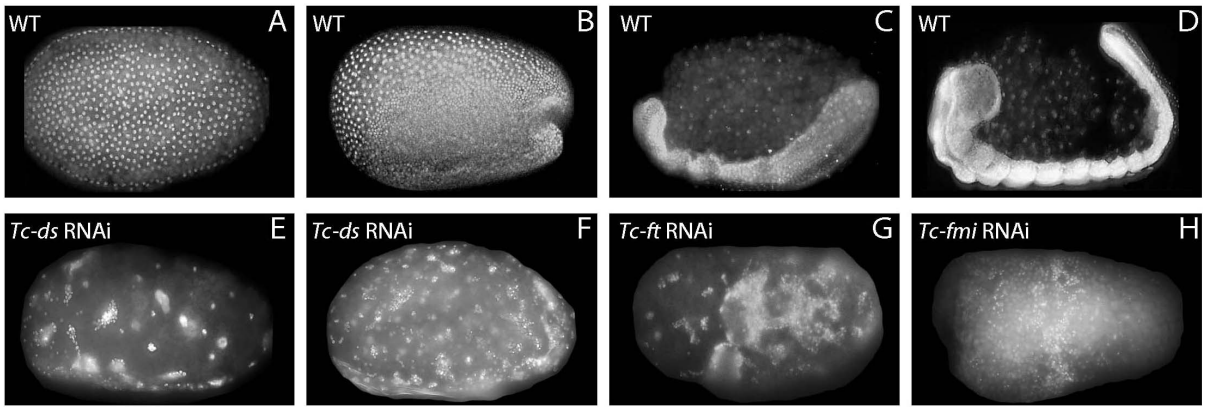

Figure A.7: *RNAi for either Tc-dachsous, Tc-fat or Tc-flamingo produced early defects before embryonic condensation. Nuclei in each embryo were stained with DAPI. Embryos are oriented laterally with anteior to the left, if known. (A-D) Different stages throughtout the age of 0-24 hours in wildtype. (A) Early blastoderm stage. All nuclei are uniformly located on the surface of the egg. (B) Early gastrulation stage. Germ rudiment cells are condensed in the ventral side with pit formed in the posteiror pole. (C) Early germ band elongation stage with anterior abdominal segments sequentially added from the growth zone. (D) Late germ band elongation stage with posterior abdominal segments added sequentially from the growth zone. (E-H) Collected RNAi progeny were incubated for another 24 hours before cuticle preparation, so that they were at least as old as 24 hours. However, instead of being similar to the 24 hours old wildtype embryo in (D), RNAi progeny stopped development at early stage before embryonic condensation. (E-F) Tc-dachsous RNAi progeny. (G) Tc-fat RNAi progeny. (H) Tc-flamingo RNAi progeny.*

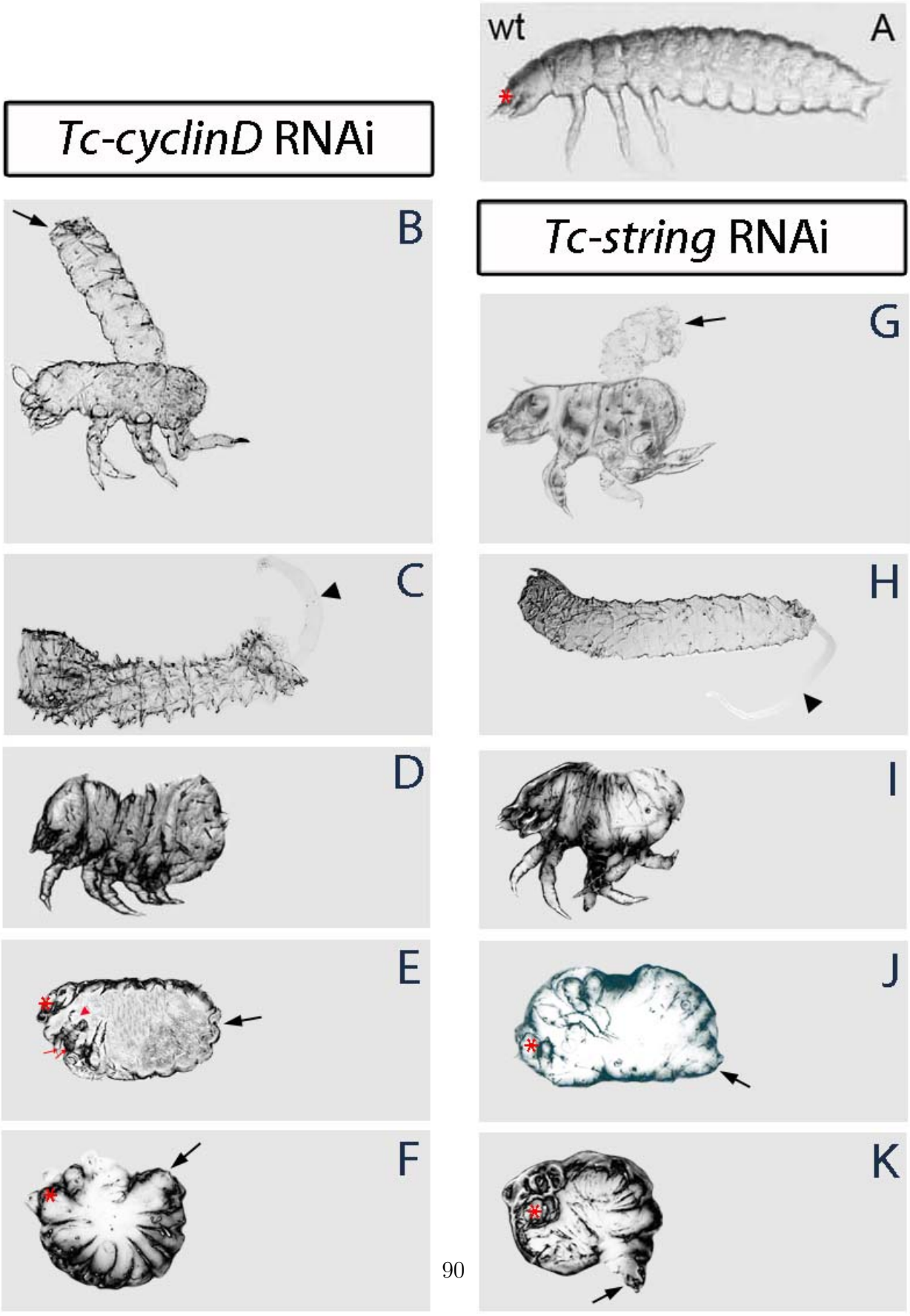

Figure A.8: *(Caption next page.)*

Figure A.8: *(Previous page.) Comparison of wildtype and RNAi (cell division genes) cuticles. Images in E, F, J, K are ventral view with anterior to the left. The rest images are lateral view with anterior to the left. (A) Wildtype cuticle. From anterior to posterior there are head, thorax with three pairs of legs and eight abdominal segments. (B-F) Tc-cyclin D RNAi cuticles. (B) Abdomen was inversed, though segmentation was fine. (C) The whole embryo was inversed (see the black arrow head pointing to the exposed gut). (D) Abdominal truncation and dorsal open. (E) Head was tiny with incomplete head appendages. Thorax was asymmetrically formed, with three thorax segments containing three legs formed in the bottom side and only one thorax segment (see the red arrow head) with two bifurated legs (see the red arrow) formed in the top side. Abdomen was also truncated. (F) Cuticle with reduced head lacking appendages and asymmetric segmentation in both thorax and abdomen. (G-K) Tc-string RNAi cuticles. (G) Abdominal part was inversed. (H) Inversed embryo (see the black arrow head pointing to the exposed gut). (I) Truncation in abdomen and defect in dorsal closure. (J) Head was tiny with incomplete head appendages. Thorax was asymmetrically formed, with three thorax segments containg three legs formed in the top side and no thorax segment in the other. Abdomen was also truncated. (K) Cuticle with reduced head in lack of head appendages and asymmetric segmentation in both thorax and abdomen.The red star marks labrum, and the black arrow points to the pit of the embryo.*

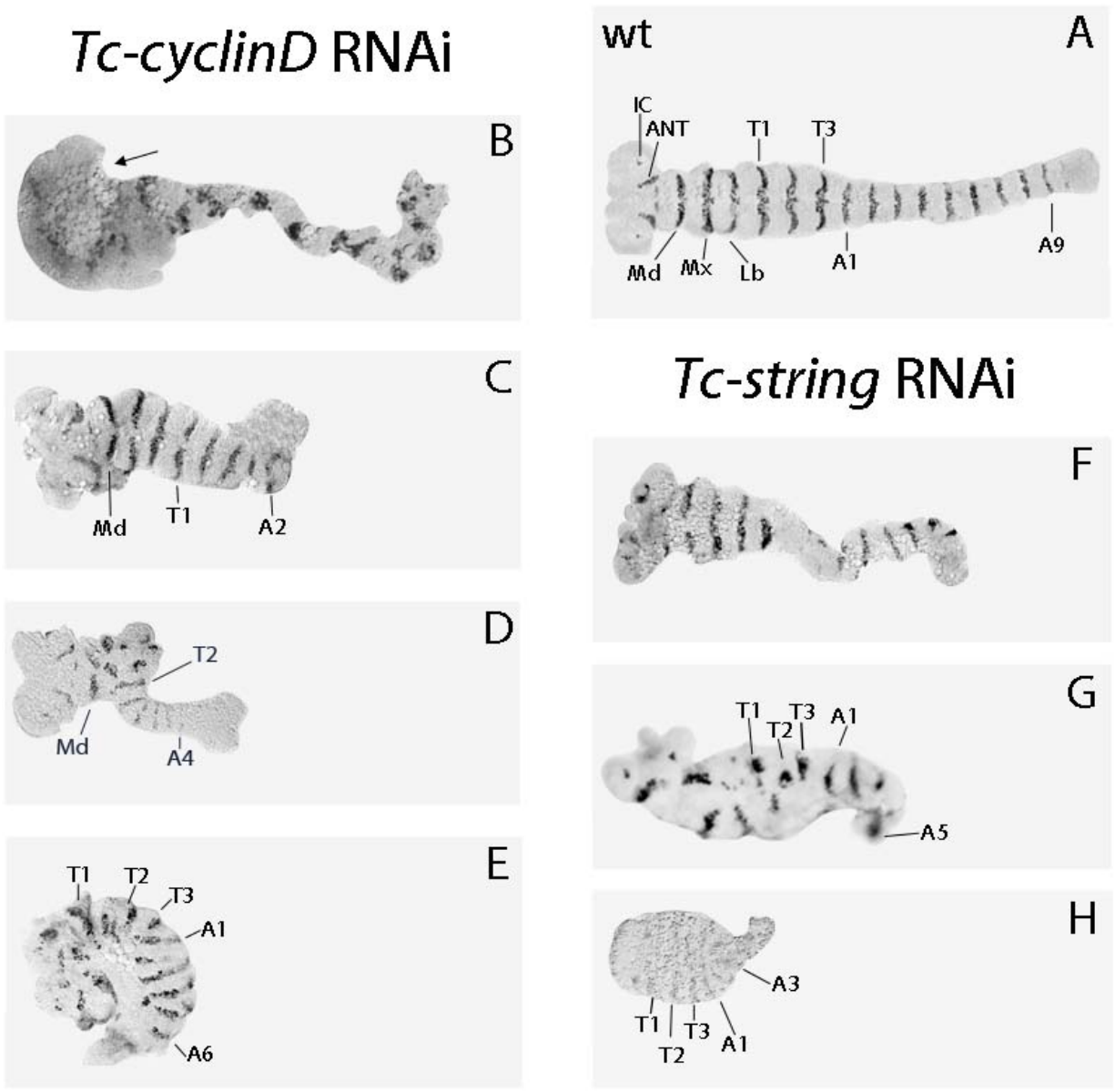

Figure A.9: *(Caption next page.)*

Figure A.9: *(Previous page.) Tc-Engrailed staining in RNAi (the cell division genes) embryos confirmed the late phenotypes in cuticle preparation. (A) Wildtype with each segment stained with one stripe of Tc-engrailed. (B-E) Tc-cyclin D RNAi embryos. (B) Anterior part was tightly sticked with the eggshell and hard to be dissected. The whole embryo looked very skinny and twisted. (C) Posterior abdomen segments were truncated. (D) Segments between Md and T2 clumped to the one side and posterior segements were lost, consistent with the late phenotypes in Fig. A.8 E. (E) On one side (top) of the embryo there were intact thorax segments and partial abdomen segements, while on the other side (bottom) there was no segment formed. This is consistent with the late phenotype in Fig. A.8 F. (F-H) Tc-string RNAi embryos. (F) Skinny and twisted embryo with messy stainings. (G) Posterior segments were lost. Messy stainings in the middle part of the embryo implicating a possible assymetrical throax formation as described in Fig. A.8 K. (H) Posterior segments were lost. Abbreviation used: Oc: ocular segment; Ant, antenna; Md, mandible; Mx, maxilla; Lb, labium; T1-T3, thoracic segments; A1-A9, abdominal segments.*